Flammability, corrosion resistance, and environmental friendliness of coal composites produced from various coal fines

A Master's dissertation submitted to the Faculty of Engineering and the Built Environment, University of the Witwatersrand, Johannesburg, South Africa, in fulfilment of the requirements for the degree of Master of Science in Engineering

by

Mhlawakhe Vatsha (1741475)

Submitted to

School of Chemical and Metallurgical Engineering, Faculty of Engineering and Built Environment, University of the Witwatersrand, Johannesburg, South Africa.

Supervisor: Prof. Samson O. Bada

May 2024

Declaration

I declare that this dissertation is my own unaided work. It is being submitted for the degree of Master of Science in Engineering to the University of the Witwatersrand, Johannesburg, South Africa. It has not been submitted before for any degree or examination to any other University.

……

(Signature of Candidate)

……..2nd …day of ……May……2024

(Day) / (Month) / (Year)

Abstract

The concept of recycling carbon-containing waste into secondary raw materials is highly promising for fostering a resource-efficient and circular economy, given the increasing scarcity of natural resources and growing population. The effectiveness of coal tar modified by air-blowing technique as a binder "pitch" for coal fines in the production of structural composites is highlighted in this study. In addition, the feasibility of commercial dimethylpolysiloxane as a binder for coal carbon composite production was assessed and compared to that produced using coal tar-pitch.

The two coal fines (GG1 and GS) used in this study have an ash content of 84.02% and 62.27%, respectively, and can be classified as rock. Their fixed carbon content ranges between 5.44% and 16.27%, compared to coal tar (35.23%). The coal tar has a volatile matter content of 64.50%, and with the air-blowing pretreatment, the tar was converted to pitch with a low volatile matter content of 11.27%. A pitch with the highest fixed carbon content of 87.68% and total carbon content of 96.01% was produced. Various ASTM standard test methods were used in the investigation to characterise and evaluate samples, including mineral phases and functional groups in the raw and coal composites produced.

The composites were fabricated using a circular mould with a diameter of 30 mm and a 40 mm square mould. In the study, it was found that composites with a low H/C atomic ratio had low water absorption. Additionally, composites with high volatile matter content had high water absorption. However, the sample with the highest water absorption (19%) was the GG1 50/50 coal tar pitch 400-composite, which falls within the range (0-25%) for building materials. The composites with an intense O-H group had high compressive and flexural strengths ranging from 106.58 to 344.71 MPa and 48.75 to 159.30 MPa, respectively. The flammability of all composites was low. The highest flammability mass ablation rate and linear ablation rate were found to be 0.008 g/sec and 0.00983 mm/sec, respectively. In terms of the corrosion rate, the GS 80%/20% dimethylpolysiloxane coal composite had the highest corrosion rate (0.081 μmpy), which is minimal compared to some commercial ceramic tiles.

The composites' environmental friendliness was determined by leaching them at various pH levels. The test was conducted by comparing the concentration of heavy toxic elements in the solution to the leachable concentration threshold for waste management standards (NEM WA Act No. 59 of 2008). All composites were environmentally friendly, meeting the moderate risk leaching concentration threshold. The composites that were produced in this study from South

African discard coal can be used in large quantities in the environment without any danger or hazards, as demonstrated. Based on this study's overall results, repurposing South African discard coal as carbon/ceramic composites for building materials could play a role in the country's Just Transition initiatives. In addition to waste reduction, this strategy could reduce operational emissions, improve circularity, and address associated environmental risks.

Acknowledgements

I want to express my sincere gratitude to my supervisor, Prof. Samson Bada, who has consistently been involved in this project to ensure its completion and has provided complete assistance and guidance. Without my supervisor, I doubt that this study would be successful in the manner it is currently conducted. He ensured that I had all the necessary equipment and facilities to conduct my experimental work. Prof. Nicholas Wagner of the University of Johannesburg has been extremely helpful in assisting and guiding with the petrographic analysis of the pitch. I also appreciate the assistance and guidance I received from my colleague, Dr. Orevaoghene Eterigho-Ikelegbe. His expertise in this field was instrumental in the successful completion of this research by assisting with the necessary methods and standards to be employed in the study.

My family and extended family, particularly my father, deserve my sincere gratitude for encouraging me to pursue my Masters degree even though he was unable to see it happen; may his wonderful soul REST IN ETERNAL PEACE. Jalamba, I am eternally grateful for your support. I have witnessed your love, and you have always made sure that I accomplish what I want and have guided me to achieve in everything.

I am grateful to my mother, six siblings, and daughter Luminjalo for their happiness and love, which have kept me going despite the challenges I have faced on the road. Every time I had to speak with you, I found a reason to keep pursuing my ambitions. The emotional support I receive from my family is beyond my expectations. I have never felt neglected once in my life because you were always there as my family to support me in all walks of life. Your contributions should never be taken lightly because that is what made me reach where I am today. Also, my great uncle, Senzile Vatsha, played a pivotal role in my career; without him, I doubt I would have enrolled at this institution for an engineering degree. He has done everything you can imagine as a parent to a child. I express my gratitude to the Fourways family, my aunt Tily, and all my cousins for their role in my life.

I am also grateful to the Coaltech Research Association of South Africa for their financial support, the Helmut and Babs Amos Scholarship from the DAAD-Stiftung – DAAD South Africa and the DS/NRF Clean Coal Technology Group at the University of the Witwatersrand, Johannesburg. I would also like to thank the School of Chemical and Metallurgical Engineering for access to their research facilities.

I appreciate Mr. Andrew Morgan's committed support and assistance, this research would be extremely challenging and would result in delays in finishing the study. He ensured that the equipment I used was serviced, repaired, and fabricated on time. The Chemical and Metallurgy workshop team really assisted me in fixing our reactor every time I encountered problems with it. For that, a special thank you goes to Mr. Hopewell Gumede. To Dimakatso Ramohaladi and Jimmy Alade for their assistance to conduct some analyses, Msizi Mkhize, Sifiso Ngcobo, and John Nkuna for their help and support in making some decisions – I appreciate you all. To the entire Clean Coal Technology Research Group at the University of the Witwatersrand, I express my sincere gratitude for your support and guidance.

Yanga uThixo woxolo anganisikelela nonke anithamsaqelise anembese ingubo yeentsikelelo kwaye anivambe entendelezweni yesandla sakhe sobubele.

List of Acronyms

A	Water absorption
ASTM	American society for testing materials
B	Bulk density
C	Carbon
CPCC	CTP carbon composites
C_{pr}	Corrosion rate
CTP	Coal tar pitch
DMPS	Dimethylpolysiloxane
F	Flexural strength
F_a	Aromatic ratio
FTIR	Fourier transform infrared
GO	Graphene oxide
GS	Greenside coal fines
H	Hydrogen
H/C	Hydrogen-total carbon ratio
L_a	Crystal size
LAR	Linear ablation rate
LCT	Leachable concentration threshold
MAR	Mass ablation rate
M_G	Mass of the green body (before pyrolysis)
M_P	Mass of the pyrolysed composites
MPa	Megapascals
MXCC	CPCC and PPCC mixture
N	Nitrogen
N/A	Not applicable
p	Apparent porosity
PET	Polyethylene terephthalane
PPCC	Petroleum pitch carbon composites
S	Sulphur
SEM	Scanning electronic microscopy
T	Apparent specific gravity
XRD	X-ray diffraction
ρ	Relative density

Table of Contents

List of Tables

List of Figures

Chapter 1

1.1 Background and motivation

Coal is the most abundant and inexpensive natural resource influencing global economic growth (Magazzino *et al*., 2020). It has numerous global applications, including as a precursor to produce building materials, feedstock for over 200 chemicals, steam for electricity generation, and a reductant for metallurgical applications (Longwell, 1995; Miller, 2005; Letcher, 2008). According to the Energy Data report published by Enerdata (2022), South Africa produces about 244 Mt of coal and is the world's seventh largest coal producer. Technological development and the need for cheap carbon sources have increased the alternate uses of coal beyond power generation (Gagarin *et al*., 2020). As a result, coal is now being used as a feedstock to produce carbon composites, fibres, and foams with excellent physicochemical properties (Petrova *et al*., 2005; Liu *et al*., 2018; Sharma *et al*., 2020). In addition, coal is also used as a carbon source to prepare activated carbons for adsorbed natural gas storage (Abdulsalam *et al*., 2020). Some types of coal are also used to produce graphite electrodes for electric arc furnaces and carbon anodes for the low-cost aluminium industry (Banerjee, 2021). More so, some coals are adapted for applications where mechanical properties such as micro-wear, low coefficient of friction, and high-temperature stability are required (Sharma *et al*., 2020).

The coal and mining industries face environmental pollution challenges, just like any other industry, despite their significant contribution to global technological development. Coal uses generate millions of tonnes of coal waste during coal beneficiation. In addition, metallurgical coal produces coal tar, which has highly volatile matter and is difficult to manage as it poses environmental risks. The current method of managing coal discard and other pollutants is inadequate, as the accumulation of discard could lead to spontaneous combustion and leaching of trace elements (Onifade and Genc, 2018). The rewashing or beneficiation of the discard coal to recover the carbon in the dump is a strategy put in place by most mining houses. This approach has drawbacks because little or no separation is achieved due to the association of carbon and inorganic minerals in the coal discards. As a result, it is critical to identify alternative and efficient uses of coal waste. Eterigho-Ikelegbe *et al.* (2021a) showed that South African coal waste is suitable for producing coal composites for construction purposes. Also, Taha *et al*. (2017) reported that using coal waste to produce high-quality construction materials can solve the coal industry's environmental contamination challenges.

According to the International Energy Agency (2023), global coal demand reached a new all-time high in 2022, surpassing 8.3 billion tonnes. Thus, this would lead to more coal waste and the need for adequate management or utilisation of this waste. Many innovative studies have been conducted in the field of coal waste utilisation, including being used as a filler with conventional polymers to produce ceramic materials and processes such as moulding and firing in ceramic bricks making (Stolboushkin *et al.,* 2016; Xu *et al.,* 2017; Al-Majali *et al.,* 2019; Bai *et al.,* 2019; Phillips *et al.,* 2019; Vasić *et al.,* 2021). In the recent study by Hill *et al.* (2022), raw coal from the United States of America and preceramic polymer were used to produce composites for building materials. These composites are produced through curing and pyrolysis of the coal/ preceramic polymer mixture under an inert atmosphere. The resulting composites exhibited properties such as lightweight, adequate strength, thermal stability, fire resistance, chemical resistance, etc. Such properties made them suitable for roofing tiles, bricks, panels, and blocks (Hill and Easter, 2021).

In this study, an alternative composite, "coal composite", which is less flammable than polymeric composites, known to be flammable with high levels of toxic gases (Liu *et al*., 2018) was produced. Coal discards were used as a precursor for these coal composites, while coal tar was used to produce coal tar pitch (CTP). CTP and dimethylpolysiloxane (DMPS) were used as binders. The fabrication process involved blending the materials in suitable proportions, followed by carbonisation under an inert atmosphere to prevent the combustion of the carbon in the samples (Banerjee *et al*., 2019; Sharma *et al*., 2020). The fabrication produced composites with high-quality engineering properties such as tensile strength and modulus (Hill *et al*., 2019; Sharma *et al*., 2020). Some of the composites also exhibited low thermal conductivity, low coefficient of thermal expansion, hydrophobicity, and high strength, which makes them applicable in the aerospace industry (Liu *et al*., 2018; Sharma *et al*., 2020). The coal type or rank, precursor-to-binder ratio, processing methods, and pretreatment of the binder influence the composites' properties.

This research was necessary given that little information is available on fabricating coal composites applicable for construction purposes using CTP. The properties of the two coals used, the CTP, and the coal composites were determined along with composites produced from DMPS. The properties of the resulting composites were determined using the standards for conventional building/construction composites reported in the literature. This reasonably justifies using modified CTP as a binder to fabricate coal composites.

1.2 Problem statement

Over 8 billion metric tons of coal was mined globally in 2022, resulting in the generation of significant amounts of coal fines and waste during mining and beneficiation. In addition, fine coal processing is challenged when there is no adequate plan for its use while the cost of maintaining the dumps continues to increase. Most dumps comprise coal characterised by its diverse qualities and rich in inorganic compounds and could be valuable resources for the construction industry. On the other hand, the rapid growth of the world population is straining the sustainable use of Earth's natural resources due to modern society's extensive use of building and construction raw materials. In practice, this industry is threatened by resource exhaustion, providing a powerful platform for the use of fine coal waste.

Similar environmental hazards experienced by the coal processing industry is also experienced by the metallurgical industry, as about 30 million tons of coal tar are produced per annum. Disposing of the tar is also a major challenge to the metallurgical industry. For every tonne of tar produced by the coking plant, only 60% is converted to pitch during the distillation process. This made it difficult to manage thousands of tonnes of tar without causing environmental contamination, such as acid mine drainages and fire hazards (Roberts, 2014). Coal tar is not suitable to be used directly in the industry because of its high volatile matter. Therefore, it must be modified before it is used as a suitable precursor with excellent properties for the carbonisation process (Sharma *et al*., 2020). In this study, coal tar was modified using air-blowing process to produce pitch, and the best-produced pitch was used as the binder for the coal composites. The modification of the tar plays a crucial role in influencing the mechanical strength of composite materials produced due to its volatile matter, total carbon, H/C atomic ratio, and aromatic ratio. In addition, the nature of the binder's hydrogen bonding with carbon-carbon covalent bonds, which causes the fusibility of coal composites during pyrolysis, is also important.

The variability of the coal fine may also influence the quality of the structural composite produced. The physico-mechanical properties, such as density, water absorption, and compression test, were used to evaluate the composites. Furthermore, the corrosion, leaching, and flammability properties, such as oxidation induction time, (OIT) which may pose environmental uncertainties for the application of the composites, were investigated.

1.3 Hypothesis

CTP and coal discards can be blended to produce coal-based structural composites with excellent physicochemical, mechanical, and thermal properties with low flammability, low water absorption, and low porosity.

1.4 Research questions

The research effort on this study seeks to address the following research questions:

i. What optimum pretreatment conditions are required for coal tar to produce CTP appropriate to produce an inflammable coal composite?
ii. What process conditions will be undertaken to achieve mesophase pitch?
iii. Does coal-DMPS composites have better quality than coal-CTP composites?
iv. Can a composite with high flexural and compressive strength, low bulk density, and non-corrosive properties be produced from blended coal discard and CTP?
v. Does the composite produced meet the required standards for construction according to conventional building/construction testing standards?

1.5 Aim and objectives

The aim of this study is to produce coal composite materials for building applications using South African coal fines and coal tar pitch. The objectives of the study are:

i. To investigate the physicochemical, mineralogical, and textural properties of the as-received coal fines, coal tar, and the produced CTP;
ii. To investigate the optimum pretreatment conditions for coal tar to produce coal tar pitch;
iii. To compare the properties of the coal-CTP composites produced at different ratios and coal-DMPS composites;
iv. To determine the physical properties, mechanical strength, water absorption, corrosion, and flammability behaviour of the produced coal composites;
v. To determine the commercial suitability of the produced coal composites using the existing commercial building material testing and standard analyses.

1.6 Research benefits

The following benefits could be accomplished from the successful completions of this study:

i. Repurposing coal fines to produce value-added composite materials will reduce the cost of waste disposal.

ii. Coal-based composites will help to meet the growing demand for construction materials.
iii. The application of coal fines and CTP to produce composite will protect the environment, preserve our natural resources, and help conserve energy.

1.7 Research layout

This dissertation is divided into five chapters, each serving a distinct purpose in the exploration of the research topic. The brief description of each chapter is provided below.

Chapter 1 introduces the research and provides the study's background and motivation, problem statement, hypothesis, research questions, aim and objectives, and research benefits.

Chapter 2 reviews the uses and properties of coal, coal tar, and CTP, particularly in the building industry. The binding nature of coal tar pitch and the structure of coal, as well as their implications to coal composite materials, were discussed.

Chapter 3 details the research methodology. The methodology used to characterise the raw materials, produce CTP from coal tar by the air-blowing method, and the fabrication and characterisation of the coal composites are outlined. The standard methods followed in this research are also provided.

Chapter 4 presents and discusses the results obtained to show the significance of this research. The results of the materials and the produced coal composites are discussed utilizing literature, engineering, and scientific analysis tools.

Chapter 5 concludes the study and offers recommendations for further research. Based on the obtained results, it is demonstrated that South African coal fines and coal tar pitch can be effectively utilised to produce coal composites suitable for building applications.

Chapter 2

Literature review

This chapter reviews the extensive literature on coal and its applications that result in the generation of coal waste. It outlines the use of coal in various industries based on its characteristics. The widespread use of coal, particularly for energy generation, generates coal wastes that pose environmental hazards. Alternative methods for using coal waste to reduce the environmental footprint have been demonstrated in recent studies. However, that does not appear to be sufficient, given the significant amounts of coal waste generated worldwide. It is now essential to conduct a study on using coal waste for industries that consume a substantial quantity of this waste. As a result, this study explores how coal waste can be used to produce coal composites that can be used in the construction industry. This industry has been identified as one that can consume large amounts of materials due to population growth, which leads to a demand for shelters. The method of producing CTP as a suitable binder with excellent physicochemical properties for coal composites is discussed in this chapter. The literature review covers certain characteristics of coal waste and CTP that could be attributed to their use as building materials. In addition, other precursors increase their potentials to produce tiles, bricks, etc., are discussed.

2.1 Introduction

The beneficiation of coal in the preparation plant results in a significant amount of coal being lost to tailings and disposed of for no purpose (Li and Wang, 2020). On the other hand, during the carbonisation of coking coal to produce coke "reductant" in the metallurgical industry, coal tar is produced as a by-product. Both coal tar and coal fines are difficult to manage due to their environmental impact. Repurposing these wastes from the metallurgical and coal processing industry would enable waste valorisation and management, the circular economy, and the sustainability of the construction industry. In addition, the threat of resource exhaustion provides a powerful platform for the use of fine coal waste for building components rather than conventional soil.

Clay and sand are the conventional materials used to manufacture bricks in the construction industry (Alonso-Santurde *et al*., 2012). In a study conducted by Manjarekar *et al.* (2017), plastic waste was mixed in small amounts with sand and cement to make bricks. According to the author, the increase in plastic content in the mix decreased the bricks' compressive strength. In another study, polyethylene terephthalate (PET) waste was also utilised to manufacture cement sand bricks (Rafikullah-Deraman *et al*., 2021). The author also observed a decrease in

the concrete's bond and its compressive strength when PET was used. Furthermore, with the addition of PET, a low density, low weight brick was produced (Rafikullah-Deraman *et al*., 2021), but the brick did not meet the required properties. Several studies investigated the use polymer composites in biomedical applications (medical implants) and engineering applications for construction purposes (Ramakrishna *et al*., 2001; Gao, 2004; Sheikh-Ahmad, 2009; Rahman *et al*., 2011; Galande, 2016; Li *et al*., 2022; Turvey, 2023). These composites are typically made with thermosets and thermoplastics such as epoxy resins, phenolic, polycarbonates, polyvinylchloride, nylon, acrylics, glass, carbon and Kevlar fibres (Mouzakis, 2013; Greene, 2021; Liew *et al*., 2021). In a recent study conducted by Eterigho-Ikelegbe *et al*. (2021a), a "preceramic polymer" was mixed with discard coal to produce a coal composite suitable for use in the construction industry. The coal composites produced demonstrated excellent water absorption, compressive strength, flexural strength, and thermal stability.

Fly ash, which is a by-product of coal combustion, was also used as a supplementary cementitious material at 15 to 25% to produce concrete (Romadhon, 2021). According to the author, using fly ash increased the bond strength of concrete compared to normal concrete. A similar approach was also used by Mandal *et al*. (2017) to produce construction bricks with excellent compressive strength and durability that were chemically inert. Guo *et al*. (2019) likewise used biomass fly ash and coal fines to replace clay in the production of bricks, and the bricks made from coal fines were more thermally stable than those produced from biomass ash. The use of coal slag to produce tiles, which is another waste, was investigated by Kim and Pandy (2019). The tiles produced from the mixture of this waste, clay and a binder proved to be durable, hard, and resistant to abrasion. The use of coal waste to produce building materials would lead to a decline in the use of conventional raw materials or natural resources, saving energy and reducing greenhouse gas emissions (Kumar *et al*., 2020).

In the current study, coal tar "metallurgical coke oven waste" was used as a precursor to make an appropriate pitch that acts as a binder and is mixed with coal fines to produce coal composites. The coal tar was modified to produce pitch with a high total carbon content, a highly aromatic and anisotropic liquid with uniform pores and low voids. With a modified tar "pitch" blended with coal, coal composites with excellent physicochemical and mechanical properties, such as high compressive and flexural strength, low flammability, and high corrosion resistance, were produced. Specifically, different shapes of these composites were produced, which could be used in applications requiring micro-wear resistance.

2.2 Coal overview

Coal is a heterogeneous sedimentary rock composed mainly of molecular organic and inorganic matter from dead plants buried millions of years ago (Wong, 2009; Jurisch *et al*., 2012). Most coal deposits began in peat bogs, where water was stagnant, and plant remains accumulated. Depending on the region, the deposit and the environmental conditions prevailing during the formation, each deposit has its own vegetal raw material (Vassilev and Vassileva, 2009; Wong, 2009). The first phase of coal maturity is lignite, which has a low carbon content, followed by sub-bituminous and bituminous coals, which are intermediates. The last of the coal ranks is anthracite, which may have a total carbon content of about 90% and is the purest and hardest coal (Tishmack and Burns, 2004). The organic matters of coal are known as macerals and are composed of non-crystalline constituents such as lithotypes and micro-lithotypes groups (petrographic ingredients) (Whitehurst, 1978; Nip *et al*., 1992; Vassilev and Vassileva, 2009). The minerals and mineraloids within the coal consist of inorganic matter (mineral matter). According to Wu *et al*. (2020), the inorganic matter in coal is brittle, whereas its organic matter is flexible and exhibits properties such as plasticity, toughness, and ductility. The plasticity of coal is one of the characteristics required for coal composite applications (Chelgani and Matin, 2018; Fraga *et al*., 2020).

Coal is the most inexpensive fossil fuel in the world (IEA, 2021). According to Mazumder *et al*. (2020), the use of coal to provide energy for the world's 9.49 billion people could be increased by 17.6% in 2040. This will further increase coal discard generated worldwide, as only 60 to 70% of the total run of mine washed is recovered. As coal discard is a by-product of both mining and processing plants, its low calorific value limits its application for power generation (Sekhohola and Cowan, 2017). It contains unrecoverable carbon that interlocks with inorganic minerals and rocks, which is difficult to separate. Consequently, this resource, normally stockpiled in South Africa for no economic use, was used to produce structural coal composites in this study.

2.3 Overview of coal tar as a by-product

Coal tar is a by-product of the coke (industrial coal) manufacturing process, and is a mixture of aliphatic, aromatic, alicyclic, and heterocyclic compounds (Yuan *et al*., 2016; Liu *et al*., 2018; Sinaga *et al*., 2021). Coal tar is produced from the coke oven, which produces about 22 metric tonnes of coke per day from 30 tonnes of coking coal (DoESA, 2021). According to SteelMint (2023), about 819 million tons of coking coal was used in the production of coke as a reductant in the global production of over 1.8 billion tons of crude steel. During coke

production, the gas released from the coke oven, which may represent a quarter of the coal once cooled, produces about 37 kg of coal tar per tonne of coking coal charged into the oven (Zhang and Zhang, 2020; Britannica Kids, 2022). Therefore, it is estimated that coal tar produced globally in 2023 should be around 30.3 million tons. Coal tar is characterised by its molecular structure, which contains an aromatic core to which methyl groups are attached (Huang *et al*., 2023a). As a result, CTP has superior aromatic properties, resulting in a lower degree of substitution than petroleum pitch (Das Lala *et al.*, 2018). Aromatic compounds have delocalised electrons in their π-π orbitals, which improves structural stability (Fan *et al*., 2017; Yang *et al*., 2022). The distillation of coal tar produces numerous products such as carbolic oil, anthracene oil, naphthalene oil, creosote oil, and CTP as a residue (non-volatile at 450°C) (Das Lala *et al*., 2018; Ispatguru.com, 2018). Coal tar is used in various industries, including chemical, medicine, and engineering. The primary use of coal tar is the production of electrodes for the aluminium and steel industry (Future Market Insights, 2022), as well as a carbon precursor for carbon materials due to its high carbon content of about 53 wt.% (Liu *et al*., 2018). The following sections provide information on selected sectors and commodities derived from coal tar.

2.3.1 Chemical and crude oil industry

During World War II, the Germans relied completely on the production of synthetic fuels from tar oils and gasoline produced from creosote oil (coal tar product) by hydrogenation (Clough, 1957). As more crude oil was discovered, there was a shift to use crude oil for producing premium petroleum products rather than tars. However, coal tar contains contaminants in the form of heteroatoms like sulphur, nitrogen, and metals (Ancheyta *et al*., 2005; Marafi *et al*., 2006). To produce transportation fuels from coal tar, the heteroatom content of the tar must be removed. According to Šafářová *et al*. (2010), a clean fuel can be produced from tar using a hydrotreating process. Clean liquid oil was produced by hydrotreating coal tar at 600°C in a trickle bed reactor system filled with a commercial catalyst (Li *et al*., 2013). Using a distillation process, the same author also produced gasoline and diesel from the liquid fuel oil, as shown in Figure 2.1.

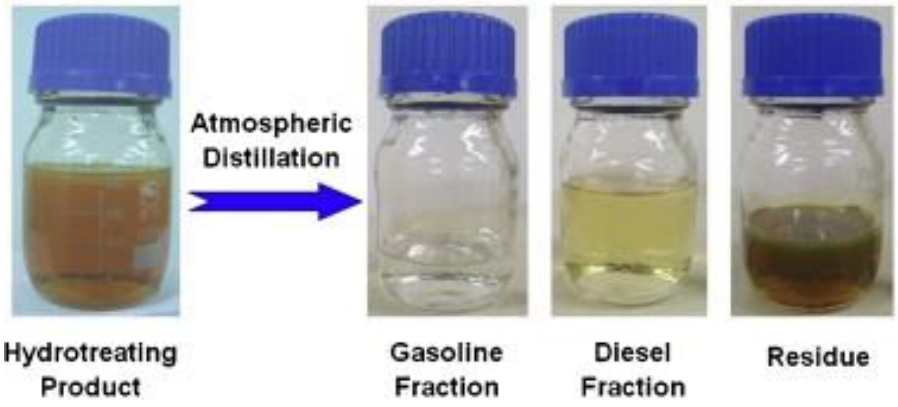

Figure 2.1: Hydrotreating products after distillation (Li *et al*., 2013)

The polycyclic aromatic hydrocarbon structures in coal tar also influence its use in the petroleum industry (Ma *et al*., 2021). With these structure variations, different products, such as BTX (comprising benzene, toluene, and xylene), can be produced. Other highly demanded products are carbolic oil (phenols, cresols, and xylenols), resins, herbicides, fungicides, disinfectants, and plasticisers. Other products include carbolic fractions, which are used in the production of polymers and flux oils for bitumen production (Granda *et al*., 2013).

The agricultural, construction, photography, rubber, tanning, dye, and polymer industries also rely on naphthalene oil produced from coal tar. Wash oil is another nitrogen-containing product, i.e., it contains quinolone, isoquinoline, carbozol, and acridine. These are aromatic chemicals with very low freezing points and good solvent characteristics. As a result, wash oil is commonly used in coke battery ovens to remove impurities from pipelines and valves. Anthracene oil is another coal tar product, characterised as the heaviest oil and composed of two to five aromatic rings. These rings include acenaphthene, fluoranthene, fluorine, phenanthrene, anthracene, and pyrene. The major use of anthracene is to produce carbon black that is used to produce tyres and rubbers. The residue of this oil is CTP, which is left after the distillation process, and it is widely used as a binder and impregnating agent in the aluminium and steel industries for manufacturing carbon anodes and graphite electrodes (Granda *et al*., 2013).

2.3.2 Carbon fibres

Carbon fibres are materials comprised of more than 92 wt.% carbon, and fibres with 99 wt.% carbon are referred to as graphite (Huang, 2009). Graphite is a high-performance material with a threaded structure and a carbon backbone (Banerjee *et al*., 2021). The history of carbon fibres can be traced back to 1860 when Sir Joseph Wilson Swan first produced them by heating cotton

fibres in an inert environment for lighting incandescent light bulbs (Peijs *et al*., 2022). As of 1961, Akio Shindo (1961) pioneered the use of polyacrylonitrile as a precursor for carbon fibres, and other sources like CTP and rayon are now being used. CTP, as a precursor, has a couple of advantages over peroxyacetyl nitrate (PAN). It is an inexpensive material with a higher degree of orientation and a higher char yield than polyacrylonitrile (Berrueco *et al*., 2012). The graphic structure of pitch provides a carbon fibre with higher elastic modulus and higher thermal and electric conductivity. The modification of the pitch could lead to either isotropic or anisotropic (mesophase), and these two pitches are used depending on the field of application (Kim *et al*., 2016). According to Yang *et al*. (2014), carbon fibres produced from CTP are most applicable in the automotive industry as brakes or insulators for high-temperature performance.

2.3.3 Carbon porous materials for supercapacitors

Coal tar pitch has also found applications as a carbon source in the making of an electrode material for supercapacitors (Wei *et al*., 2020). A supercapacitor is an electric double-layer capacitor that stores electrical energy by absorbing the charge on the electrode's surface (Wei *et al*., 2020; Bi *et al*., 2021). Low-cost carbon material with excellent electrical conductivity and physical or chemical stability is appropriate for making a porous electrode material. The same material must have a high specific surface area to provide a large electrode-electrolyte interface and good conductivity to ensure quick electron transport, as well as the appropriate distribution of pore size to optimise ion transport for high power and energy density output (Fang *et al*., 2016; Yao *et al*., 2017; Chen *et al*., 2018).

According to Wang *et al*. (2020), CTP can be carbonised (activated carbon) and used as a porous electrode material for supercapacitor applications. Figure 2.2 shows the process involved in synthesising activated carbon from CTP for supercapacitor applications. In another investigation, graphene nanocapsules were also synthesised from CTP, which showed properties such as interconnected porous and thin shells with well-balanced micropores and mesopores (He *et al*., 2017). According to the author, a porous material with exceptional electron conductivity, high ion transport in small pores, and an abundance of pores for ion storage was achieved. Jiang *et al*. (2021) also manufactured porous carbon-sheet microspheres as an electrode material. This was achieved by covering the basic zinc carbonate microspheres with CTP, carbonising them, and then activating them with KOH. The produced porous carbon-sheet microspheres had template morphology and a large surface area of about 1359.88 to

2059.43 m^2/g. Yang *et al*. (2020b) also produced nanosheets from CTP doped with MnO_2 for improved asymmetric supercapacitors.

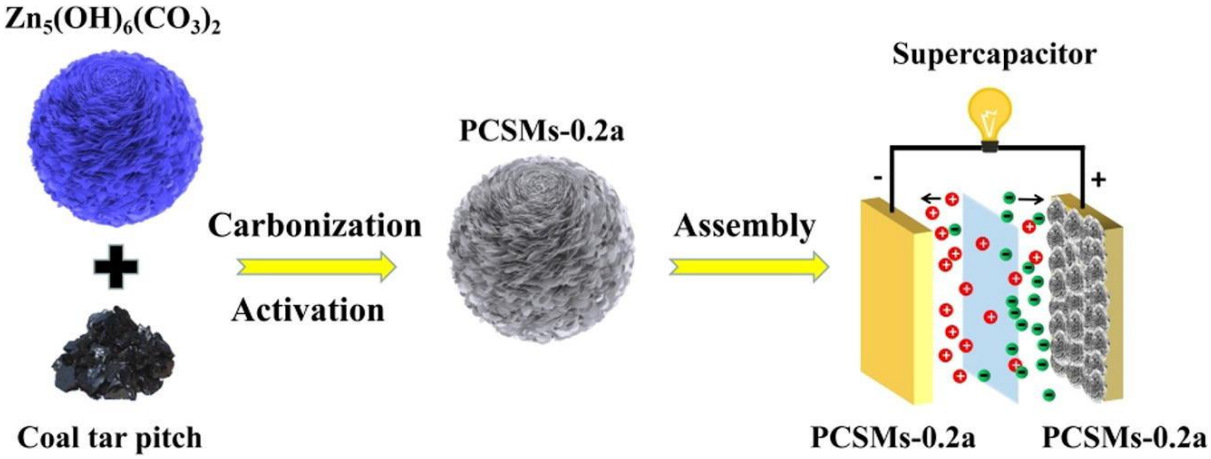

Figure 2.2: Producing supercapacitor from coal tar pitch (Jiang *et al*., 2020)

2.3.4 Coal tar pitch as binder for engineering applications

Over the past decade, carbon-carbon (C-C) composites have become the material of interest because of their ease of manufacture and low-cost carbon precursor (Shirvanimoghaddam *et al*., 2017; Mehmandoust *et al*., 2022). C-C composites have demonstrated exceptional reliability in engineering applications where low friction coefficient and high-temperature stability are required (Patel *et al*., 2016). As a result, it has found an application in aerospace as a thermal barrier for re-entry spacecraft (Song *et al*., 2012; Gao *et al*., 2016; Chowdhury *et al*., 2018). C-C composites can be formed by thermally treating modified pitch and through fibre reinforcement. C-C composites made from CTP are superior in mechanical and thermal properties compared to C-C composites made from petroleum pitch (Sharma *et al*., 2020). The mesophase constituent in a CTP is responsible for the binding nature of the pitch produced. Incorporating mesophase pitch as a binder in a boron-phenolic resin improves the compression strength and ablation rate of phenolic fibre (Huang *et al*., 2022). Huang *et al*. (2023a) reported that using CTP with high mesophase constituent led to the conversion of composites with thermoplastic properties to thermoset properties.

As justified above, CTP improves mechanical and thermal qualities for high-performance applications. However, there is minimal research on how CTP can be blended with coal fines to produce construction materials. Given the different attributes of CTP provided in the literature, the current study aimed to produce coal-based composites of coal fines mixed with CTP to produce construction materials.

2.4 Global market of coal tar pitch

The global market of coal tar is growing, as reported by Globe Newswire in 2022. Low-level coal tar manufacturers account for 60 to 70% of total market revenues (Globe Newswire, 2022). On the other hand, the CTP market is also growing at a rate of 5.5% per annum and was valued at 3.75 billion dollars by the end of 2022 (Globe Newswire, 2022). The global business also projects a compound annual growth rate of 5.4% between 2022 and 2028 (Future Market Insights, 2022). The world's major leaders in the CTP ecosystem are China, India, Russia, and Western Europe (Chai *et al*., 2021). China alone forecasts annual sales growth of 6.0%, reflecting numerous growth opportunities for CTP manufacturers (Globe Newswire, 2022). The growth rate in developing countries is also expected to reach 7.0% (Future Market Insights, 2022). The industry is expected to grow further by the end of 2023 owing to the increased use of CTP in road construction in China and India (Future Market Insights, 2022.). In addition, the increase in demand for automobiles worldwide also leads to the use of aluminium-grade CTP, thus influencing the growth of the industry (Future Market Insights, 2022).

The major challenge to the global CTP market is the hazardous potential of CTP. As a result, various studies are being conducted to improve the quality of CTP as an environmentally friendly raw material. Liu *et al*. (2018) developed a method for modifying CTP for construction purposes. In another study, Patel *et al*. (2020) suggested that CTP must be pre-treated prior to use to reduce the impurities associated with it. Pitch pretreatment is carried out to modify the plastic properties of the pitch and convert the raw pitch to mesophase pitch that is suitable to be used as a precursor to produce high-performance carbon materials (Oh *et al*., 1991; Banerjee *et al*., 2019). In the current study, the pitch used as a binder was prepared from coal tar using one of the methods for the modification of CTP (Section 2.5). In other words, the coal tar was converted to CTP by thermal treatment and modified using the air-blowing method.

2.5 Pretreatment and modification of CTP

The modification or pretreatment of CTP can be achieved by various methods, including toluene extraction, vacuum distillation, and cross-linking with bifunctional group chemicals (Banerjee *et al*., 2019). The pretreatment of CTP influences subsequent stages, such as pyrolysis, carbonisation, graphitisation, and the structural performance of the final product (Prauchner *et al*., 2001). Hence, the main goal of pretreatment is to control the softening point of the pitch and to control the viscosity's flowability at high temperatures. This is often achieved by heating the CTP molecules to increase their molecular weight through a process

known as "polymerisation" (Prauchner *et al.*, 2003). Pitch polymerisation implies the release of side chains to form radicals, resulting in large molecules and an increase in tar aromaticity (Prauchner *et al.*, 2001). Pre-treating CTP at moderate temperatures also reduces volatile content, increases carbon content, and converts short-chain hydrocarbons to longer-chain hydrocarbons (Banerjee *et al.*, 2019). According to Banerjee *et al.* (2019) and Sharma *et al.* (2020), when the total carbon content of CTP is > 60 wt.%, a quality carbonised product with a high modulus and durability can be achieved. To produce carbon materials using pitch, the pitch "matrix" liquid's viscosity must be high enough to prevent bubbles from escaping the liquid pool (Banerjee *et al.*, 2019). The relevance of viscosity control is that the pitch may be regulated and shaped to a desired form during high-temperature treatment.

Chemically modifying the pitch with nitric acid increases its softening point. This process is conducted to ensure that raw pitches perform well during the pyrolysis (Patel *et al.*, 2020). According to Banerjee *et al.* (2019), the process must be conducted at a low pressure to release volatile matters and prevent further swelling that could result in low bulk density. With swelling, highly porous composites can be formed, leading to a negative impact on the physical properties of the coal composite. Acid modification in CTP converts aromatic compounds containing fewer aromatic nuclei to higher aromatic compounds. This raises the pitch's softening point and viscosity, allowing mesophase to form quickly during the carbonisation process (Banerjee *et al.*, 2019).

Another technique that can be used to produce high-quality pitch is air-blowing coal tar. This is a simple, low cost, highly effective, and versatile method of producing pitch with a wide range of properties and applications (Fernández *et al*., 1995; Prada *et al*., 1999; Wang *et al*., 2019). According to Fernández *et al*. (1995), air-blowing at temperatures ranging from 250 to 300°C can lead to increased aromaticity. Table 2.1 shows the data from the test carried out on two distinct pitches: binder pitch and impregnating pitch. Both pitches were subjected to air and nitrogen blowing. As the temperature increases, so does the quality of the pitch in terms of carbon yield, softening point, C/H ratio, etc. (Table 2.1)

Table 2.1: Studied properties of coal tar pitch produced using the air-blowing method (Fernández *et al*., 1995)

Pitch	Treatment	C/H ratio	SP (°C)	CY (%)	TI (%)	QI (%)
CTPA	-	1.9	72	48.4	35.7	13.0
CTPA0	250°C/N_2	2.0	92	54.3	42.9	15.8
CTPA1	250°C/Air	2.2	151	70.8	59.8	39.3
CTPA2	275°C/Air	2.2	171	72.1	62.6	49.2
CTPA3	300°C/Air	2.3	223	79.4	70.0	53.2
CTPB	-	-	54	35.2	20.8	3.0
CTPB0	250°C/N_2	1.7	70	37.8	23.7	4.2
CTPB1	250°C/Air	1.7	148	62.4	52.7	39.2
CTPB2	275°C/Air	1.9	164	64.4	53.8	42.9
CTPB3	300°C/Air	1.9	219	67.9	60.5	45.9

C: total carbon; CY: carbon yield; CTPA: binder pitch; CTPB: impregnating pitch; H: total hydrogen; N_2: nitrogen; SP: softening point; TI: toluene insoluble; QI: quinoline insoluble

The results in Table 2.1 are congruent with those reported by Prada *et al*. (1999), who investigated CTP air-blowing at three different temperatures (275, 300, and 325°C). Fernández *et al*. (1995) and Prada *et al*. (1999) varied the reaction time (8, 12, and 20 hours) for each temperature (275, 300, and 325°C), and the results show that there were significant changes in the characteristics of the modified pitch for eight hours at 300°C, but no significant changes after this period. This illustrates that temperature and reaction time are critical parameters in modifying the pitch qualities during air-blowing modification. In addition, the author reported that at 275°C of pitch air-blowing, the C/O ratio reaches a maximum for the coal tar utilised. This can be caused by oxidation-polymerisation, which has considerably increased the softening point of the treated tar. Furthermore, Fernández *et al*. (1995) and Prada *et al*. (1999) indicated that thermal treatment could reduce the aromatic and ortho-substitution index due to the distillation of smaller components. Air-blowing only reduces the ortho-substitution index and dehydrogenative polymerisation of the pitch molecules without the formation of any oxygenated compounds (Blanco *et al*., 2000). The increased aromaticity index and C/H ratio demonstrate that polymerisation reduces aliphatic hydrogen (Fernández *et al.*, 1995; Sharma *et al*., 2020). Using Fourier transform infrared (FTIR) spectra, Prauchner *et al*. (2001) also show that the air-blowing technique reduces the aliphatic stretching absorbance of the pitch

produced. Therefore, in the current study, coal tar was converted to pitch thermally and modified using the air-blowing method to produce the binder for the coal composite.

Alcañiz-Monge *et al*. (1997) investigated the effect of temperature on the H/C ratio of two CTP samples heat-treated in the presence of air and nitrogen. The samples heat-treated in air had a much lower H/C ratio than the samples treated in nitrogen at comparable temperatures, owing to the oxidative impact of air. From the aromatic-aliphatic hydrogen ratio (H_{aro}/H_{ali}) of the two samples, a modest (H_{aro}/H_{ali}) ratio for samples heat-treated in nitrogen and a large variance for samples heat-treated in air was obtained (Figure 2.3).

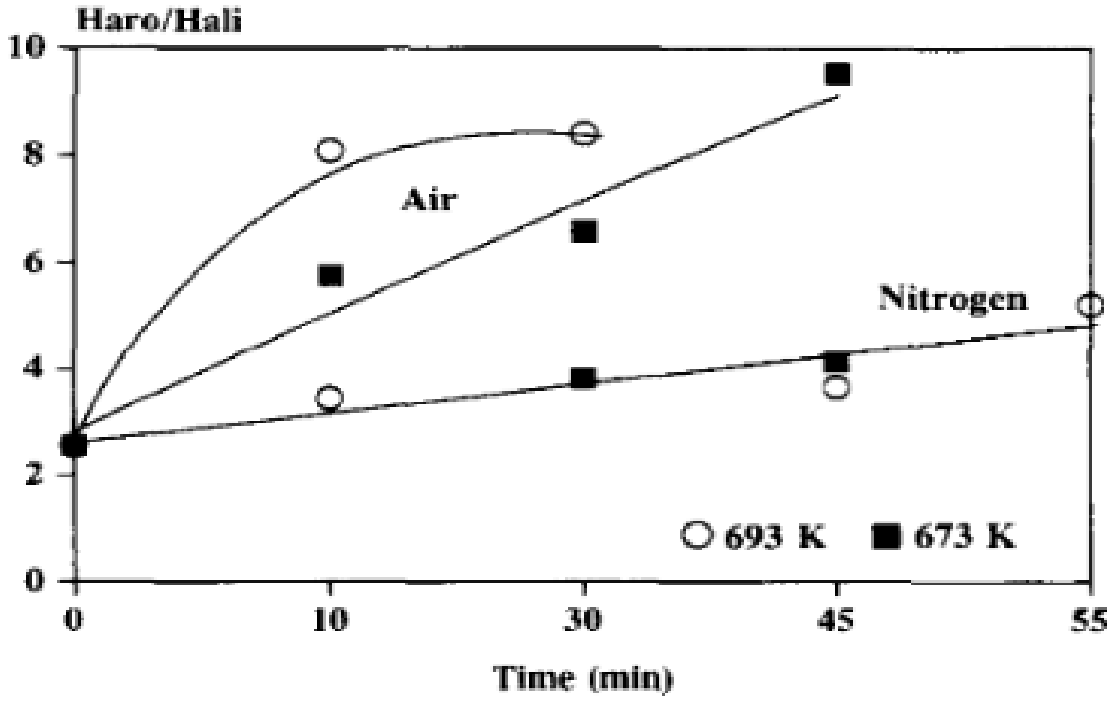

Figure 2.3: H_{aro}/H_{ali} (aromatic-aliphatic hydrogen) ratio for coal tar pitch samples treated in air and nitrogen at different temperatures for different periods (Alcañiz-Monge *et al*., 1997)

In an investigation by Prauchner *et al*. (2003), it was reported that the loss of alkoxyl carbons occurred during the modification of pitch at temperatures lower than 300°C. In addition, at temperatures around 200°C, the O-C_{aliph} bond breaks in the CTP, resulting in the formation of heterolytic-hydrolytic cleavages (hydrolysis), which is important in the breakdown of hydrocarbons to form radicals. These results are favoured by the formation of phenoxy-like anions stabilised by negative charge delocalisation along the aromatic ring (Prauchner *et al*., 2003). Modification can produce an appropriate and suitable pitch for a certain application. According to Oh *et al*. (1991), isotropic raw pitch can be modified to produce quality

mesophase pitch with high anisotropy liquid crystallinity, spherule nucleation and coalescence, as well as mosaic form mesophase pitch. Figure 2.4 depicts the micrographs obtained from the modified pitch by Liu *et al*. (2014). Figure 2.4(a) and (b) have typical anisotropic mesophase spherules, with Figure 2.4(b) having more spherules due to the increased cinnamaldehyde additive content in the pitch during pretreatment process. Additionally, Figure 2.4(c) to (e) shows the merged spherules and flow domains. This is probably due to the reaction between cinnamaldehyde and small pitch molecules, which enhances the degree of pitch polymerisation.

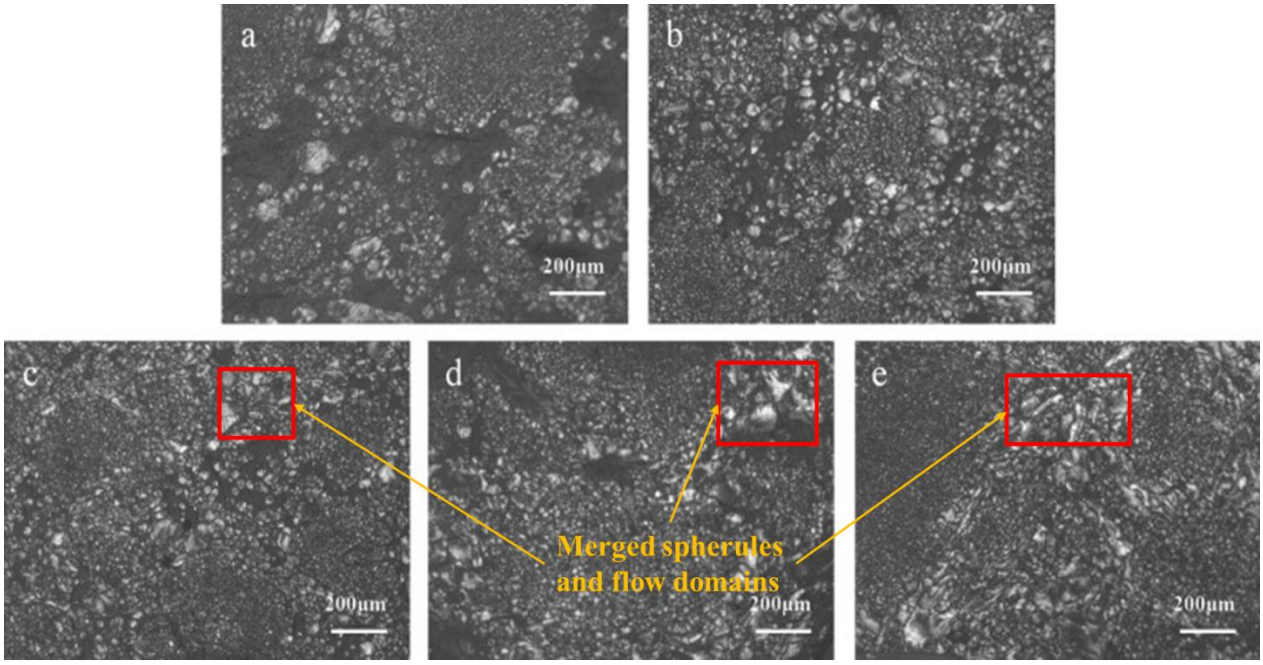

Figure 2.4: Optical results of the modified coal tar pitch showing mesophase spherules and flow domains: (a) CTP1, (b) CTP2, (c) CTP3, (d) CTP4 and (e) CTP5 (Liu *et al*., 2014). CTP1 to CTP5: resulted coal tar pitch from the additive of 0 wt%, 3 wt%, 7 wt%, 10 wt% and 13 wt% cinnamaldehyde, respectively

2.5.1 Structure of coal tar pitch

Pitch is derived from the distillation of tar at relatively low temperatures (400°C) (Savage, 2016). The two different types of CTP are isotropic and anisotropic. They are used to make low- and high-modulus carbonaceous materials, respectively (Fitzer *et al*., 1987). CTP is constituted by the system in which the aromatic units (oligo-aryls) are attached by C-C single bonds. Phenols and aromatic amines also occur in pitch but at relatively low concentrations. The structure of CTP is comprised of benzologues of pyrrole, furan, thiophene, and cyclohexane polycyclic aromatic hydrocarbons with few aliphatic chains and heteroatoms (Figure 2.5) (Yang *et al*., 2022). However, other chemicals may exist despite their low concentrations (Zander, 1987).

With advancements in technology and the requirement for various carbon materials, CTP is now used in various industries. This is possible because of its more dominant aromatic nature than petroleum pitch (Fan *et al*., 2017; Das Lala *et al*., 2018; Yang *et al*., 2022). It is less soluble in solution than petroleum pitches and contains hydrophobic polycyclic aromatic hydrocarbons compared to other forms of pitches (Kershaw and Black, 1993; Yang *et al*., 2022). According to Alcañiz-Monge *et al*. (2001), aromatic hydrogen is assigned to an aromatic ring with a low degree of substitution in the CTP structure. While in the petroleum pitch, aromatic hydrogen is bound to the aromatic ring with a high degree of substitution. The structure and aromatic content of CTP are important parameters to consider when selecting CTP for a variety of applications (Fan *et al*., 2017; Yang *et al*., 2022). To analyse the chemical and structural properties of coal tar or pitch, techniques such as FTIR spectroscopy, nuclear magnetic resonance, and X-ray diffraction (XRD) are employed. CTP samples that have been modified from the same parent pitch but under different conditions often contain the same functional groups but differ in transmittance/absorbance intensities. Figure 2.6 shows the common structure of CTP samples, which were modified at different temperatures in the experiment carried out by Chen *et al*. (2018).

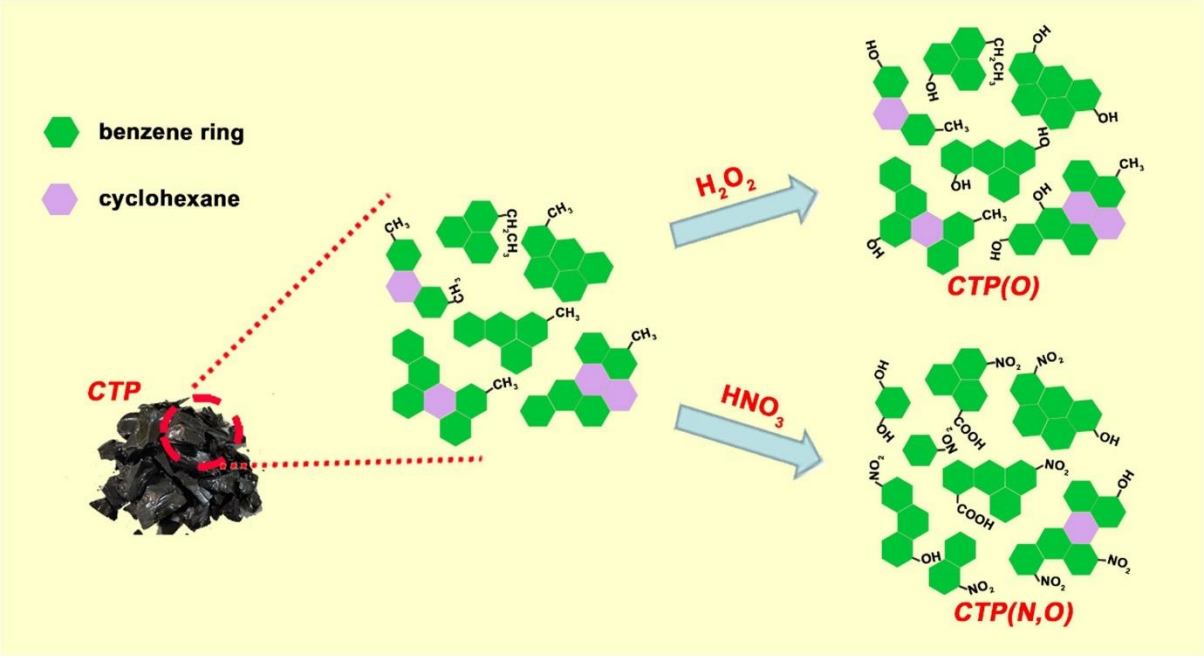

Figure 2.5: Schematic diagram for coal tar chemical structure (Yang *et al*., 2022)

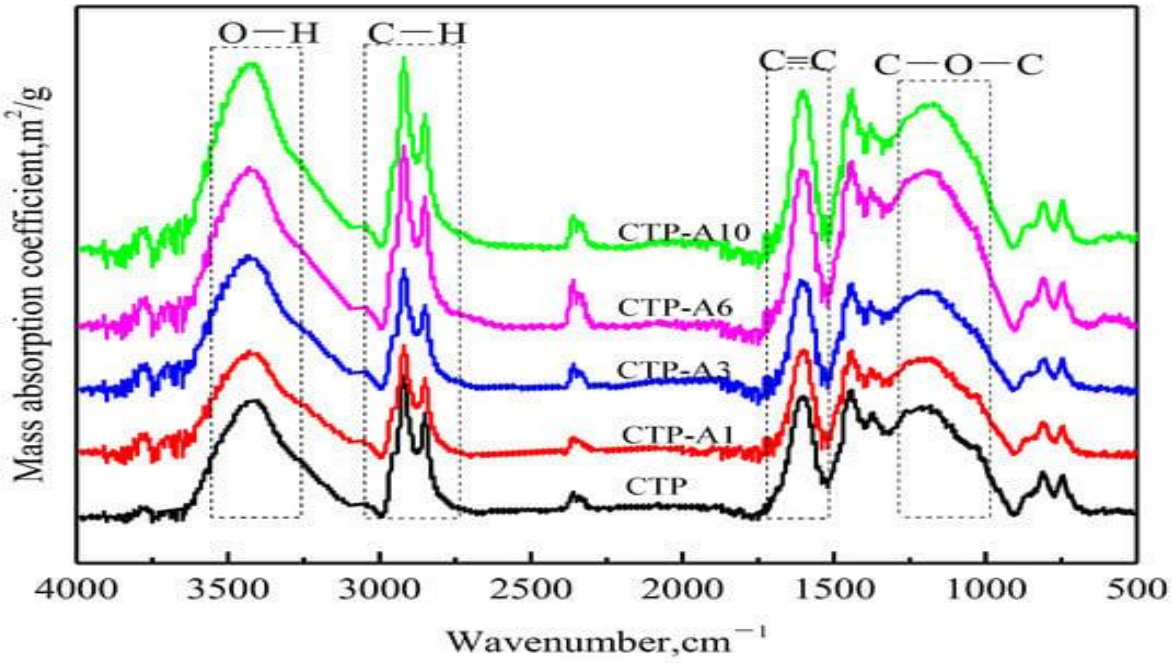

Figure 2.6: Fourier transform infrared analysis of coal tar pitch (Chen *et al*., 2018)

2.5.1.1 Mesophase pitch

Raw pitch is generally isotropic, but when heat-treated, it develops anisotropic liquid crystal phases called "mesophase". Mesophase is a complex mixture of many aromatic hydrocarbons that contains anisotropic liquid crystalline particles (carbonaceous mesophase) when observed under an optical microscope (Soni *et al*., 2013). These liquid crystals represent a state of matter defined by a combination of order and mobility (Tschierske, 2002). The removal of volatile matter led to the formation of mesophase pitch. This is accomplished by modifying parameters such as heat treatment, soaking time, heating rate, and a variety of others. Lamellar molecules are formed during heat treatment of isotropic pitch at temperatures ranging from 350 to 500°C in an inert atmosphere. This leads to the formation of nematic discotic liquid crystals. As a result of these developments, a liquid crystal system (mesophase) is formed, which is the final carbon structure that controls its flowability (Soni *et al*., 2013). Furthermore, Soni *et al*. (2013) found that the nucleation of spheres followed by the coalescence of spheres and mosaic formation is the structure that leads to the formation of mesophase spheres. Mesophase pitch has a high stabilisation reactivity and a highly oriented structure, as well as low viscosity and high purity (Mochida *et al*., 1990). These characteristics are required for the pitch used as a binder in the manufacture of high-performance carbon composites. The aromatic planes of the mesophase pitch are composed of alkyl and bulk mesophase in an isotropic matrix of coal and coal tar naphthenic groups. Furthermore, pitch heat treatment under polarised light favours these groups in terms of micro-solubility and fusibility (Mochida *et al*., 2000).

Mesophase pitches are used in a variety of applications, such as meso-carbon microbeads, carbon spheres, binder, and anode materials for lithium-ion batteries, due to their purity and high aromaticity (Soni *et al*., 2013). It does produce materials appropriate for high-performance applications due to its high degree of graphitisation after carbonisation. As Zhai *et al*. (2019) reported, producing composites from mesophase pitch enhances the mechanical properties of the composites and the material's chemical resistance. Soni *et al*. (2013) conducted a pretreatment study on pitch in an inert atmosphere at temperatures between 350°C and 500°C. The results (Table 2.2) show that the mesophase content increases with temperature. The temperature affects properties such as quinoline and toluene insolubility, coking value, softening point, weight loss, C/H ratio, and sulphur and mesophase content of the pitches (Table 2.2). Pretreatment at low temperature inhibits mesophase production, but an isotropic pitch with exceptional characteristics is produced. In cases where mesophase was not produced during pretreatment of the pitch, adding polymer additives to the pitch may improve the formation of mesophase pitch (Bardají Luna and Coco Cea, 2022).

Table 2.2: Properties of modified pitch (Soni *et al*., 2013)

Samples	**QI (%)**	**TI (%)**	**CVC (%)**	**Mesophase content (%)**	**Softening point (°C)**	**Weight loss by TGA up to 900°C (%)**	**C/H ratio**	**Sulphur (%)**
PP	0.9	14	43	0	88	72	1.71	0.66
MP_a	6	33	55	4	118	58	1.91	0.59
MP_b	43	55	60	24	125	42	2.44	0.56
MP_c	67	70	79	52	279	32	2.70	0.52
MP_d	83	86	91	90	>350	17	3.03	0.47

C/H: carbon/hydrogen; CVC: coking value; MP_a: mesophase pitch (350°C); MP_b: mesophase pitch (400°C); MP_c: mesophase pitch (450°C); MP_d: mesophase pitch (500°C); PP: precursor pitch; QI: quinoline insoluble; TI: toluene insoluble; TGA: thermogravimetric analysis

2.5.1.2 Isotropic pitch

Isotropic pitch is routinely produced at low temperatures using the same method as mesophase pitch (Yuan *et al*., 2020). It can also be obtained by filtering it out of an incomplete mesophase pitch. Isotropic pitches are used in the manufacturing process of general-purpose fibres

(Bermudez *et al*., 2018). However, mesophase pitches are used for applications requiring high strength and thermal stability because of their molecular orientation (Arai, 2016; Choi *et al*., 2019; Daulbayev *et al*., 2021). The sole difference between these two pitches is their chemical structure. According to Maeda *et al*. (1993), isotropic pitch is produced along with the mesophase pitch during the modification process of coal tar. The proportion of each phase in the mixture depends on the pretreatment temperature at which the tar is exposed. Even though isotropic pitches, like mesophase pitches, can be made from various precursors, such as naphtha split oil, anthracene oil, or CTP, the pitches had to be separated, making it possible for the pitches to be used for various high-value applications.

According to Mora *et al*. (2003), one of the methods for separating mesophase from the isotropic phase is through hot filtration, but they also indicate that the two phases may contaminate each other. Another proven process is solvent extraction (Poot and Everson, 1999). With solvent extraction, the mixture of pitch and solvents, such as quinoline, toluene, and pyridine, are heated prior to separation. This led to the isotropic pitch being dissolved while the mesophase pitch remained insoluble. The macromolecular structure and higher C/H ratio of the mesophase prevent it from dissolving in the solution, and it is recovered as a filter cake (residue) (Banerjee *et al*., 2021).

The thermal treatment of both isotropic and mesophase pitches through carbonisation or pyrolysis influences the final product. In an isotropic pitch, mosaic structures are produced through carbonisation, whereas pyrolysis produces morphological forms that change depending on the pyrolysis conditions. Changes in pyrolysis temperature have a significant influence on composite structure, with small aromatic structures clustering up to 400°C. At this temperature, crystalline properties, tensile strength, and modulus increase due to the removal of C=O functional groups. At 400 to 800°C, gases evolve, and the C-O-C, O-C-O, and O-H bonds are removed, resulting in a 2D carbon structure. Figure 2.7 shows the relationship between the tensile strength of isotropic and mesophase pitch-based structures at different pyrolysis temperatures. This temperature-induced structural change provides information on the optimal carbonisation temperature that would give acceptable characteristics for a desired product (Peng *et al*., 2020; Daulbayev *et al*., 2021). It is evident from the plot that pyrolysis must occur between 800 and 1200°C for isotropic pitch-based materials but at substantially higher temperatures for mesophase pitch-based materials, which may become graphitised (Banerjee *et al*., 2021).

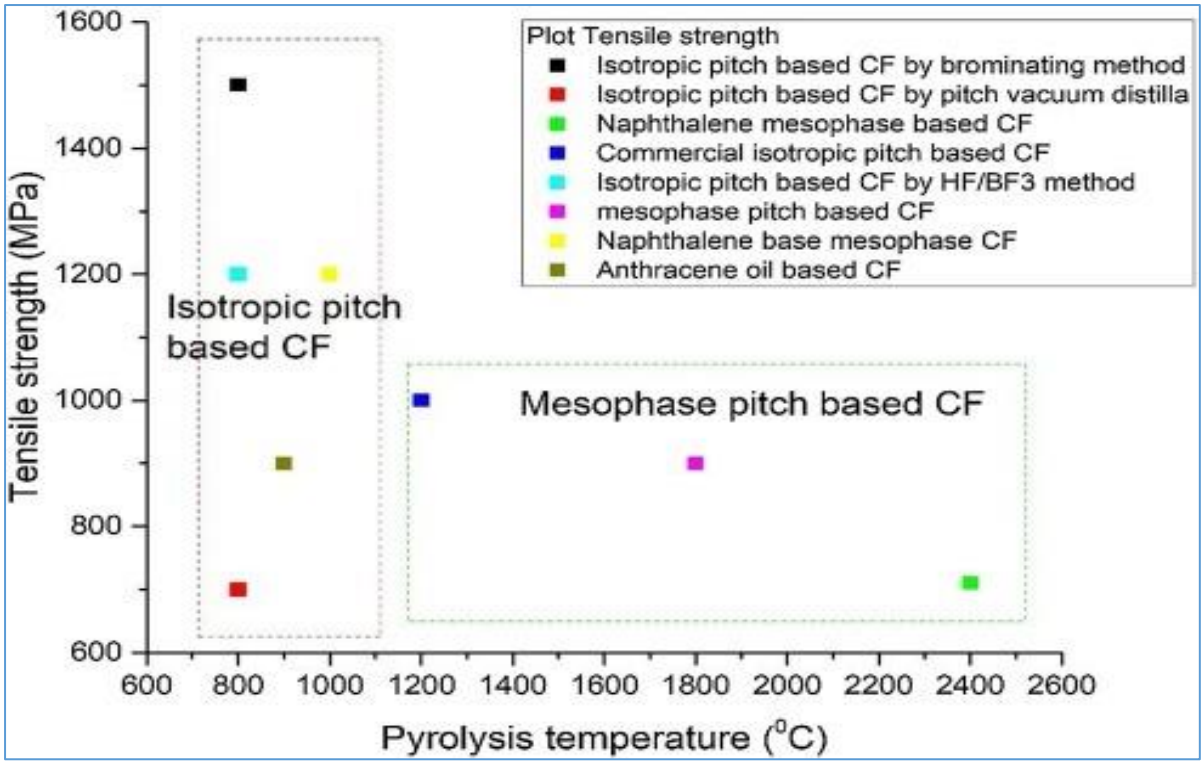

Figure 2.7: The tensile strength of isotropic and mesophase pitch-based fibres (CF) at different pyrolysis temperatures (Banerjee *et al*., 2021)

2.5.1.3 Rheological properties of coal tar pitches

The rheological properties of CTP, such as yield stress, relaxing time, viscosity, and compliance, are important in identifying the CTP's non-Newtonian behaviour. The rheological behaviour of CTPs reported by Fitzer *et al*. (1987) demonstrates that various anisotropic spheres are formed by heating CTP under various conditions, leading to nucleating an isotropic phase, growth, coalesce, and forming a material that is still plastic (bulk mesophase pitch) (Otani *et al*., 1970; Fitzer *et al*., 1987). According to Collet and Rand (1978), the degree of coalescence in heat-treated pitch can be large at 450°C, leading to the interconnected mesophasic microstructure network. The mesophase, therefore, evolved into a continuous phase in which isotropic liquid pockets were dispersed (George *et al*., 1977).

The rheological behaviour of CTP demonstrates that the solidification of pitch is affected by factors such as heat treatment, mean molecular weight, molecular weight distribution, and aromatic and heteroatomic content. In general, the melting behaviour of pitch is related to the solidification of pitch, which means that pitch that melts at low temperatures solidifies at high temperatures (Otani *et al*., 1970).

2.6 Different types of composites

Composites are categorised depending on the type of reinforcement and matrix phases used in their production. Matrix composites are classified into three categories: polymeric, ceramic, and metal (Swain, 2014; Rajak *et al*., 2019; Hunt, 2000; Hsissou *et al*., 2021). These composites can be reinforced in various ways, including fibre, particle, and sheet reinforcement (De Araújo, 2011). Fibre-reinforced composite materials offer better material qualities, such as high strength, stiffness, and resistance to chemicals, wears, and high temperatures. This is because they are composed of a dispersed phase of synthetic fibres such as glass, carbon, basalt, and Kevlar in a composite structure (Husić *et al*., 2005; De Araújo, 2011). Particle-reinforced composites have a lower strength-to-weight ratio and are often utilised in wear-resistant applications such as road surfaces (Gopalakrishnan and Murugan, 2012). For example, using gravel as a reinforcing filler ingredient in cement greatly enhances its hardness. The key advantages of particle-reinforced composites are their low cost and simplicity of manufacture and shaping (Gan *et al*., 2010; Gopalakrishnan and Murugan, 2012). Sheet-based composites, commonly known as sheet moulding composites, are thermoset-moulding materials with glass reinforcement that are typically compression moulded. In contrast, sheet-based composites use long glass fibre with unsaturated resins to produce a high-strength moulding composite. Due to their excellent strength-to-weight ratio, sheet moulding composites are appropriate for large structural components.

Nanocomposites are another class of composites, but they are produced by mixing two or more components on a nanoscale to obtain the required material characteristics (Hafeez, 2022). In general, nanocomposites are characterised as unintercalated, intercalated or exfoliated and are produced by template synthesis, polymer intercalation, in situ polymerisation, or melt compounding (Thakur *et al*., 2022). Biomedical nanocomposites are designed for biomedical purposes such as dental treatments, bone tissue engineering, cancer medication delivery, and dressings (Sharma *et al*., 2021). Biocomposites reinforced with sugar palm fibres in a sago starch matrix enhance thermal stability, minimise water absorption, and increase tensile and tearing strength and material durability. Nanoscale bionanocomposites have shown promise in a range of applications, including tissue engineering scaffolds and biopackaging. The antibacterial property of ginger fibre has been used effectively in biocomposites to maintain food packaging quality. Figure 2.8 depicts the categorisation of composites, and the following section discusses some of the fibre reinforcement materials and matrix materials.

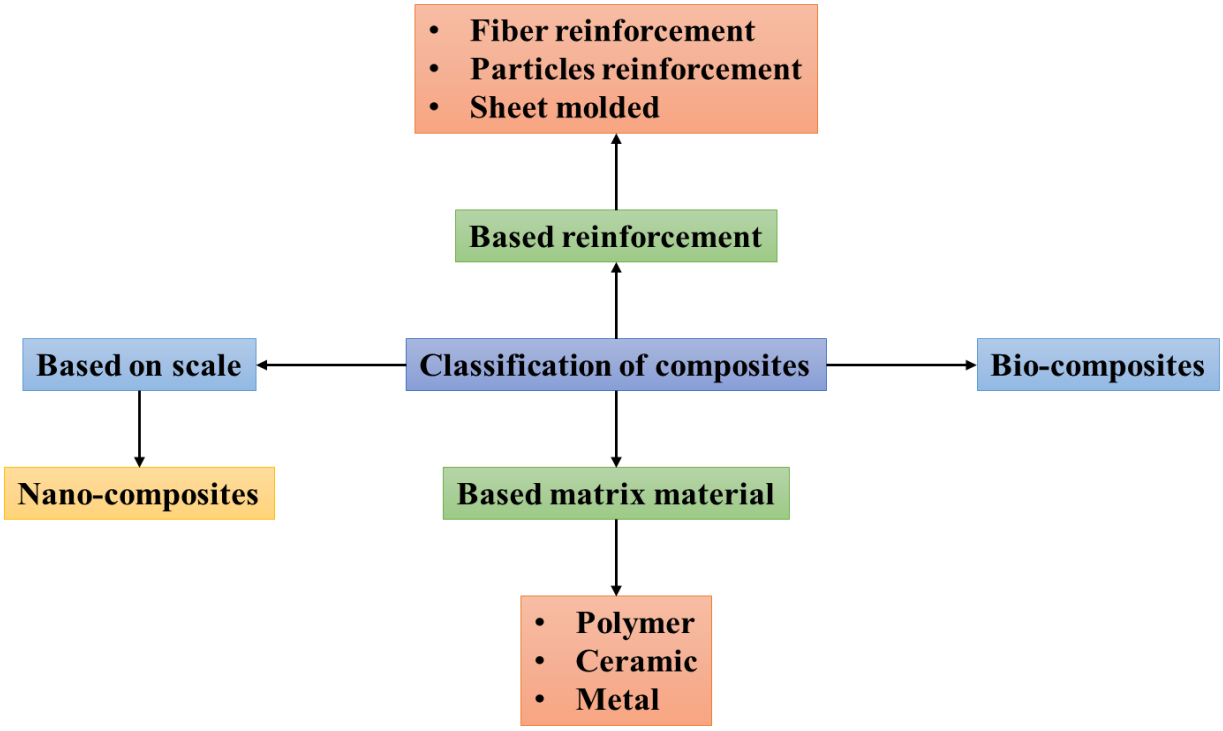

Figure 2.8: The overview of the composite's classification (Rajak *et al*., 2019)

2.6.1 Reinforcement materials

Reinforcement materials are always stiffer, tougher, and harder, while matrix materials are used to optimise the composites' qualities. The composites reinforcement phase is important because it provides the composites with the necessary characteristics to withstand heavy applied loads (Rajak *et al*., 2019). Coal has been used as a filler material in the manufacturing of polymeric composites that outperform polymers in terms of physicochemical qualities (Eterigho-Ikelegbe *et al*., 2021b). The use of coal to produce composites is environmentally friendly since it emits no carbon dioxide or other pollutants into the atmosphere. Coal has been identified as a suitable filler because of its inherent antifungal properties and lower water absorption. Furthermore, by-products of coal like fly ash and cenospheres have been investigated as thermoplastic composite fillers, yielding composites with unique properties. The fly ash composites are environmentally benign, lightweight, and have minimal water absorption. As a result, the use of coal as a filler in composites eliminates the need for additional additives to minimise water absorption and flammability. Additionally, the use of coal in this sector may raise coal demand and identify new coal applications, thus growing the coal market (Phillips *et al*., 2017).

2.6.2 Metal matrix composites

The main function of the matrix is to keep the reinforcements together so that the force applied can be passed to the reinforcement. Other functions of the matrix include protecting and preventing composite fibre damage, such as fracture propagation within the material (Muangwaeng *et al*., 2013). Metal matrix composites are made up of metal matrices such as aluminium, zinc, copper, titanium, and carbide. The reinforcement may include ceramics and carbides or metallic reinforcement such as tungsten or molybdenum. For these types of composites, reinforcement accounts for at least half of the total composite weight (Hunt, 2000). Aluminium is used as a matrix because of its low weight and ductility. Aluminium is usually reinforced with silicon carbide because alumina binds easily with it and increases its qualities, including strength, stiffness, density, and thermal expansion. Aluminium-based composites are well suited for the automobile industry due to these properties (Mallick, 2012). Metal matrix composites, on the other hand, have considerable drawbacks because of their exceptionally high stiffness and abrasive structure, resulting in a high wear rate during machining (Haghshenas, 2016).

2.6.3 Ceramic composites

Ceramic composite materials have been used for thousands of years in the construction industry due to their durability, fire resistant, thermal insulation, and chemical resistance (Singh *et al*., 2018; Santa *et al*., 2023). Building components, such as roof tiles, bricks, floor tiles, pipes, and cladding, are produced from ceramic composite (Kumar *et al*., 2019; Zhang *et al*., 2019). Some of the various ceramic materials that are used for construction include silicon carbide, alumina, and zirconia (Li *et al*., 2012; Wang *et al*., 2019). In the construction industry, a coal-based ceramic composite can be created by blending coal with matrices like alumina, silica, and zirconia. According to Kwon *et al*. (2005), coal mixed with alumina and silica matrices can produce a composite with high thermal conductivity and minimal thermal expansion. The authors also reported using fly ash to produce ceramic building components with composites with excellent mechanical properties. The advantages of these coal-based composites are that coal and its ash are cheap and abundant (Kim *et al*., 2004; Wang *et al*., 2013; Xie *et al*., 2014; Roychowdhury *et al*., 2015).

Furthermore, Eterigho-Ikelegbe *et al*. (2022) compared coal-based composites and concrete-based materials for the building industry. Both materials were subjected to different chemical conditions to assess their degradation in a harsh chemical atmosphere. According to the authors, coal-based composites have superior chemical resistance compared to conventional

feedstock materials for building materials. In another study, Yahya *et al*. (2019) investigated the influence of coal mixed with polyethylene to form coal plastic composites for construction materials. They reported that increasing the coal composition in the mix resulted in an increase in the coal plastic composites' flexural strength, which means coal enhances the mechanical properties of the ceramic composites. In the same study, the burning rate of coal plastic composites was examined, and it was reported that the rate of burning decreased when the coal content was increased. The findings on coal-based ceramic composites are opening the way for coal to continue being used to manufacture ceramic composites with excellent mechanical properties for a wide range of applications. As a result, the current study utilised coal wastes (coal fines and CTP) to produce ceramic composite materials that could be utilised in building applications.

2.6.4 Polymer matrix composites

Polymeric composites are made of thermosetting plastic or thermoset matrix and carbon reinforcement (Rajak *et al*., 2019). Polyester resin, vinyl ester resin, epoxy resin, polyethylene imine/polyphenylene sulphide, and polyamide are the polymer matrix types utilised to produce polymer composites. Thermosets are commonly used in the preparation of composite materials because of their high thermal resistance. The role of thermosets in the manufacture of polymer composites is critical because they absorb moisture through plasticisation and swelling. Plasticisation causes plastic deformation and swelling due to differential stresses caused by the expansion forces applied by the liquid during stretching of the polymeric chain. Polymeric composites are affordable due to their ease of fabrication (Rajak *et al*., 2019).

The lower price of fibre-reinforced polymer composites has led to their use in the construction industry as a substitute for steel in reinforced concrete constructions (Pendhari *et al*., 2008; Bartolomei and Wiebeck, 2019). The cohesion and direction of the load in the composite are guaranteed by the matrix of the composite material. The continuous and discontinuous phases that make up the composite are referred to as the matrix and the reinforcement, respectively. Compared to metal composites, composites made using polymer matrix may be moulded into intricate forms. High-performance composites are often constructed from epoxy resin with long fibres of glass, carbon or aramid for reinforcing. The aerospace and space industries often employ this type of composite due to its high performance (Hsissou *et al*., 2021). Table 2.3 shows different matrices that are normally used to manufacture polymer composites.

Table 2.3: Different matrices used to manufacture polymer composites (Hsissou *et al*., 2021)

Types of polymer matrices	
Thermosetting	**Thermoplastic**
Polyamides	Polypropylene
Polycarbonates	Polyoxymethylene
Polyesters	Polyesters
Phenolic	Polyether sulfone
Polyimides	Polyether ether
Silicones	Polyether ketone
Polyurethanes	Polyether ether ketone
Polyepoxides	Polyether imide

2.6.5 Carbon-carbon composites

There are currently three methods for manufacturing C-C composites: chemical vapour deposition, pyrolysis of thermoset and thermoplastic resins, and pyrolysis of hydrocarbon pitches generated from petroleum, coal tar, and synthetic mesophase products (Abali *et al*., 2003). These processes include the treatment of carbon materials during their fabrication and thus influence the mechanical properties of the finished product. C-C composites come in a variety of forms, including resin-impregnated C-C composites. These types of composites are made by impregnating carbon fibres with a matrix resin (Jayaseelan *et al*., 2013). There are also pitch-based C-C composites made from carbon fibres and a CTP matrix. These composites are commonly used in high-temperature applications, including furnace lining and power generation heat exchangers (Hegde *et al*., 2013; Chen *et al.*, 2017; Liu *et al*., 2019). C-C composites have also seen widespread usage in aircraft applications, such as rocket nozzles, braking disks, and missile guidance systems (Jayaseelan *et al*., 2012; Krenkel, 2018). Another way of making C-C composites is through chemical vapour infiltration. This involves the deposition of carbon atoms in a carbon fibre matrix followed by chemical vapour infiltration. These composites are used in the aerospace industry in a similar manner as other C-C composites (Krenkel, 2018). In addition, coal waste can be reinforced with CTP to produce C-C composites. This method involves grinding coal waste to fine particle sizes and mixing it with CTP, followed by pyrolysis or carbonisation. With this approach, composites with

excellent mechanical properties, high strength, stiffness, and thermal conductivity suitable for the construction industry can be produced (Hegde *et al*., 2013; Zhang *et al*., 2015).

Pyrolysis is one of the important steps in carbon composite manufacturing, as well as the carbonisation process. Pyrolysis involves heating green moulded bodies lead to a compacted and lightweight composite material (Banerjee *et al*., 2021). The final product's attributes are governed by the pyrolysis parameters (time and temperature). The challenge with this approach is that at high temperatures (900-1200°C), nitrogen and sulphur-containing components are liberated from the material, disrupting the ordered structure by forming pores in the material matrix. This temperature window is not suitable for producing composites with low porosity, such as those used in construction materials, but it is suitable for producing carbon fibres and carbon hollow spheres (materials with high porosity). Figure 2.9 shows the pyrolysis behaviour of carbon compounds at different temperatures and the type of structure that could be formed by changing the pyrolysis temperature.

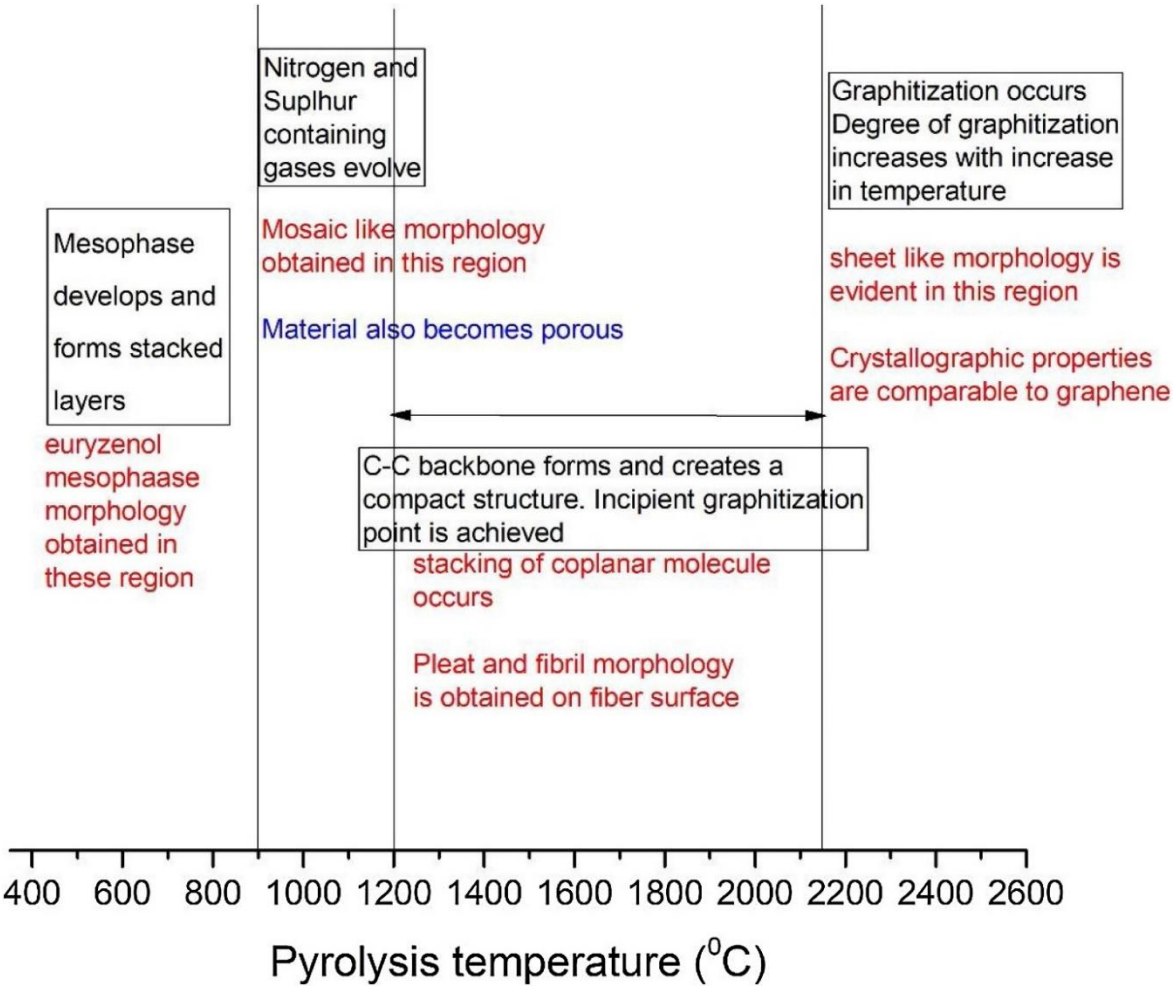

Figure 2.9: The behaviour of carbon material at different pyrolysis temperatures (Banerjee *et al*., 2021)

2.6.5.1 Thermal stability of carbon composites

It is vital to determine the thermal stability of carbon composites at the time of production. From the thermal stability test of the composite, information on the mass loss with respect to the degradation temperature of the composite can be achieved. An investigation of the thermal, physical, and chemical properties of carbon composites produced from CTP (CPCC), petroleum pitch (PPCC), and a CPCC and PPCC mixture (MXCC) was conducted by Sharma *et al*. (2020). Thermogravimetric analysis (TGA) and thermomechanical analysis were used to investigate weight loss relative to temperature for all composites produced. Figure 2.10 shows that the CPCC had the best stable thermal behaviour. This is due to the higher aromatic content of the CTP compared to petroleum pitch, which is more aliphatic. The radicals produced by the breakdown of short-chain hydrocarbons cause weight loss (Liu *et al*., 2014). The three samples (CPCC, MXCC, and PPCC) were also flame ablated in the same experiment, and the CPCC showed fewer microstructure changes than the other samples, suggesting that CTP composites had great thermal stability (Sharma *et al*., 2020). In addition, the influence of the pitch's chemical composition on the properties of the C-C composites produced was investigated. Table 2.4 shows that the density of the CPCC is higher than the other two composites. More so, the mechanical properties of the CTP composite are much higher than those of the petroleum pitch and their mixture.

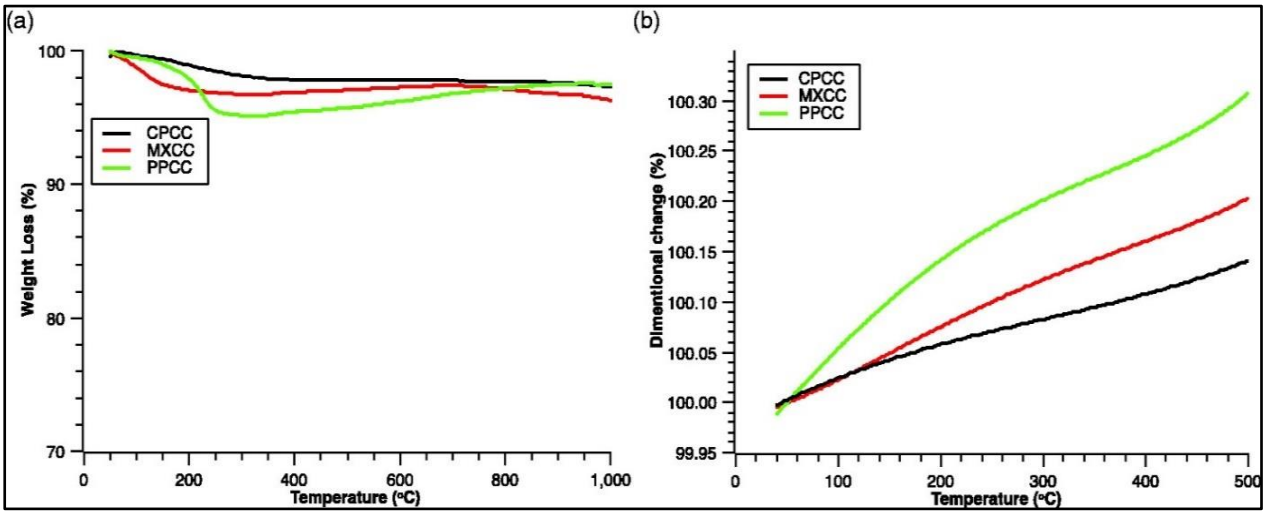

Figure 2.10: (a) Thermogravimetric analysis and (b) thermomechanical analysis plot of various composite samples. CPCC: coal tar pitch carbon composite; MXCC: CPCC and PPCC mixture; PPCC: petroleum pitch carbon composite (Sharma *et al*., 2020)

Table 2.4: Various properties of carbon composites (Sharma *et al*., 2020)

Sample code	Density (g/cm^3)	Porosity (%)	Hardness (HRC)	Impact energy (J/cm^2)	Compressive strength (MPa)
CPCC	1.72	7.6	71	36.14	138.42
MXCC	1.68	8.0	68	31.02	129.67
PPCC	1.66	8.1	62	27.76	122.98

CPCC: coal tar pitch carbon composite; MXCC: CPCC and PPCC mixture; PPCC: petroleum pitch carbon composite

In another study, Huang *et al*. (2022) used mesophase pitch as a binder and boron-phenolic resin as a precursor to produce mesophase pitch boron-phenolic resin composites. The composites were examined for thermal stability using thermogravimetric analysis in a nitrogen atmosphere. The results show that increasing the mesophase pitch content from 5% to 20% by weight decreased the weight loss from 25.85% to 24.96%, demonstrating that mesophase content impacts the thermal stability of the composites (Huang *et al*., 2022). The high aromatic content of the mesophase pitch increases the residual mass as the mesophase pitch content increases (Liu *et al*., 2014).

2.6.5.2 Advantages of C-C composites

The C-C materials have some drawbacks, such as brittleness and low fracture strength. Despite these drawbacks, C-C composites are nonetheless attractive. This is because they have a high fracture toughness value and less matrix failure strain than that of the fibre. The main properties of C-C composites include low density, low thermal conductivity and shock resistance, low thermal expansion, and high modulus. Compared to traditional graphite, C-C composites have superior mechanical properties and can maintain structural integrity at temperatures beyond 1000°C. Under interlamellar shearing, 3-D C-C composites can survive damage, and with little delamination crack development. With reference to failure, these composites do not disintegrate catastrophically but go through gradual failure that is described as "graceful failure"(Chawla, 2012).

In terms of sustainability, C-C composites are highly recyclable relative to other materials (Windhorst and Blount, 1997). When used at high temperatures, CTP has a minimal reactivity with air and CO_2 (Lu *et al*., 2020). When heated at extremely high temperatures, composite

materials created from coal tar may form a carbon sheet and graphite (Daulbayev *et al*., 2021). Pitch-based compounds are less costly to manufacture than other precursors. Figure 2.11 shows that the mechanical strength of C-C composites increases with increasing temperature as opposed to metals and ceramics, which decrease with increasing temperature (Manocha, 2003). Other advantages of C-C composites include chemical resistance, outstanding high-temperature properties, biocompatibility, shape stability, and pseudo-plastic fracture behaviour. In contrast to metals and other homogenous materials, C-C composites are anisotropic, which means they may be designed with high directional properties (Abali *et al*., 2003).

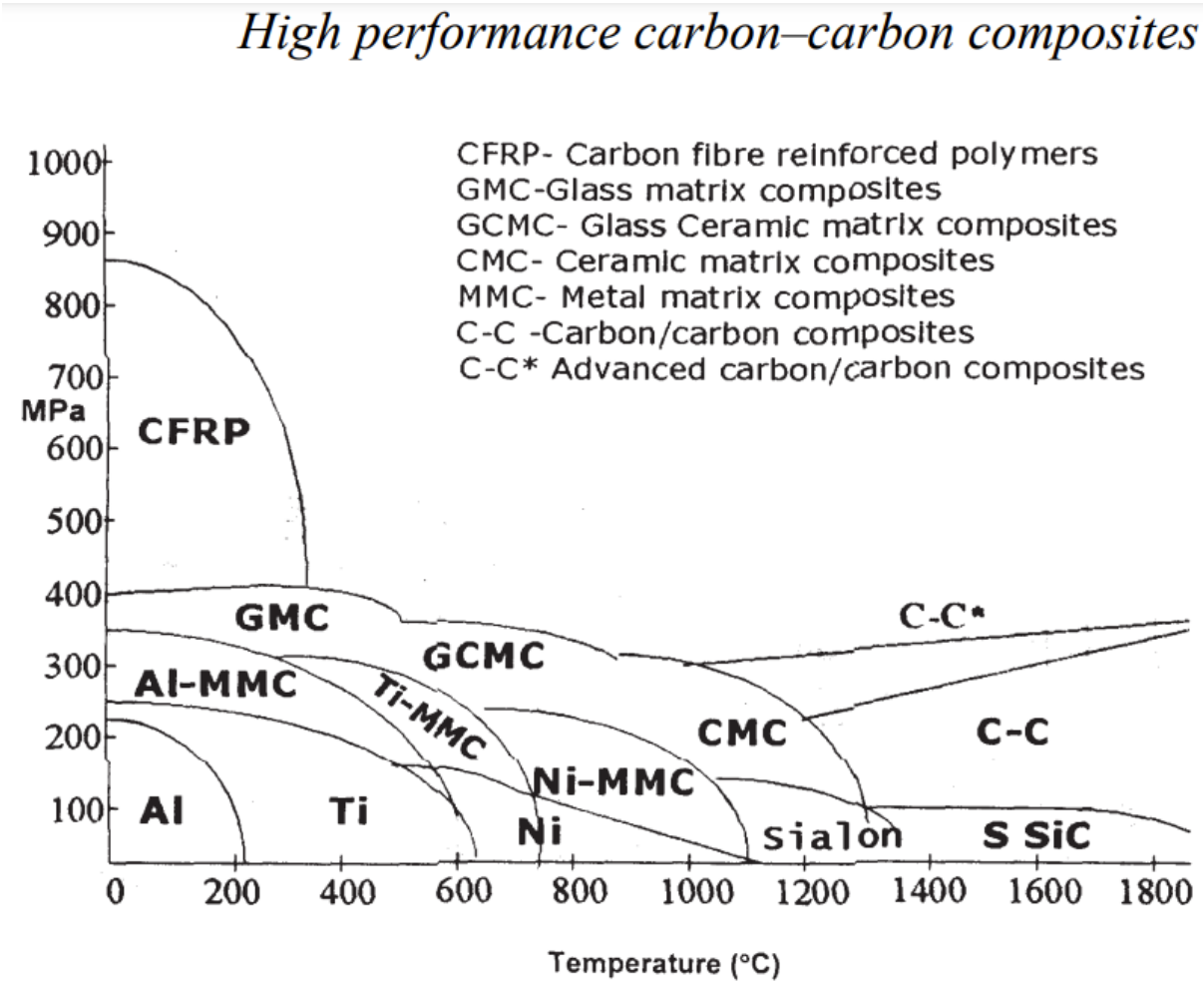

Figure 2.11: The variation of mechanical strength of different engineering materials at different temperatures (Manocha, 2003)

2.6.6 Carbon/coal-based composites for building applications

The use of coal as a carbon-based material for building applications is not as widely used as fly ash. A few studies are available in the literature. In a study conducted by Jiang et al. (2019) pyrolysed char from coal was used to produce insulated low thermal conductivity building

bricks with low bulk density. As half of the energy consumed by buildings is lost into the building envelopes, the use of building materials with low thermal conductivity to minimize energy consumption is paramount (Sutcu & Akkurt, 2009; Cha *et al*., 2011). According to Yu et al. (2023) coal char-based bricks were found to exhibit a high compressive strength (49.2-52.5 MPa). This surpasses that of normal clay bricks with a compression strength ranging from 10 to 20 MPa (ASTM, 2017). A study in the use of inexpensive pyrolysed hazelnut shells containing 98% carbon incorporated into cement has shown that carbon has a role to play in building applications. According to Restuccia & Ferro (2016), the use of pyrolysed hazelnut shells improved the blending and compression strength of the composite produced. In another study, geopolymer cement was incorporated with graphene oxide (GO) to improve the mechanical properties of geopolymer composites. With the addition of 0.25% pure GO polymers with high strength values of 27.8 and 43.9 MPa after 7 and 28 days of curing was produced, respectively. The polymers also have a strength increase of 79% and 52% when compared to geopolymer matrix with no GO (Shamsol *et al*., 2024).

An investigation into the use of coal ash for brick making was conducted by Vidhya and Kandasamy (2016). According to the author, all the bricks were found to have a water absorption of less than 15%, which is within the IS 3495 code for class 12.5 bricks (Bureau of Indian Standards, 1992). In another investigation, coal-plastic composite (CPC) building materials were made using High-Density Polyethylene (HDPE), bituminous Pittsburgh No. 8 (P8, and sub-bituminous Powder River Basin (PRB) as ingredients. The ultimate tensile strength of the coal-plastic composites decreased with an increase in coal content during the analysis of their tensile strength. The flexural strength of these composites increased to its maximum as the coal content increased (Al-Majali *et al*., 2023). The use of South African discards coals together with the preceramic polymer resin to produce coal composites for building applications was reported by Eterigho-Ikelegbe *et al*. (2021a). The coal composites produced in this study met the sufficient standard for water absorption, flexural, and compressive strength of building materials. Even though there are few literatures on the direct use of coal for building applications, there is evidence that coal can be blended with various binders or matrices to manufacture carbon-based materials suitable for building applications. Therefore, it is crucial to examine the suitability of South African coal fines and modified coal tar pitch to determine if they meet the necessary qualities for these purposes.

2.7 Wettability of binders

The high-temperature binding properties of CTP make it suitable for use in the anode manufacturing industry (Lu *et al*., 2020). Among other things, CTP has great rheological qualities, good interaction with carbon fillers and can penetrate the pores of material, leading to an improved density. The wettability qualities of carbon materials should be considered during the process of producing carbon materials. During the wettability analysis, the surface tension, viscosity, and angle of contact between the binder and filler particles should be considered. Wetting can occur because of the coal and pitch interactions through adhesive and cohesion forces (intermolecular interactions). The contact angle and interaction trend that lead to complete wettability are shown in Equation 2.1 and Figure 2.12 (Lu *et al*., 2020). According to Lu *et al*. (2016), the good wettability of the filler and binder improves these qualities. In addition, decreasing the angle of contact of the binder with the duration of the reaction with other materials increases the wettability. Both pitch and coal have chemical characteristics that contribute to the composite's wettability.

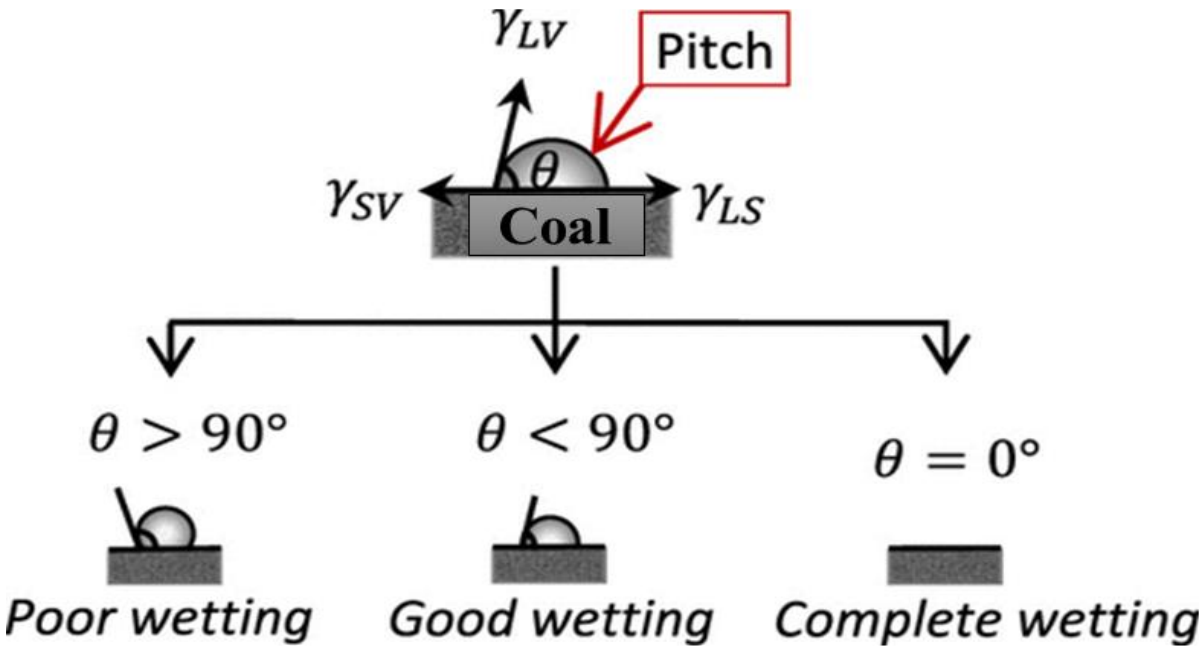

Figure 2.12: Relationship of contact angle and wettability (Lu *et al*., 2020)

$$\gamma_{Lv} Cos\theta = \gamma_{sv} - \gamma_{Ls} \quad (2.1)$$

Where Y_{sv} is the interfacial tension of the solid–vapor interface, γ_{LS} is the interfacial tension of the solid–liquid interface, γ_{LV} is the interfacial tension of the liquid–vapor interface (also known as the surface tension), and θ is the contact angle.

2.8 Summary

The literature reviewed showed that carbon composites can be used to produce high-quality building materials such as bricks, tiles, etc. The carbon-based materials reported in most of the articles reviewed for building applications outperform the normal building materials. The use of different carbon materials to produce carbon composites resulted in materials with high compression, flexural, and tensile strengths greater than 20 MPa, which is normal for conventional building materials. The various carbon composites highlighted showed high chemical resistance, which is attributed to the aromatic nature associated with high carbon materials. The results of coal-based composites also align with those produced from other carbon materials. However, coal composite properties may differ between regions, so it is important to explore the use of South African coal to produce coal composites for building applications.

Chapter 3

Materials and experimental methods

This chapter describes the analytical methods used to determine the physiochemical properties of coal, coal tar, and pitch produced at different temperatures, and the composite produced. The process (air-blowing pretreatment) method used to convert coal tar into pitch at different temperatures is outlined. In addition, the composite fabrication procedure of blending coal with CTP and DMPS binders is presented. Lastly, the chapter presents the procedures for characterising the physical, mechanical, and chemical properties of the composites produced. Figure 3.1 presents the study's process flow diagram to produce coal composites.

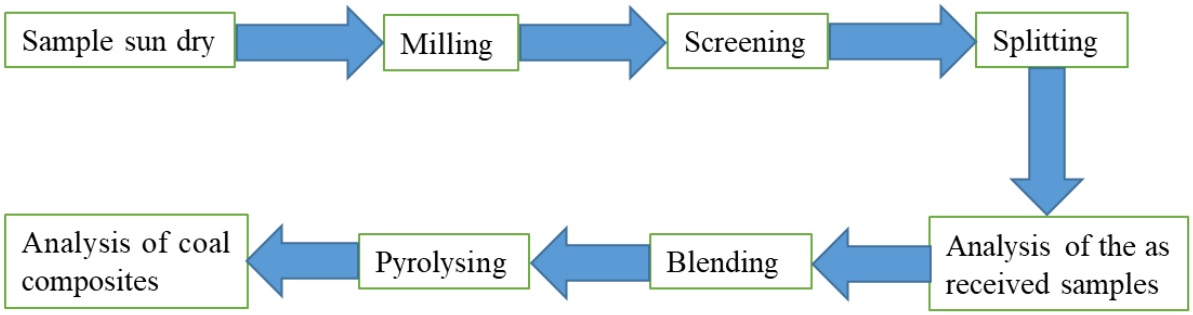

Figure 3.1: Process flow diagram for production of coal composites

3.1 Sample receipt and preparation

The coal samples (GG1 and GS) received were first sun-dried to remove excess moisture. The samples were then subjected to crushing, followed by milling, screening, and splitting using a rotary divider to obtain representative samples at particle sizes of −212 and −53 micrometres (µm). Afterwards, the −212 µm coal samples, along with the coal tar and pitches produced at different temperatures, were analysed, according to Figure 3.2.

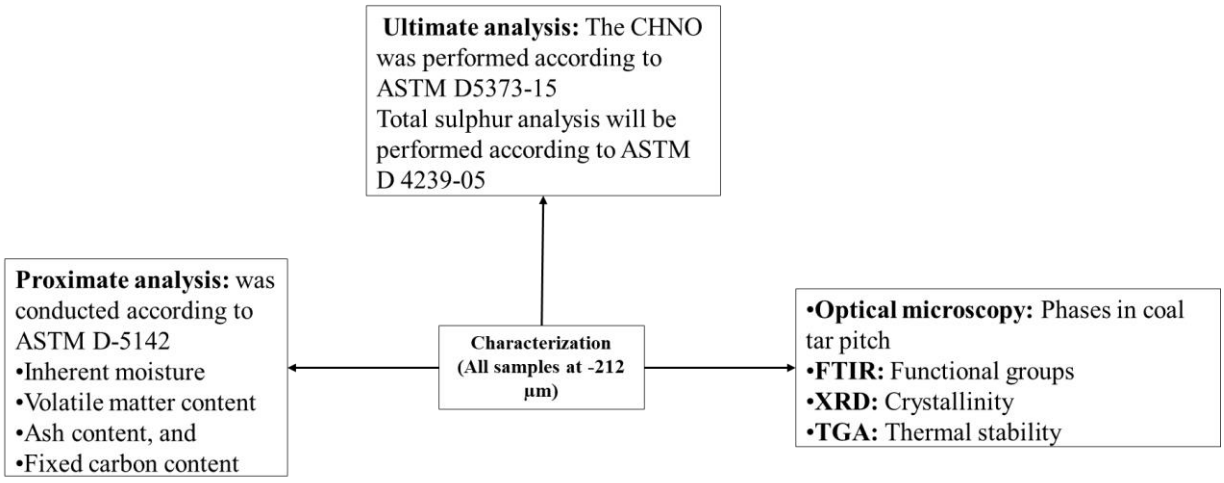

Figure 3.2: Physicochemical analysis techniques

3.2 Analytical methods for the coal and coal tar pitch characterisation

3.2.1 Proximate analysis

The proximate analysis for the coal fines (−212 µm), coal tar, and CTP (−212 µm) was conducted using a Leco thermogravimetric analyser 701 instrument to determine the sample's inherent moisture content, volatile matter, ash content, and fixed carbon content. The method utilised was the American Society for Testing and Materials (ASTM) D-5142, where 1.0 g of sample was placed in a crucible for analysis. The fixed carbon was expressed as the difference between the sum of the other parameters (ash content + inherent moisture content + volatile matter) and 100%.

3.2.2 Ultimate analysis and total sulphur

Ultimate analysis determines the percentage mass fractions of carbon, hydrogen, sulphur, nitrogen, and oxygen in the samples, calculated by difference as in Equation 3.1.

$$O = 100 - (C + H + N + S + A + M) \quad (3.1)$$

Where A and M represent the ash content and inherent moisture content, respectively, C is total carbon, H is hydrogen, S is total sulphur, O is oxygen, and N is nitrogen.

The ultimate analysis of all samples was conducted at the Bureau Veritas Testing and Inspections South Africa (Pty) Ltd. A 0.25 g sample was used, and analysis for carbon, hydrogen and nitrogen was carried out according to the ASTM D 5373-14:2015 using the Leco CHN 628. Total sulphur was determined following ISO 19579: 2006.

3.2.3 X-ray diffraction

The identification of the mineral phases in the samples (coals, coal tar and pitch) was determined using XRD according to the ASTM D 3682-13 method. The analysis was done using a Bruker D2 phaser diffractometer equipped with Cu-Kα radiation, k = 1.54184 Å. This was operated at 50 kV and 23 mA in the 2-theta range of 10 to 90ºC. The outcome provided information on the mineral phases in the coal fines, coal tar, CTP and coal composite samples and the crystallinity of the coal tar before and after air-blowing pretreatment.

3.2.4 FTIR analysis

FTIR spectroscopy (PerkinElmer Spectrum version 10.5.4) equipped with an attenuated total reflectance accessory was used to determine the aromaticity, chemical bond configuration, and functional groups in the coal fines, coal tar, CTP, and coal composites. All samples were scanned using FTIR at the range of 4000 to 400 cm^{-1}.

3.2.5 Petrography optical microscope analysis

All modified CTP samples were characterised using cross-polarised light optical microscopy to determine the growth and content of the bulk liquid crystalline mesophase. The CTP samples were crushed to -1.0 mm with fines included. The particles were put in epoxy resin in 30 mm silicon moulds and vacuum-cured for 24 hours. The surface of the hardened blocks was subsequently polished, as per ISO 7404, using a Struers Tegraforce polisher. The polished blocks were assessed petrographically using a Zeiss AxioImager M2M petrographic microscope fitted with a Fossil Hilgers system at a magnification of 100 X using an air lens and 500 X under oil immersion. Microphotographs were captured as optical textures observed in each sample, taken using white light and polarised light with cross nicols (cross polars with lambda plate) rotated by 45ºC to observe anisotropy.

3.3 Air-blowing pretreatment method

The coal tar was modified in a one-litre cylindrical stainless-steel reactor using the air-blowing method. The reactor was equipped with inlet and outlet valves and a pressure gauge to monitor the pressure within the vessel. For each experiment, 200 g of coal tar was charged into the vessel and heated at a constant heating rate of 3°C/min using a heating jacket to pre-determine temperatures of 350°C, 400°C, and 450°C. When the proper temperature was reached, air was blown into the reactor at a steady rate of 0.060 m^3/h for three, six and nine hours at each temperature. This was in accordance with Prada *et al*. (1999), which reported that a gas flowrate of 0.060 m^3/h is adequate to remove light components from tar.

Before reaching the optimal temperature, the pressure inside the vessel was maintained at a constant pressure of 10 bars. During air-blowing, the inlet and outlet valves were opened to allow air into the reactor and discharge volatile matter, respectively. The reactor vessel was removed from the heating jacket at the end of the experiment and cooled to room temperature. After the reactor had cooled, the product within was chipped out, weighed for mass loss, and placed in a clean container. Figure 3.3 gives an overview of the coal tar air-blowing process,

and Figure 3.4 shows the procedure used to modify coal tar in different conditions using the air-blowing method.

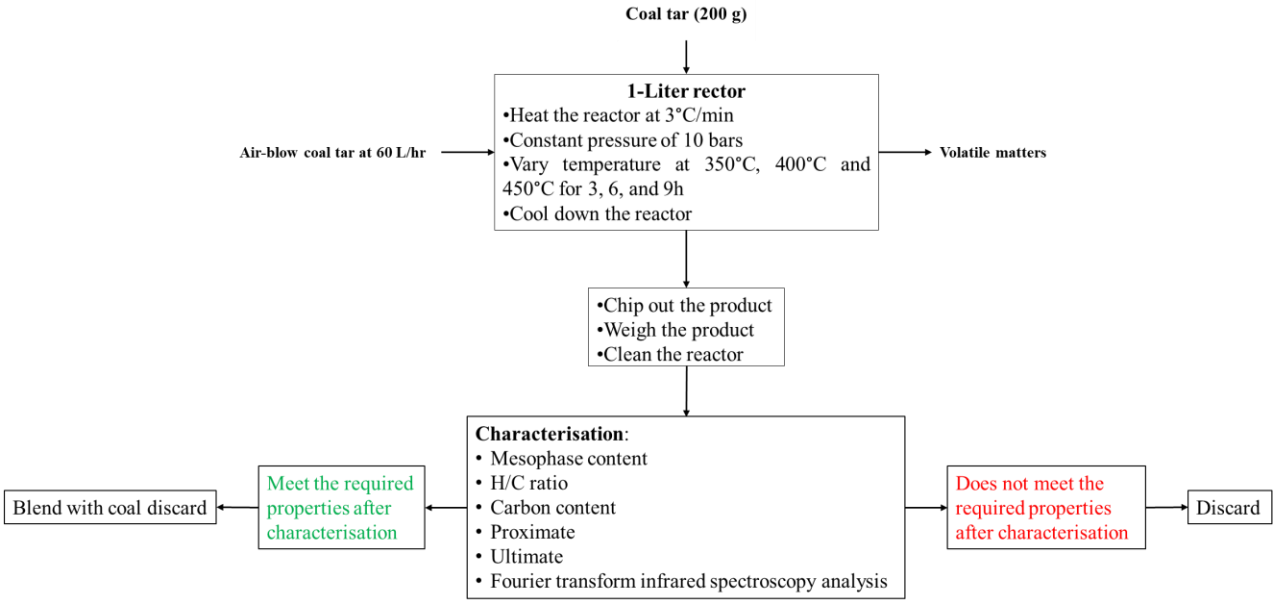

Figure 3.3: Coal tar air-blowing process

Figure 3.4: Coal tar pitch (CTP) modification process at different conditions

3.4 Fabrication of coal composites

Coal composites were produced with varying ratios of coal discards to CTP by weight per cent (wt.%) (Table 3.1). The blend ratio for composites made from DMPS and coal fines was constant at 20 and 80 wt.%, respectively. The ratio was chosen because a blend with more than

20% DMPS creates a watery paste, which makes it challenging to control the fluidity during pressing. A total blend of 2.0 g of coal fines (−53 µm) and CTP (−53 µm) was moulded into square and circular shapes. After compacting the green composite with a hydraulic press at 10 tons, it was tested for its thermal stability. The thermal stability test provides information regarding the temperature at which the sample must be pyrolysed.

The green bodies/composites were pyrolysed in an airtight furnace under argon at a heating rate of 5°C/min from 25°C to 600°C and hold time of five hours. Figure 3.5 depicts the coal composites' fabrication process. Section 3.6 describes the analytical test conducted on the composites produced, such as mechanical, physical, chemical, linear shrinkage, weight loss, and thermal stability.

Table 3.1: Proposed blending ratio of coal discards to coal tar pitch

Coal discard (%)	**Coal tar pitch (%)**	**Dimethylpolysiloxane (%)**
90	10	-
80	-	20
70	30	-
50	50	-

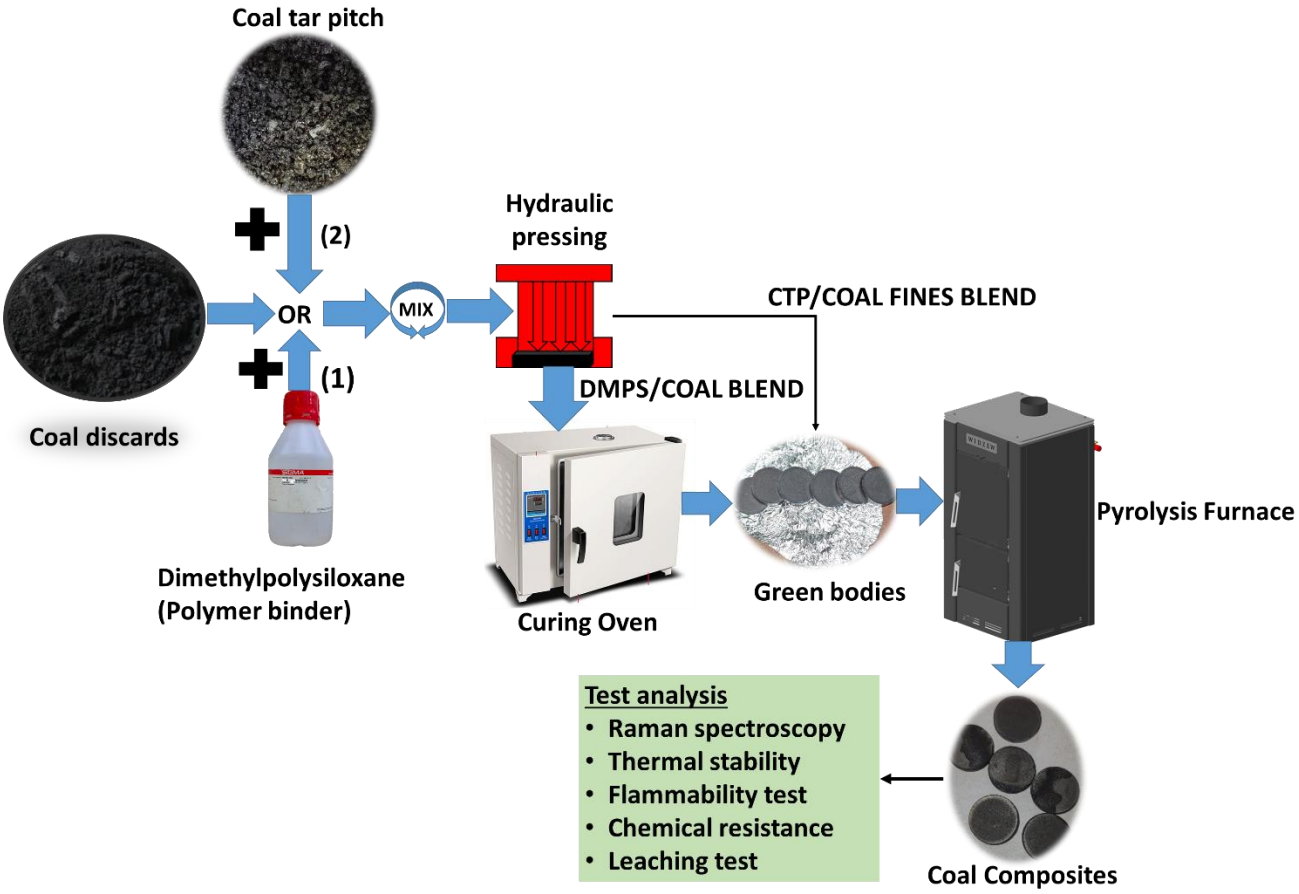

Figure 3.5: Fabrication procedure of coal composites

3.5 Characterisation of coal composites

It was essential to characterise the coal composites based on their properties to determine whether the composites met the standard for construction materials. To ensure the accuracy of the results, all characterisation analyses were repeated at least three times. Figure 3.6 outlines all the analytical tests to which the coal composites produced were subjected.

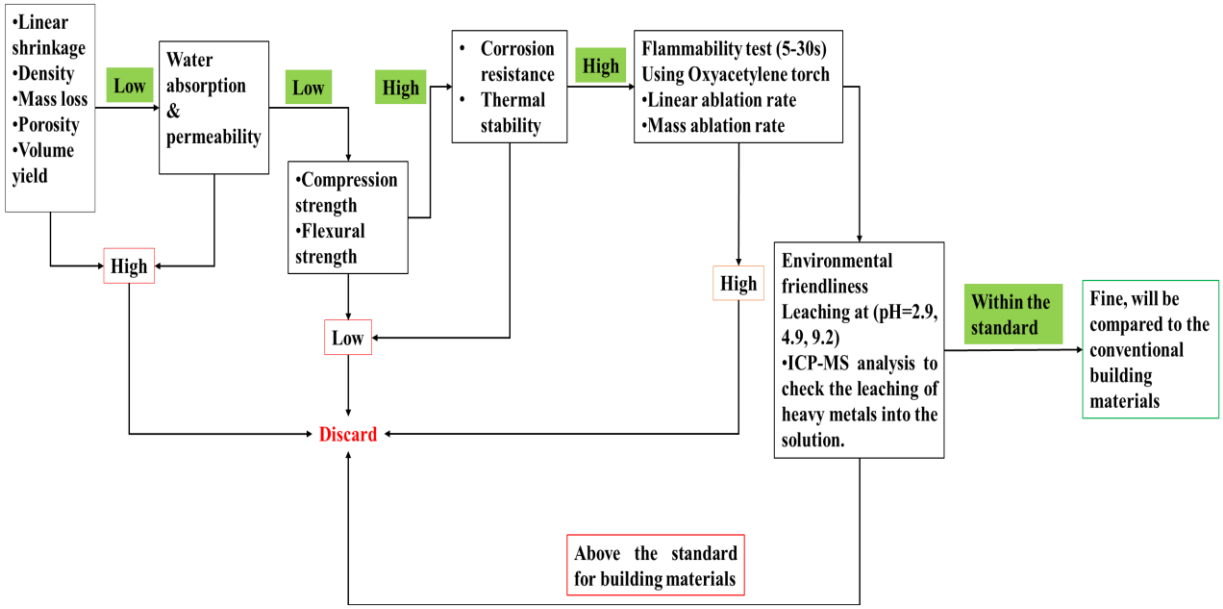

Figure 3.6: Characterisation techniques for coal composites

3.5.1 Linear shrinkage and weight loss

The mass loss of the coal composites after pyrolysis was evaluated by weighing the mass of coal composite samples before (M_G) and after (M_P) pyrolysis. This was determined using equation 3.2. Whereas the linear shrinkage of the coal composite samples was calculated as shrinkage before pyrolysis (L_g) and after pyrolysis (L_p). This was measured using a Vernier caliper with a precision of ± 0.01 mm, and the percentage linear shrinkage was determined from equation 3.3.

$$\%\, Weight\ loss = \frac{M_G - M_P}{M_G} \times 100 \qquad (3.\ 2)$$

$$\%\, Linear\ Shrinakge = \frac{L_G - L_P}{L_G} \times 100 \qquad (3.\ 3)$$

Where M_G is the mass (g) of the green specimen before and M_P is the mass (g) of the green specimen after pyrolysis. L_G is the length (mm) of the green specimen and L_P is the length (mm) of the pyrolysed specimen.

3.5.2 Relative and bulk density, water absorption, apparent porosity, and apparent specific gravity

The relative density, apparent porosity, apparent specific gravity, bulk density, and water absorption were determined according to the ASTM C373 standard test method for ceramic tiles using equations 3.4, 3.5, 3.6, 3.7 and 3.8, respectively (ASTM, 2018).

$$Relative\ density, \rho = 1 - p \quad (3.4)$$

$$Apparent\ porosity, P = \frac{M-D}{V} \times 100 \quad (3.5)$$

$$Apparent\ specific\ gravity, T = \frac{D}{D-S} \quad (3.6)$$

$$Bulk\ density, B = \frac{D}{V} \quad (3.7)$$

$$Water\ absorption, A = \frac{M-D}{D} \times 100 \quad (3.8)$$

Where ρ is the relative density, P is apparent porosity (%), M is the moisten mass of the composite (g), D is the dry mass of the composite (g), T is the apparent specific gravity, S is the suspended mass of the composite (g), B is the bulk density (g/cm^3), and A is the water absorption (%).

To determine the water absorption capacity of the samples, the dry mass, D, of the composites was heated to a constant mass in an oven at 110°C. Thereafter, the composites were immersed in distilled water for five and 24h at room temperature (Figure 3.7a) and later immersed in boiled water (Figure 3.7b) at 105°C for 5h as described by Eterigho-Ikelegbe *et al* (2021a).

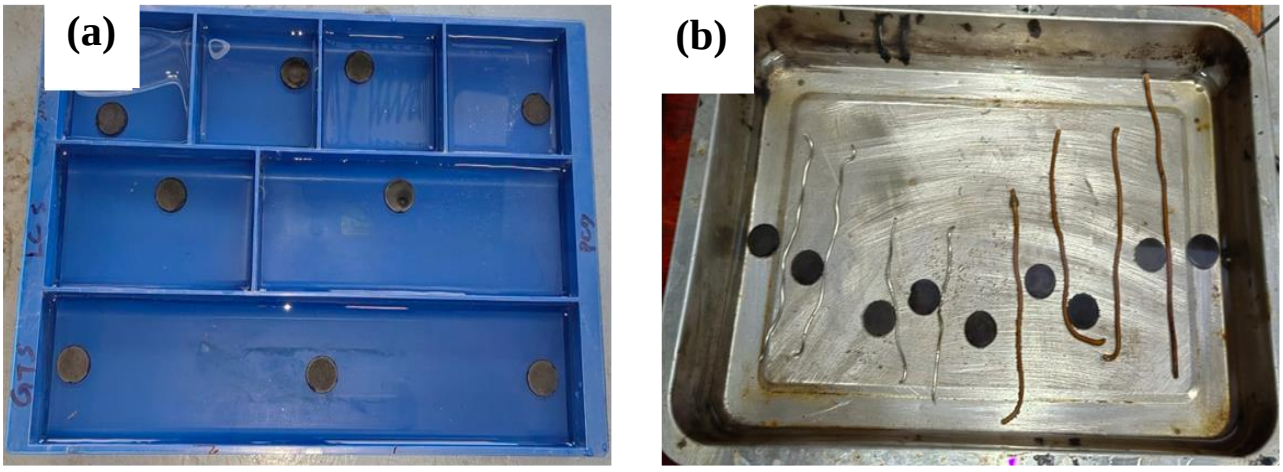

Figure 3.7: Water absorption test (a) at room temperature for five and 24 hours, (b) at 105°C for 5 hours

3.5.3 Compressive strength

The composite specimens were subsequently evaluated for compressive strength to measure their capacity to resist crushing loads. The test pieces were evaluated using the compression test machine, and the constant load of about 1.0 mm/min was applied to them until they fractured. The compression strength was calculated using Equation 3.9 from the ASTM C67 standard (ASTM, 2003).

$$C = W/A \tag{3.9}$$

Where C is the compression strength in MPa, W is the maximum compression load, A is the average lower and upper bearing surface in mm.

3.5.4 Flexural strength

The flexural strength of the composites was determined to assess their ability to withstand bending load. The specimens were evaluated using the flexural test machine, and the constant load of around 1.0 mm/min was applied to them until their failure. The flexural strength was calculated using Equation 3.10 from the ASTM C67 standard for building materials (ASTM, 2003).

$$F = \frac{P \times L}{b.d^2} \tag{3.10}$$

Where F is the flexural strength (MPa), L is the length of the beam (mm), b is the breadth of the beam (mm), and d is the thickness of the specimen (mm).

3.5.5 Flammability test

The flammability of the composite specimens was determined to investigate their ablation behaviour. In accordance with the GJB 32 3A-1996 standard, a butane oxylane torch was utilised for this test (Huang *et al*., 2022). The centre of the specimens was exposed to the torch's flames for 10, 20, 30 and 40 seconds. Following flame exposure, the linear ablation rate (LAR, mm/sec) and mass ablation rate (MAR, g/sec) were calculated using Equations 3.11 and 3.12, respectively. Three specimens (ø30×10 mm) of the same samples were tested.

$$LAR = \frac{d_1 - d_2}{t} \tag{3.11}$$

$$MAR = \frac{m_1 - m_2}{t} \quad (3.12)$$

Where $d1$ $(m1)$ and $d2$ $(m2)$ are the thickness (mass) in mm (g), respectively, and t is the duration of the flame ablation in seconds.

3.5.6 Corrosion test

To estimate the corrosion rate of the samples, hydrochloric acid was added dropwise to a beaker containing a mixture of 3.5% concentration sodium chloride solution, hydrochloric acid, and distilled water, to obtain a pH of 3.7. Subsequently, the composites were suspended from a stick and immersed in the solution, with the beakers securely covered in glad wrap to prevent evaporation. Allowing ample time for the samples to interact with the solution, they were left undisturbed in the beakers for a duration of seven days. After which, the coal composite samples were gently removed from the beakers. The weight of each specimen was recorded before and after immersion to obtain weight loss and the corrosion rate was calculated using Equation 3.13:

$$C_{pr} = \frac{87.6\Delta W}{\rho A t} \quad (3.13)$$

where C_{pr} is the corrosion rate (micrometer per year: μmy^{-1} or μmpy), ΔW is the weight loss (mg), ρ is the density of the composite ($g.cm^{-3}$), A is the surface area (cm^2), and t is the time (year).

3.5.7 SEM analysis

A ZEISS Sigma 300 VP scanning electron microscope was used to determine the microstructure and morphology of the surface and sectioned coal composite specimens. The specimens were coated with at least two gold coats prior to scanning to enhance conductivity and obtain high-resolution images. The surface morphology of the coal composite samples was examined using low magnification at 500 X and 1000 X.

3.5.8 Leaching behaviour

The composites were examined for leaching behaviour to assess the potential release of trace elements. Acetate buffer and glacial acetic acid (leachant) were utilised as leaching reagents, and 1M concentrated sodium hydroxide was used to control the pH of the solution. The test was conducted according to EPA Method 1311. The leachant was added to deionised water,

and the pH used for the solutions were 2.9, 5.0 and 9.2. The pH values of the solution were recorded using a pH metre (SevenCompact^{TM} S220 and S230). The slurry ratio of 1:20 (coal composites (10 g) and solution (200 mL)) was prepared in a screw bottle for each sample. The screw bottles were then placed in a roller mixer and rotated at 30 rpm for 18 hours (U.S EPA, 1992).

Thereafter, the slurry was filtered using a 0.45 µm syringe filter to separate solids from the solution. Inductively coupled plasma-mass spectrometry was used to determine the concentration of chromium (Cr), copper (Cu), silver (Ag), barium (Ba), mercury (Hg), selenium (Se), nickel (Ni), cadmium (Cd), arsenic (As), lead (Pb), and zinc (Zn). The results obtained were then compared to the limits for the trace elements in accordance with the leachable concentration threshold (LCT) from NEM: WA Act No. 59 of 2008 (South Africa) (Molewa, 2013).

3.5.9 Thermal stability

The weight loss and thermal stability, as well as the optimum carbonisation/continuous operating temperature and combustion behaviour of the samples, were determined using a thermogravimetric analyser (TGA701, LECO Corp. USA). Approximately 1.0 g of coal composite sample was placed in a crucible and heated under a nitrogen and air atmosphere from 20 to 950°C at a heating rate of 10°C/min and held constant for 5 hours. After the test finished, the data was recorded.

3.6 Summary

The characterisation of coal fines, coal tar, and coal tar pitch provides insights into the nature, structure, and properties of these materials. Coal tar pitch with a high mesophase and aromaticity ratio, characterised using proximate and ultimate analysis, is blended with coal fines to produce coal composites. The composites that are produced are analysed for weight loss and linear shrinkage. Composites that show cracks and swelling are discarded. Water absorption is measured to determine the extent of water intrusion into the composites. Mechanical strength is also evaluated, with composites surpassing the standard for building materials considered the most favourable. Additionally, leaching behaviour is assessed to determine the environmental safety of the composites.

Chapter 4

Results and Discussion

This chapter presents the results of the tests on the coal fines, coal tar, CTP and the coal composites produced in this study, including the particle size distribution, physicochemical analysis, FTIR, and XRD analysis. The optical microscopic results of the CTP produced using the air-blowing method at 350°C, 400°C, and 450°C at residence times of 3, 6 and 9 hours are discussed. The physical, chemical and mechanical properties of coal-CTP composites and coal-DMPS composites are also discussed, as well as the influence of the pyrolysis process on the weight and thickness of the various composites produced.

4.1 Characterisation results for the coal fines, coal tar, coal tar pitch and composites

4.1.1 Particle size distribution, proximate and ultimate analysis

The particle size distribution for the pulverised CTP, GG1, and GS coal fines are shown in Appendix B.1. At 100% volume, CTP, GG1 and GS coal fines were observed to pass −416, −181, and −239 µm, respectively. The CTP, GG1 and GS had about 49.73%, 92.73% and 76.67% passing −75 µm. The result illustrates that GG1 presented the highest proportion of fines compared to the other samples tested.

The physiochemical analysis results for the coal fines, coal tar, and CTP produced at different temperatures are presented in Table 4.1. The GG1 and GS coal fines have the highest ash content of 84.02% and 62.27%, respectively, compared to coal tar (0.28%) and the CTP samples (0.24 to 0.84%). In terms of the volatile matter content, the as-received coal tar had the highest volatile matter content of 64.50%, which decreased as the tar was subjected to air-blowing at high temperatures. This is similar to the result obtained by Banerjee *et al*. (2019), as well as Zhang and Zhang (2020) during the air-blowing of coal tar. Table 4.1 indicates that the fixed carbon content of the pitch produced increased as the temperature and residence time for the modification of the tar increased. This is expected because the structure of coal tar changes as the moisture and volatile matter are released, resulting in more and denser aromatic hydrocarbons. The fixed carbon content for CTP produced at 400°C (six and nine hours) and 450°C (three and six hours) varied between 82.42% and 88.3% from the raw coal tar, which had a fixed carbon content of 35.23%. Based on these results, the optimal conditions for producing pitch used as a binder in the production of coal composites were 400°C and a residence time of 9 hours. This decision was based on the microscopic results reported in section 4.2, where pitch produced at 400°C for 9 hours had a coarser and more circular anisotropic phase. The proximate analysis of all the composites produced are shown in Table

A.3.

The ultimate analysis results presented in Table 4.1 reveal that the pitch produced at 400°C and 450°C for 9 and 6 hours, respectively, had the highest total carbon content. The increase in the total carbon of both pitches is because of the increase in their aromaticity and polymerisation, which lowers their aliphatic hydrogen content (Fernández *et al.*, 1995; Sharma *et al*., 2020). The H/C ratio of the samples was determined, including their aromatic ratio (f_a) and number of rings of atomic C $(R/C)_u$, using Equation 4.1 and 4.2, respectively. The results showed that f_a is inversely proportional to volatile matter content in the coal tar pitch. As the air-blowing residence time increased, volatile matter decreased and f_a increased. The same trend was observed with heating temperature. The pitch produced at 400°C and 450°C for 9 and 6 hours, respectively, had the lowest H/C ratio of all the samples, as well as the highest $(\mathrm{R/C})_{\mathrm{u}}$ value. A decrease in the H/C ratio indicated dehydrogenative polymerisation of the tar components with significant loss of aliphatic hydrogen (Prada *et al*., 1999). This also indicates the degree of the formation of the mesophase in the pitch, which is responsible for the pitch's binding nature (Yang *et al*., 2022).

$$f_a = \left(100 - V_{d.a.f}\right) \times \frac{0.9677}{C} \tag{4.1}$$

$$(R/C)_u = 1 - \frac{f_a}{2} - \frac{\left(\frac{H}{C}\right)}{2} \tag{4.2}$$

Where f_a is the aromatic ratio, C is the total carbon content, $V_{d.a.f}$ is the volatile matters in dry ash free basis; $(R/C)_u$ is Kasttners' equation to represent the number of rings of atomic C in the monomer, and H/C is the hydrogen-total carbon ratio.

Table 4.1: Proximate and ultimate analysis of coal fines, coal tar, and coal tar pitch samples

Sample	Proximate analysis			Elemental compositions (%)							
	Dry basis (%)										
	VM (%)	Ash (%)	FC (%)	N	C	H	S	O	H/C	f_a	$(R/C)_u$
GG1	10.34	84.02	5.62	0.18	8.79	1.44	0.21	4.84	1.95	0.60	-
GS	20.72	62.73	16.55	0.63	23.77	1.744	2.48	8.02	0.87	0.66	0.23
CT	64.50	0.28	35.23	-	-	-	-	-	-	-	-
CTP 350°C 3h	28.80	0.28	70.92	0.91	77.42	3.54	0.00	18.13	0.54	0.88	0.29
CTP 350°C 6h	26.10	0.24	73.66	1.18	88.05	3.48	0.00	7.30	0.47	0.81	0.36
CTP 350°C 9h	22.74	0.33	76.93	1.00	89.78	3.33	1.02	4.87	0.44	0.83	0.37
CTP 400°C 3h	22.34	0.29	77.36	0.83	95.06	3.51	0.50	0.11	0.44	0.79	0.39
CTP 400°C 6h	16.74	0.84	82.42	0.88	73.74	3.11	1.03	21.26	0.50	1.07	0.21
CTP 400°C 9h	11.33	0.49	88.17	0.94	96.01	2.05	0.00	1.00	0.25	0.88	0.43
CTP 450°C 3h	12.11	0.55	87.33	0.90	88.58	3.01	0.96	6.56	0.40	0.95	0.32
CTP 450°C 6h	11.19	0.49	88.31	1.05	96.92	2.02	0.00	0.01	0.24	0.88	0.44

GG1: coal fines; GS: Greenside coal fines; CT: as-received coal tar; CTP: coal tar pitch produced at different conditions; f_a: Aromatic ratio; FC: fixed carbon h: hours; $(R/C)_u$: Kasttners' equation to represent the number of rings of atomic C in the monomer; H/C: hydrogen to total carbon ratio; N: nitrogen; S: total sulphur; VM: volatile matter

4.1.2 Optical analysis of coal tar pitch

It is critical to determine the optical properties of CTP as this indicates the type, amount, and development of anisotropic (mesophase) spherules in the pitch. The type of phase formed from the conversion of coal tar suggests its application area. The presence of a high anisotropic phase in a pitch enables it to be used as a binder and anisotropic phase is composed of more aromatic compounds and carbon atoms than the isotropic phase (Choi *et al*., 2019; Daulbayev *et al*., 2021). From this study, the CTPs produced at 350°C for nine hours, 400°C for six and nine hours, and 450°C for 6 hours were evaluated for their mesophase development (Figure 4.1).

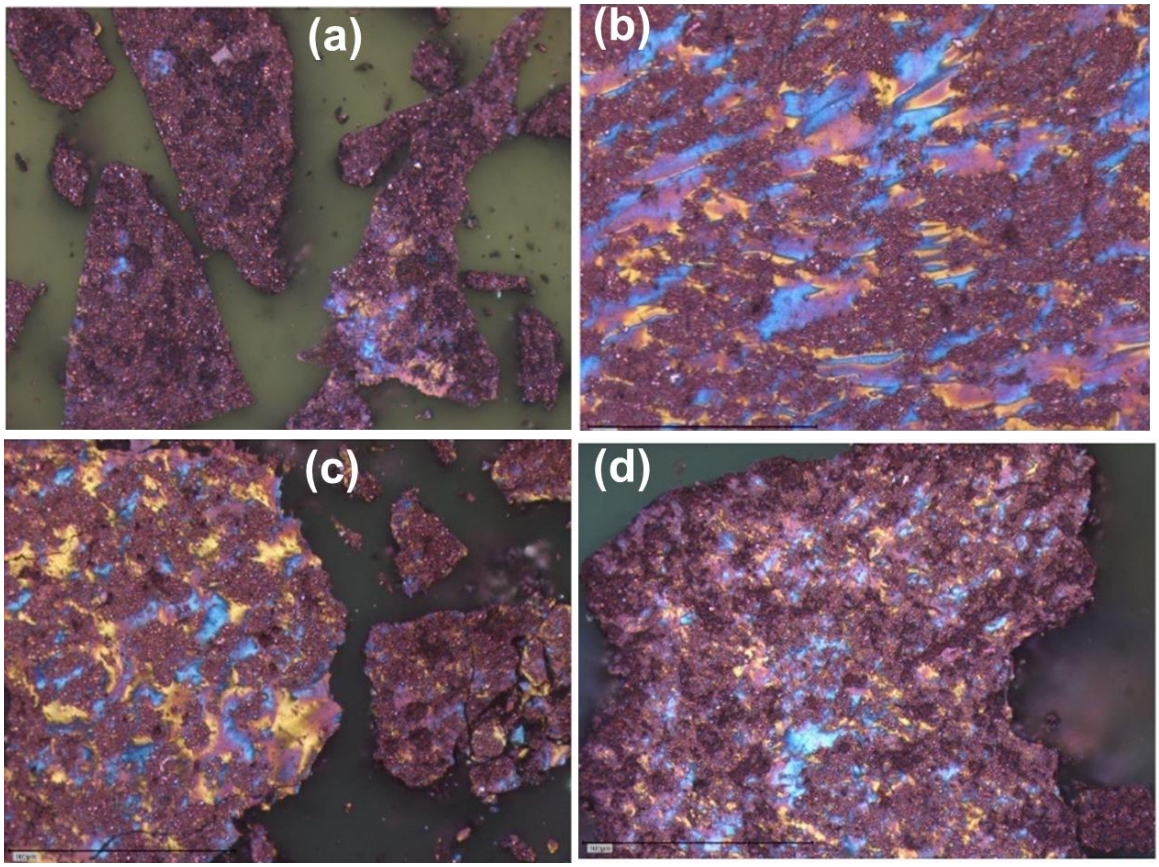

Figure 4.1: Optical observation of CTPs produced at (a) 350°C for nine hours, (b) 400°C for six hours, (c) 400°C for nine hours coarse circular anisotropic phase texture, (d) 450°C for six hours

The CTP produced at 350°C for 9 hours (Figure 4.1a) shows a smooth component that displays epoxy resin, and the embedded particles reveal an incipient anisotropic binder phase with filler fragments. Mesophase and cenospheres are not apparent for these parameters. The pitch produced at 400°C for 6 hours (Figure 4.1b) showed coarse circular anisotropic phase

development, whereas the pitch produced at 400°C for 9 hours had coarser circular anisotropic phase texture (Figure 4.1c). At 450°C for six hours (Figure 4.1d), a pitch with variable texture was produced with evidence of a circular anisotropic phase. The results are consistent with those reported by Liu *et al*. (2014), who observed that increasing the temperature and reaction time causes the spherules to merge due to a prolonged reaction between the pitch and air. The optical microscopic results are evidence that the pitch with the lowest H/C ratio and highest carbon content (pitch produced at 400°C for 9 hours and 450°C for 6 hours) exhibit more anisotropic spherules. These pitches appear to be more uniform than those produced at lower temperatures and shorter reaction times, thereby can be used as a binder.

4.1.3 FTIR results

Coal has a complex structure with many functional groups that enhance chemical bonding (Eterigho-Ikelegbe *et al*., 2021a; Sinaga *et al*., 2021). The structural properties and functional groups in coal fines, coal tar, CTP, and coal composites are either aliphatic or aromatic (Dun *et al*., 2013; Yuan *et al*., 2016). The degree of aromaticity in coal is crucial to the stability of coal and coal composites at high temperatures, which is why FTIR spectroscopy was used to determine these properties (Dun *et al*., 2013). Figure 4.2 shows the FTIR spectroscopic results of two raw coal fines, coal tar, and CTPs produced at 350, 400, and 450°C for 3, 6, and 9 hour reaction times. The presence of the O-H (hydroxyl) group in the coal fines and coal tar samples was detected at 3690 to 3622 cm^{-1}, with the coal fines having the highest peak intensity.

The aliphatic C-H stretch in CH_3 was detected between 3054 and 2895 cm^{-1} in the coal tar and in the DMPS binder at 2962 cm^{-1} (Figure 4.2b). DMPS consists of CH_3 groups, which show a higher aliphatic level than coal tar (Igisu *et al*., 2022). These CH_3 groups were detected at 2692, 1412, 863 and 745 cm^{-1}. The peak disappeared in every CTP produced at different temperatures. According to Prauchner *et al*. (2003), the pretreatment temperature causes polymerisation in the pitch, resulting in the release of side chains that form more aromatic radicals. Aromatic hydrocarbons were observed at 2995 to 2890 cm^{-1} (Figure 4.2d) in the CTP that was produced at 400°C for three hours. This is due to the coal tar air-blowing, which led to the breakdown of the aliphatic hydrocarbons to form aromatic hydrocarbons. The peak at 2336 cm^{-1} indicates the presence of the C≡C alkyne group. This appeared in all CTPs produced, with the double bonds indicating low H/C atomic ratio in the pitch than coal tar.

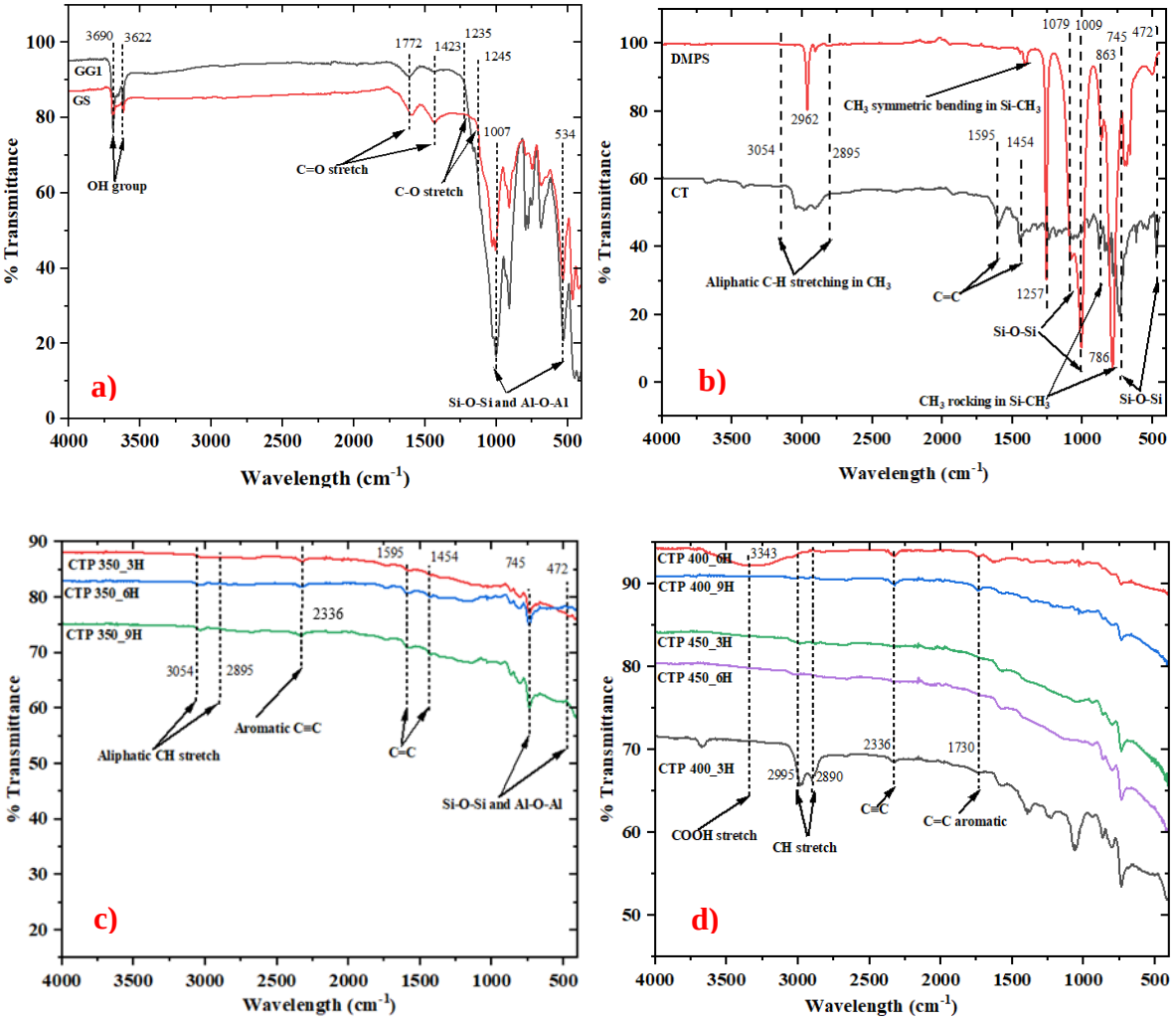

Figure 4.2: The FTIR results of (a) coal fine samples, (b) coal tar and dimethylpolysiloxane, (c) coal tar pitch produced at 350°C and (d) coal tar pitch produced at 400 and 450°C for three different reaction times.

The functional groups of the composites produced from the two binders (pitch and DMPS) blended with coal and pyrolysed at 600°C for five hours are presented in Figure 4.3. The results indicate that all composites, except for those made from GS coal and CTP produced at 400°C for nine hours, consist of an O-H and aromatic CH stretch group. According to Zhang *et al.* (2014), the O-H group facilitates the bonding between coal and the binder. The minerals in the composites are represented in the range of 1032 to 432 cm^{-1}, which is similar to that observed by Eterigho-Ikelegbe *et al.* (2021a). The bend seen at 745 cm^{-1} is the strongest intense aromatic out-of-plane bend. The presence of the aromatic out-of-plane bends indicates that the aromatic hydrogen is present in the aromatic ring with a relatively low degree of substitution (Alcañiz-Monge *et al.*, 2001; Papole *et al.*, 2012). Additionally, a C=O stretch is visible at 1394 to

1245 cm^{-1}; the composites with this peak have a dipole moment that varies with bond length (Li *et al*., 2015). The C=O group is formed during oxidation, replacing hydrogen with oxygen and generating an aryloxy radical that acts as an active site in the polymerisation of pitch during air-blowing pitch pretreatment (Miyajima *et al*., 2000). The composites with C=O (carbonyl) groups are aromatic in nature and characterised by strong electronegativity, leading to the formation of strong bonds in the composites.

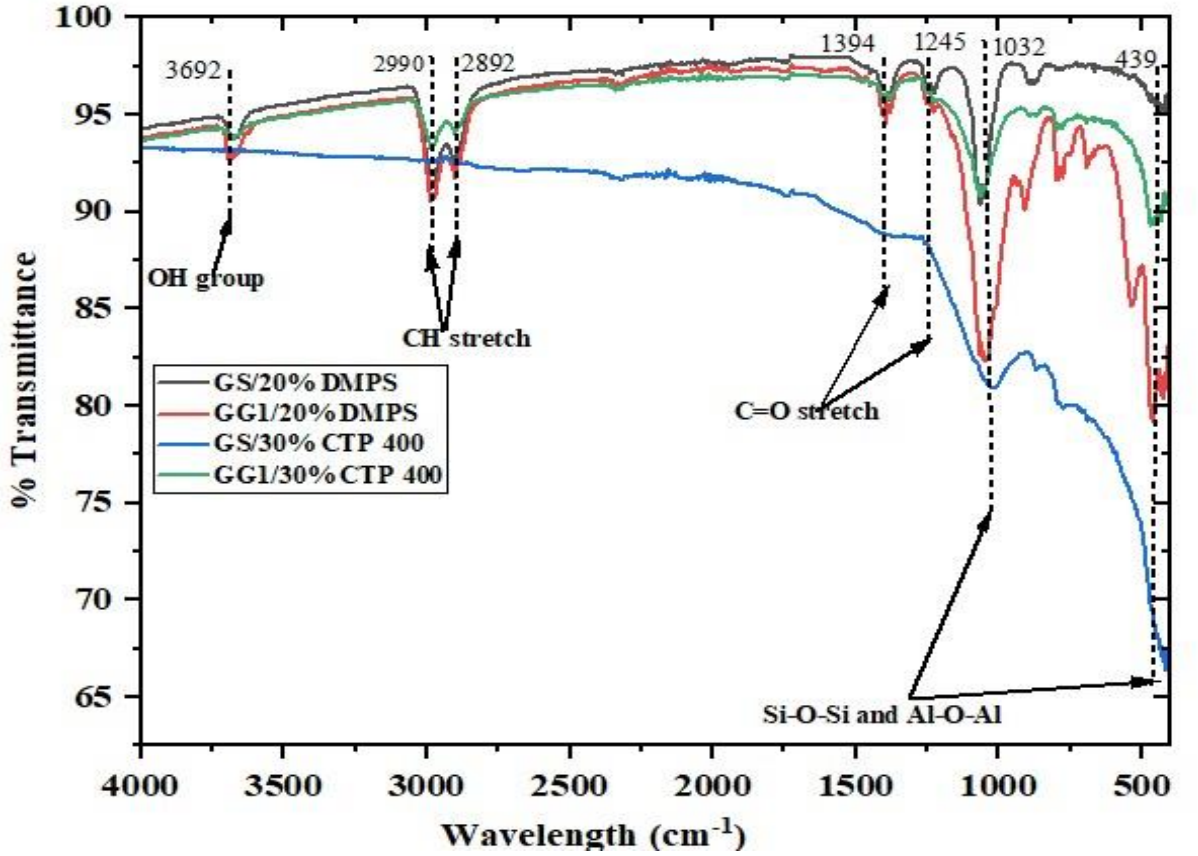

Figure 4.3: Fourier transform infrared spectroscopy results for the coal-coal tar pitch produced at 400°C for nine hours and coal-dimethylpolysiloxane composites

4.1.4 X-ray diffraction results

X-ray diffraction analysis was conducted to assess the crystallinity and identify the mineral phases in the coal fines, coal tar, CTP, and produced coal composites (Figure 4.4a, b, and c). Kaolinite, quartz, muscovite, feldspar, pyrite, and calcite (Figure 4.13a) are among the minerals identified in the coal samples. Due to the high number of peaks and/or the presence of multiple minerals with overlapping peaks, all the peaks were not matched. GG1 fines exhibited higher intensity peaks, which indicates a higher inorganic mineral content compared to GS fines. This is consistent with the higher ash content of GG1 (Table 4.1). The heat treatment of coal tar

resulted in a more graphite-like carbon structure, evident in peaks around 2 theta = 24° and 45°, caused by polycondensation in the binder pitch. Low crystallinity peaks are evidenced by the CTP produced by air-blowing treatment, which is mostly composed of organic compounds (amorphous carbons). Regarding the mineral composition of coal composites, mixture blends containing up to 30% CTP resulted in composites with fewer mineral phases or impurities.

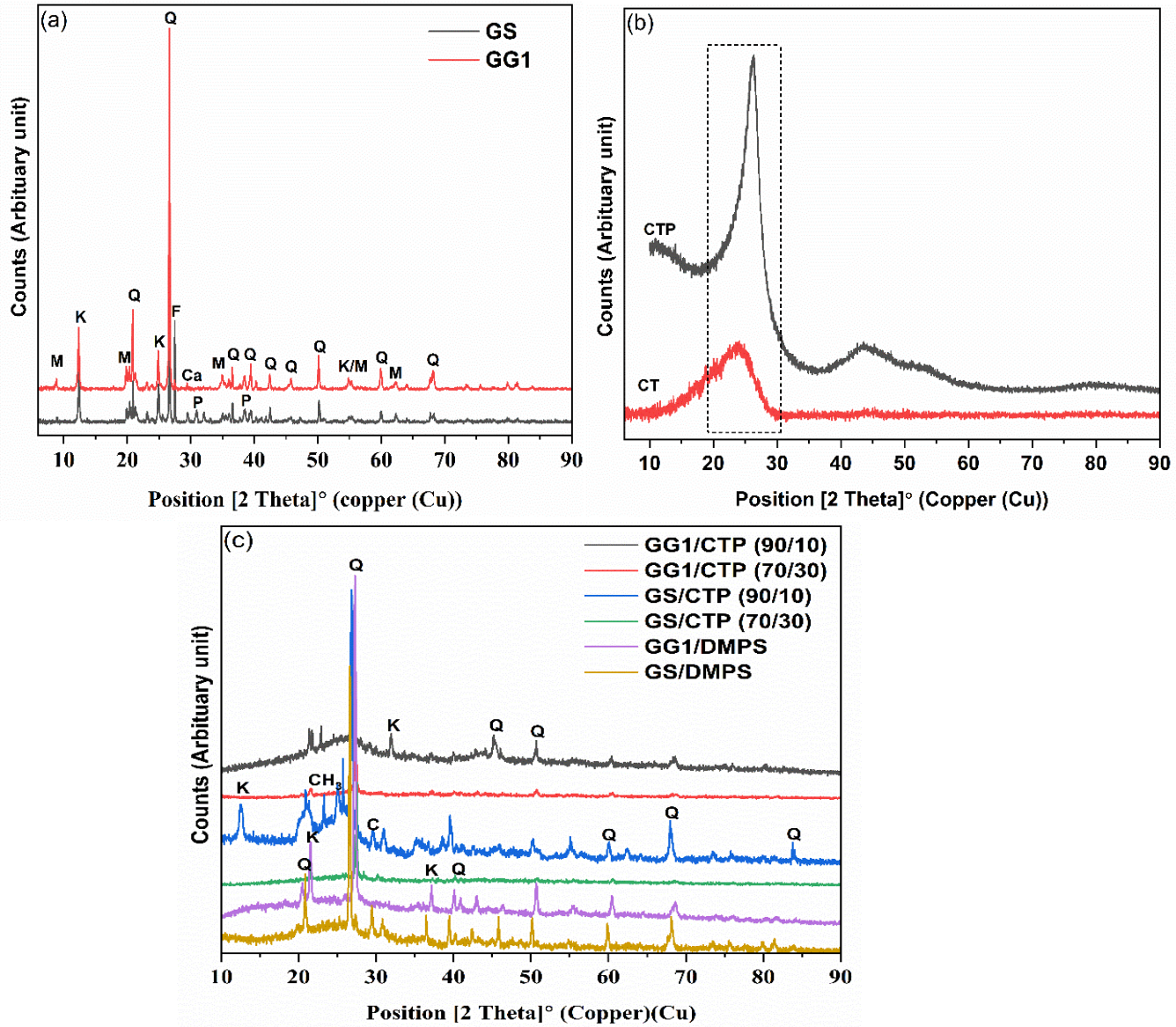

Figure 4.4: Comparison of the powder XRD patterns (a) coal fines, (b) coal tar and coal tar pitch, (c) coal composites [K: kaolinite-1A ($Al_2Si_2O_5(OH)_4$); Q: quartz (SiO_2); M: muscovite ($KSi_3Al_3O_{12}H_2$); F: feldspar $(K,Na)AlSi_3O_8$; P: pyrite (FeS_2); Ca: calcite ($CaCO_3$)]

4.1.5 Raman analysis

Raman spectroscopy was used to determine the structure of the carbon atoms in coal fines, CTP, and all the coal composites produced. It is important for carbon-bound composite formation, as pyrolysis of the composite may lead to changes in the carbon structure or its degree of graphitisation. The carbon atom structure provides the appropriate chemical orientation of the composite structure, rendering it suitable for building applications. The intensity ratio of the disordered and graphitised (I_D/I_G) peak was used to determine the crystallite size (L_a) using Equation 4.3 (Dresselhaus *et al*., 2010). The (L_a), which is the size of the carbon crystallite, is used to quantify the carbon phase disorder, and it is inversely proportional to the (I_D/I_G) ratio. The graph of the Raman fitted spectrum is shown in Figure 4.5.

$$L_a = 4.4\left(\frac{I(D)}{I(G)}\right)^{-1} \quad (4.\ 3)$$

Where L_a is the crystallite size (nm), and (I_D/I_G) is the intensity ratio for disordered and graphitic peaks.

The intensity ratio (I_D/I_G) results can be seen in Figure 4.6. The D and G bands for the CTP are shown at 1366 and 1603 cm^{-1}, which demonstrate aromatic sp^2 bonded atoms (Ruz *et al*., 2016; Sazali *et al*., 2016). For all the coal composites, the D and G band ranges from 1338 to 1366 and 1588 to 1603 cm^{-1}, respectively. The G band is due to the stretching of sp^2 atoms in rings and chains, while the D band is because of the breathing modes of sp^2 atoms in rings (Ferrari, 2007). The order in which the I_D/I_G ratio increases is GG1/30% CTP, GG1/10% CTP, GS/10% CTP, GS/30% CTP, GS/20% DMPS, and GG1/20% DMPS. The higher concentration of graphitised carbon phases in GG1/30% CTP can be attributed to the sp^2 C-C bonds in the raw GG1 coal fines (Figure 4.5a). Although GS has more carbon content than GG1 (Table 4.1), it is less graphitised than the GG1 composites. Figure 4.5a shows that GS coal fines have a stronger D band than G band, which may be caused by structural defects, edge effects, and dangling sp^2 carbon bonds (Swapna *et al*., 2018). As the disordered band decreases, the crystallite size increases (Figure 4.6). The decrease in the I_D/I_G ratio results in a high L_a, which is evidence of an amorphous carbon structure (disordered carbon ring) (Eterigho-Ikelegbe *et al*., 2023b). The calculated ID/IG ratios show that the addition of CTP in the coal matrix resulted in a low degree of disordered carbon in the composites, compared to coal fines. This

means that sp2 atoms in rings and chains were stretched during pyrolysis. The structural changes of coal composites show that they undergo graphitization during pyrolysis. The graphitized structure increases resistance to oxidation, reduces reactivity, and stabilizes thermal behavior of the composites.

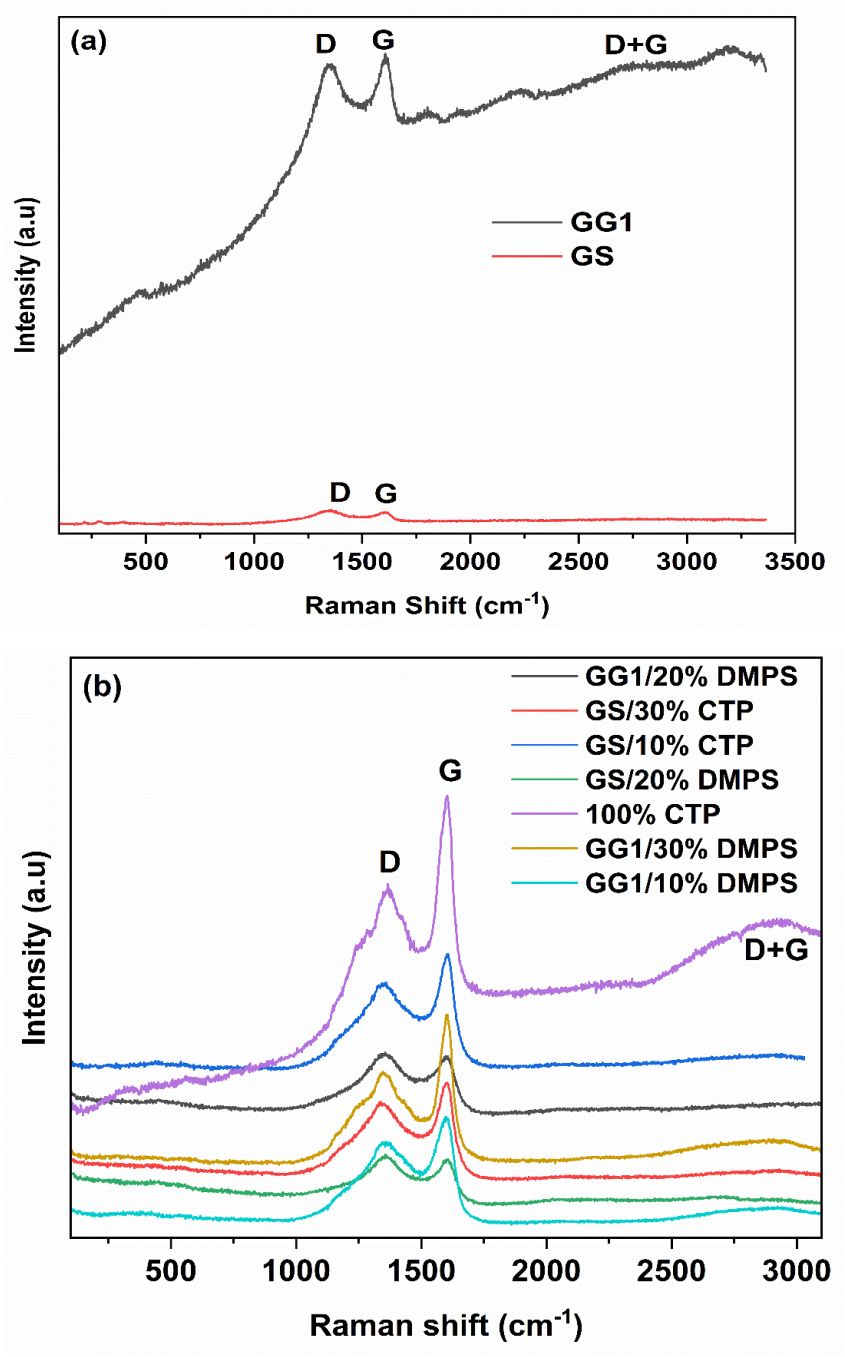

Figure 4.5: a) Raman spectroscopy for (a) raw GG1 and GS coal fines and (b) coal tar pitch and coal composites

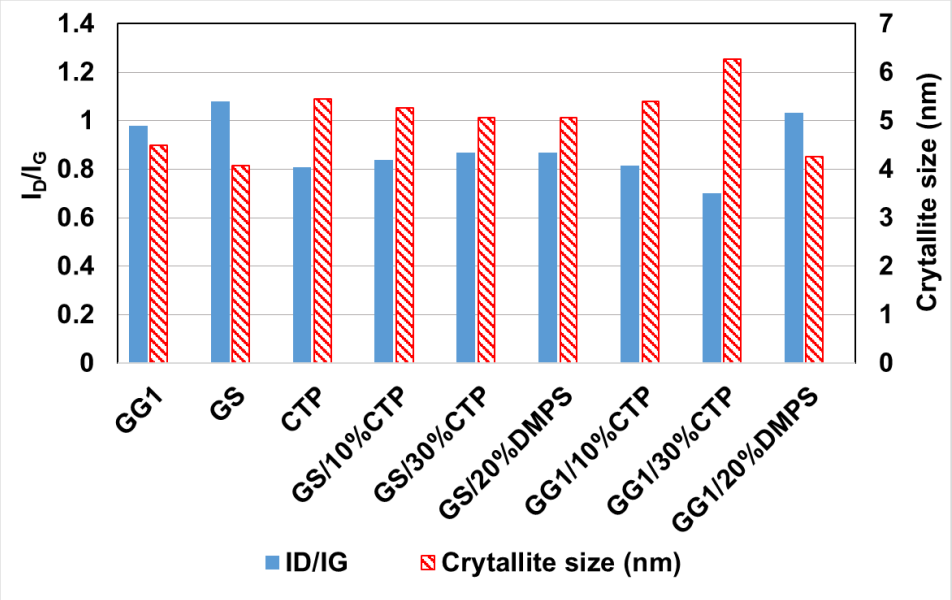

Figure 4.6: The I_D/I_G ratio and crystallite size for coal tar pitch (CTP) and all CTP and dimethylpolysiloxane (DMPS) composites

4.2 Thermal, textural, mechanical, and chemical properties of the composites

The results from the physicochemical and mechanical properties of the coal composites produced are presented in this section, including the linear shrinkage and weight loss, water absorption, bulk density and specific gravity, exterior volume, flammability test, corrosion resistance, compressive strength, flexural strength, SEM analysis, and environmental behaviour. A DMPS-coal composite with 20% DMPS and 80% coal was prepared and analysed with other different coal composites. The composites with more than 20% DMPS resulted in a watery and fluid-like coal mix.

4.2.1 Thermal stability of the composites

The thermal stability of the compressed bodies (Figure 4.7) produced was determined using a thermogravimetric analyser. TGA of the compressed green bodies was done to identify the temperature suitable for pyrolysing the composites in an inert atmosphere. The analysis was conducted at a heating rate of 10°C /min from 25 to 950°C in nitrogen.

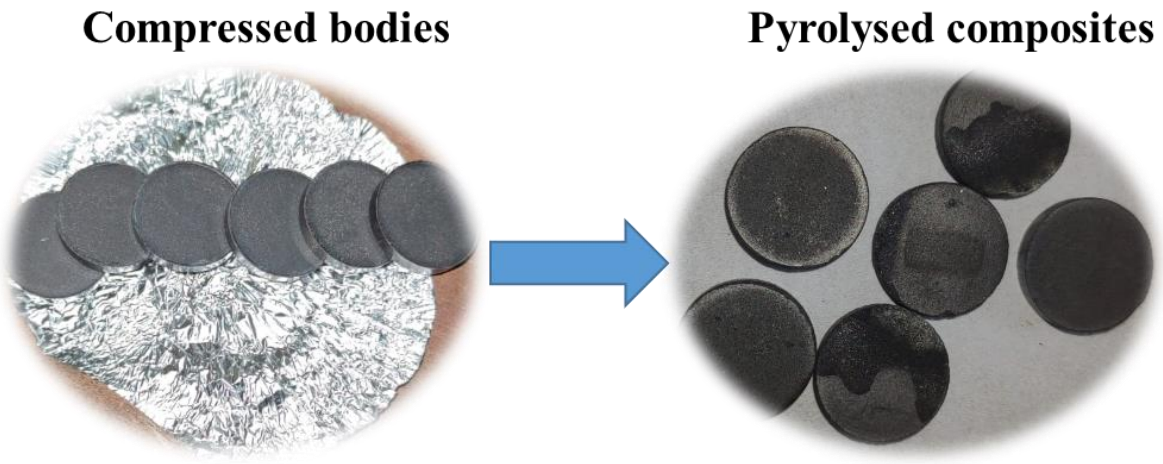

Figure 4.7: Compressed and pyrolysed composites

The weight loss observed between 40 and 150°C is due to the release of moisture in the samples, as seen in Figure 4.8a. As the temperature increased to around 400°C, the samples lost a significant amount of weight. This is due to the degradation of the low molecular compounds in the green composites. Both GG1/10 CTP and GS/10 CTP decomposed first with higher weight loss than the other samples. As seen in Figure 4.8a, the residual mass around 600 °C is more than 75%. Hence, 600 °C was selected as the pyrolysis temperature for all the composites to conserve energy. Notably, the pure CTP (100%) binder lacks thermal stability beyond 600 °C based on the rapid decrease in weight loss. Generally, GG1/CTP green composites exhibit better stability compared to GS/CTP green composites. This suggests a stronger chemical interaction between GG1 particles and the CTP. However, with the DMPS binder, GS green composites outperform GG1 green composites. Subsequently, the thermal decomposition of the pyrolyzed coal composites in air atmospheres (thermal oxidation) employing a heating rate of 10 °C/min from 25 to 950 °C is depicted in Figure 4.8b.

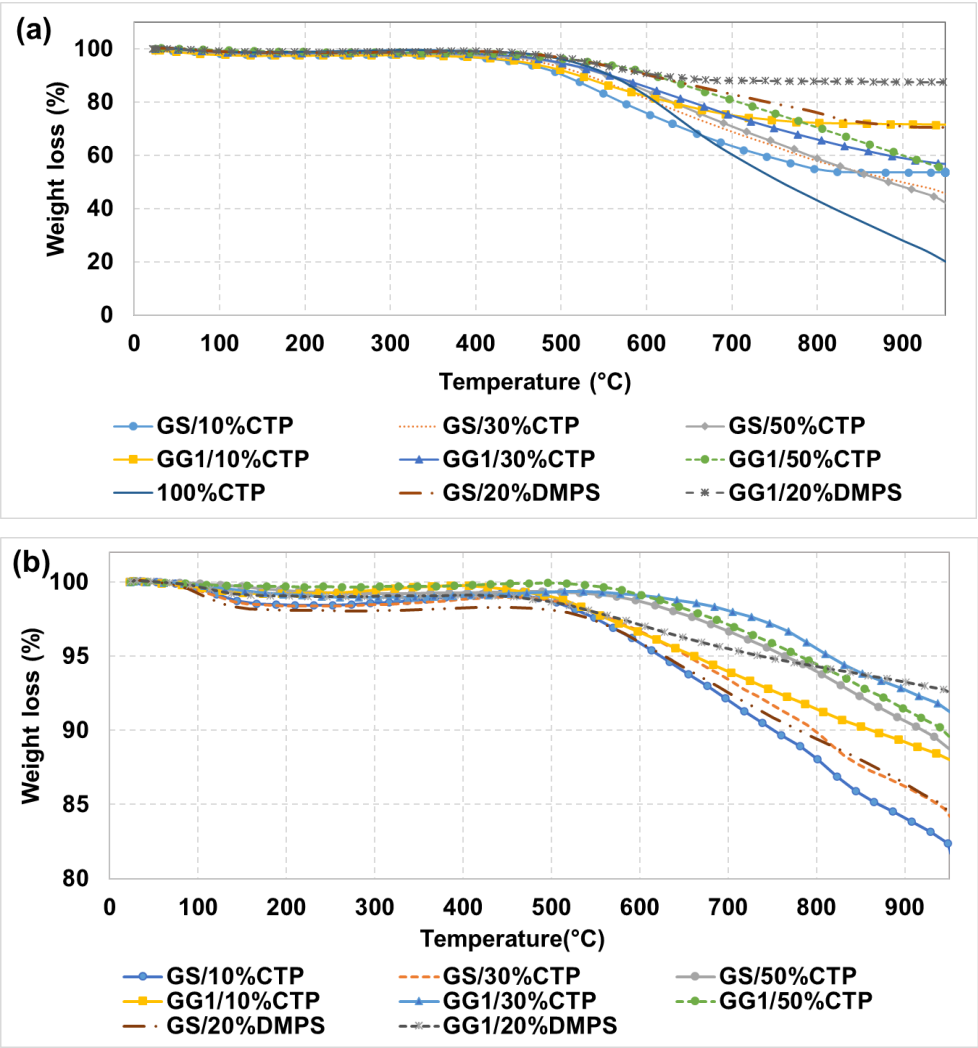

Figure 4.8: Thermal stability of (a) green bodies in nitrogen atmosphere and (b) composites in air atmosphere

For the pyrolysed coal composites produced (Figure 4.8b), the stability of the composites in air atmospheres at a heating rate of 10°C /min from 25 to 950°C was conducted. The composite body GG1 50% CTP was the most thermally stable among all the composites in air until around 550°C. This sample had the lowest volatile matter content of 3.62% (Appendix A.3) compared to GG1 10% CTP and GS 10% CTP with volatile matter content of 6.79% and 7.35%, respectively. Both GG1 10% CTP and GS 10% CTP were more reactive in air according to the thermograph (Figure 4.8b). Table 4.2 shows the residual mass for the green bodies and the coal composites produced after being heated in nitrogen and air atmosphere, respectively. According to Table 4.2, coal composites were observed with higher masses remaining after pyrolysis at 950ºC, indicating higher thermal stability than green bodies. GG1 coal, regardless of the binder used, showed superior thermal stability compared to GS coal. The DMPS-based

composite (GG1 20%/DMPS) was the most thermally stable composite with the lowest fixed carbon available for combustion and the highest ash residue.

Table 4.2: Residual mass after thermogravimetric analysis

Samples	$R_{950°C}$ (%)	
	Green bodies	Composites
100% CTP	4.00	-
GS/10%CTP	53.66	70.06
GS/30%CTP	42.58	84.19
GS/50%CTP	32.26	88.74
GG1/10%CTP	71.39	88.01
GG1/30%CTP	56.66	91.23
GG1/50%CTP	42.57	89.51
GS/20%DMPS	70.42	84.29
GG1/20%DMPS	87.39	92.53

CTP: coal tar pitch; GS: greenside coal; GG1: GG1 coal discard; DMPS: dimethylpolysiloxane

4.2.2 Composites linear shrinkage and weight loss

The linear shrinkage and weight loss of the composites were determined by pyrolysing the composites using argon gas at 600°C for five hours. The change in thickness and weight of the samples after pyrolysing provides insight into the required mould size to produce a predetermined composite size. Increasing the CTP content decreased the percentage weight loss for all composites made from two distinct coal fines, as shown in Figure 4.9. For example, the composite produced from 10, 30, and 50% CTP with GS resulted in a weight loss of 16.61, 13.92, and 10.96%, respectively. The weight and thickness of the composites before and after pyrolysis are provided in Table A.4 and A.5, respectively. The composites made with GS and 20% DMPS experienced the highest weight loss, which was 17.43%. This indicates that the composite made with DMPS is not as stable as CTP when pyrolysed at 600°C. This could be attributed because of the breakdown in the polymer network, as well as the release of unreacted monomers (Huang *et al*., 2022).

The linear shrinkage for the same samples decreased slightly as the binder concentration (CTP) increased (Figure 4.9). This is caused by the pyrolysis temperature, which leads to the volume shrinkage of the compacted composite specimens. During pyrolysis, the coal fines swell if it is a high-rank coal, allowing the binder to fill the pores of the composite. Composites with a high porosity volume have more volume shrinkage (Xie *et al*., 2007; Eckel *et al*., 2016). The GS 90% + 10% CTP sample had the highest linear shrinkage. GS has higher volatile matter than GG1, which may lead to higher porosity, degradation in sample mass, and increased volume shrinkage. The findings by Eterigho-Ikelegbe *et al*. (2023b) suggest that composites with high shrinkage may experience cracks, deformation, and warping during pyrolysis and subsequent cooling.

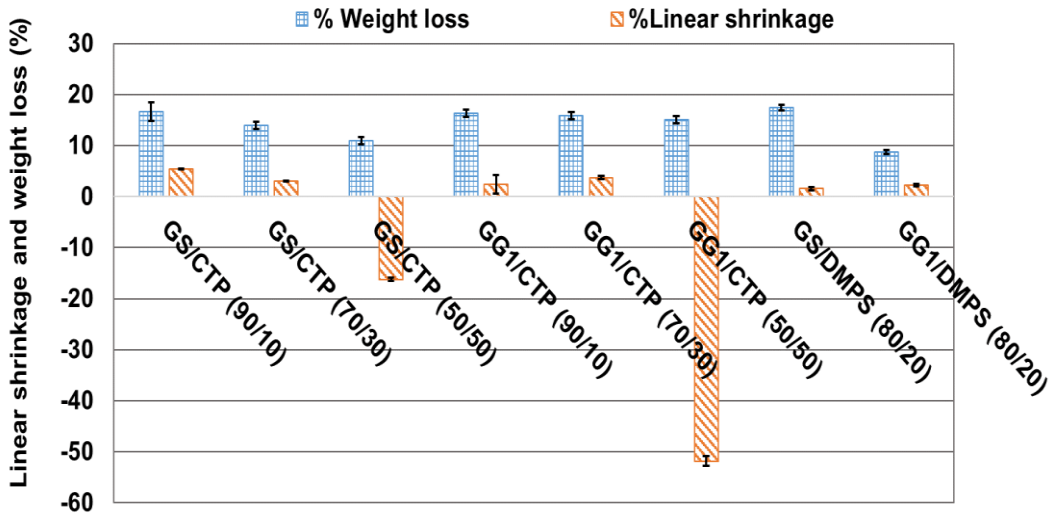

Figure 4.9: Weight loss and linear shrinkage of the composites

4.2.3 Water absorption, bulk density, exterior volume, apparent specific density, and porosity

Exterior volume, apparent porosity, apparent specific gravity, bulk density, and water absorption are some of the important properties of the composites used in the construction industry (see Table A.6-A.9). Figure 4.10a and b illustrate the water absorption test, which shows how much water the composites can absorb at room temperature and when boiling at 105°C. Table 4.3 provides the results of apparent porosity, apparent specific gravity, and bulk density at different water immersion conditions (5 and 24 hour cold water test and five-hour boiling water test, as shown in Figure 4.10).

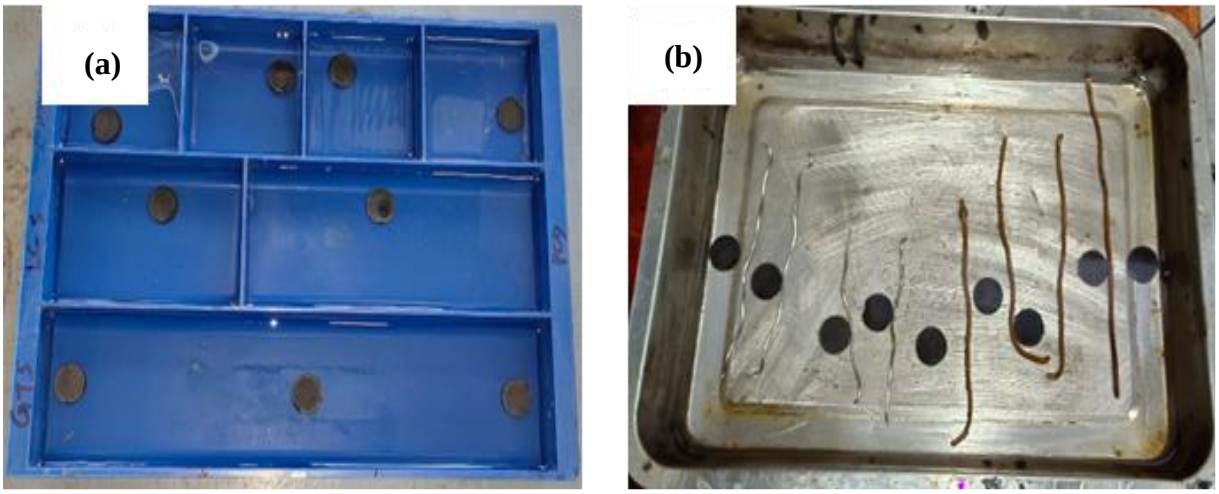

Figure 4.10: Water absorption test (a) at room temperature for five and 24 hours, (b) at 105°C for five hours

In terms of the bulk density for all the composites produced, the percentage of coal in the blend with the CTP influences the composites' bulk density. GG1 90% and GS 70% with CTP had higher bulk density than the GS 90% and GS 70% CTP composites. The high ash content and mineral functional groups found in GG1 coal can lead to this, as evidenced by the FTIR spectroscopic data. The composite decreases in bulk density with increasing CPT, and under the five-hour cold test, 24-hour cold test and five-hour boiling test, there were no changes in the bulk density of the individual composites. This indicates that a low-density composite can be produced from the coal and CTP used in this study, which is relatively lower than the standard ceramic construction materials that have a bulk density ranging from 2.05 to 2.17 $g.cm^{-3}$ (Pavlova *et al*., 2019). A similar trend was observed for the composites' apparent density in this study. Adding more CTP to the blend causes the composite to become lighter because it is less dense than the coal fines. Regarding porosity, the composites became less porous with the addition of more binder, and more compacted and fused together during pyrolysis.

The apparent porosity of the composites is affected by the severity of the process such as pyrolysis. The composite subjected to five hours in boiling water, regardless of the percentage CTP or coal used, had the highest porosity. The CTP ratio increase resulted in a decrease in composite porosity, which enhanced its quality as a construction material.

Table 4.3: Bulk density, apparent specific density, and apparent porosity of the composites

Composites	Bulk density (g/cm^3)			Apparent specific gravity			Apparent porosity (%)		
	5-h cold	24-h cold	5-h boil	5-h cold	24-h cold	5-h boil	5-h cold	24-h cold	5-h boil
GS/CTP (90/10)	1.637	1.681	1.675	1.898	2.046	2.047	13.724	17.341	18.176
GS/CTP (70/30)	1.588	1.628	1.619	1.715	1.846	1.874	7.428	11.532	13.620
GS/CTP (50/50)	1.456	1.449	1.460	1.493	1.527	1.709	2.482	5.188	14.570
GG1/CTP (90/10)	2.013	1.900	1.890	2.354	2.241	2.296	14.467	16.311	17.678
GG1/CTP (70/30)	1.778	1.812	1.775	1.857	1.989	2.049	4.258	8.697	13.399
GG1/CTP (50/50)	1.343	1.365	1.322	1.365	1.430	1.744	1.590	4.507	24.236
GS/DMPS (80/20)	1.568	1.556	1.557	2.116	2.115	2.151	25.902	26.634	27.643
GG1/DMPS (80/20)	2.044	2.062	2.038	2.090	2.150	2.127	2.228	4.050	4.200

CTP: coal tar pitch; GS: greenside coal; GG1: GG1 coal discard; DMPS: dimethylpolysiloxane

The results for the exterior volume of the composites are shown in Figure 4.11. Each composite's exterior volume remained the same regardless of the water immersion test conditions. However, when the CTP content increased, the exterior volume of the composites increased marginally with the severity of the test condition. This might be due to the lower density of CTP (1.15 to 1.4 g/cm^3) compared to the higher density of coal, especially the high ash coal used in this study (Daguerre *et al*., 1998). Composites with a higher CTP ratio are likely to expand more due to the structure of the CTP and its lower viscosity (Daguerre *et al*., 1998). Composites made from coal fines and the DMPS blend had the lowest exterior volume because DMPS is denser than CTP, with a density of around 9.65 g/cm^3 (American Elements, 2023).

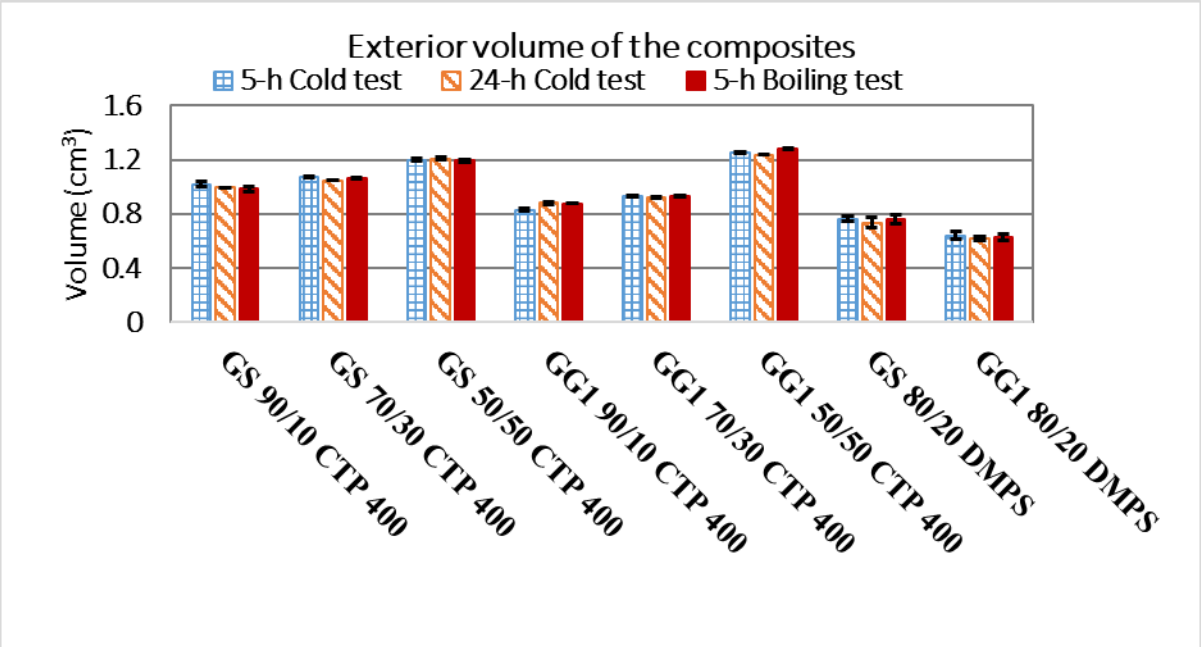

Figure 4.11: Exterior volume of the composites

The results from the water absorption test for all the composites can be seen in Figure 4.12. This test provides insight into the extent to which a building material can resist water ingress and its quality for building purposes. The water absorption of all coal composites was less than 20%, indicating that all composites meet the criterion for water absorption in building materials, which ranges between 0 and 25% (Kelham, 1988; Eterigho-Ikelegbe *et al*., 2023b). From the plot, it can be observed that the water absorption of the composite decreased as the CTP ratio increased in the composites produced from both coal samples. The results for apparent porosity agree with these, indicating that increasing the binder content decreased the

porosity of the composites. In the boiling water test, composites produced with 50% CTP, especially with GG1 coal, had the highest water absorption. While GG1 coal composites produced with 10% and 30% CTP and 20% DPMS had lower water absorption than the GS coal composites. Overall, composites made from coal with a strong, intense O-H group, low volatile matter content, and a high H/C ratio (GG1) outperform other composites. This is similar to the results obtained by Eterigho-Ikelegbe *et al*. (2021a), where coal waste with a higher H/C atomic ratio produced composites with better or lower water absorption. Furthermore, a relationship has been observed between apparent porosity and water absorption, wherein a decrease in porosity results in a decrease in water absorption for all composites. This trend can be attributed to the fewer interconnected spaces and voids present in the coal composite material. The result was a material that is less permeable to water and has low water absorption.

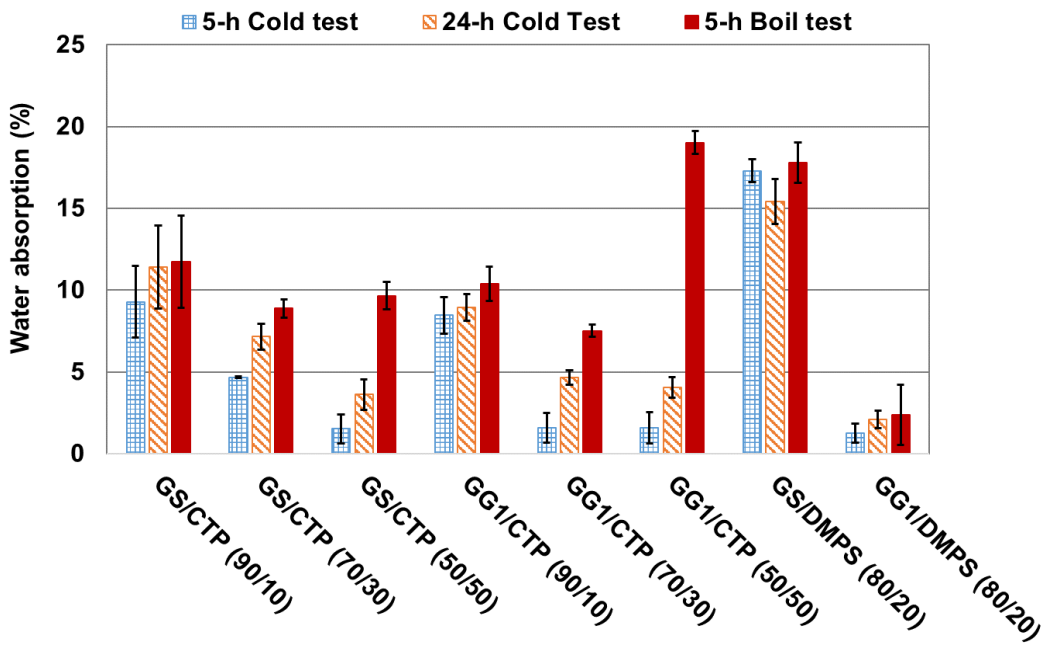

Figure 4.12: Water absorption of the composites

4.2.4 Scanning electron microscopy analysis

The morphology of the composites produced from the blend of the two coal fines, CTP, and DMPS at different ratios was determined using a scanning electronic microscope. The morphologies of the fracture coal composites produced are shown in Figure 4.13a-f. Figure 4.13a and b shows the microstructure of GS/10% CTP and GS/30% CTP, respectively. It is evident from the micrographs of the coal composites that the crack sizes decreased when

increasing the CTP weight percentage. The cracks seen might be a result of thermal stress resulting from the expansion of the composites as the pyrolysis temperature increased. The same results can be seen for GG1/10% CTP and GG1/30% CTP in Figures 4.13c and d. The filling of cracks in the composites may have been a result of the CTP percentage increase. Compared to the composites made from CTP, the surface of the two composites produced from DMPS (Figures 4.13e and f) was the smoothest. The smoothness in the surface of these composites might be due to the DMPS being a soluble binder, which wetted the coal surface and fused it homogeneously. It can also be observed that the composites produced from GG1 coal fines with both binders had the smoothest surface compared to those from GS coal. Surface inhomogeneity and lack of fusibility were observed in the composites made from GS coal fines. The porosity of the GS composites, which is determined by apparent porosity, can be attributed to this, and it is similar to the findings of Eterigho-Ikelegbe *et al*. (2021a). The GG1 composites exhibited homogeneous surfaces and minimal cracks.

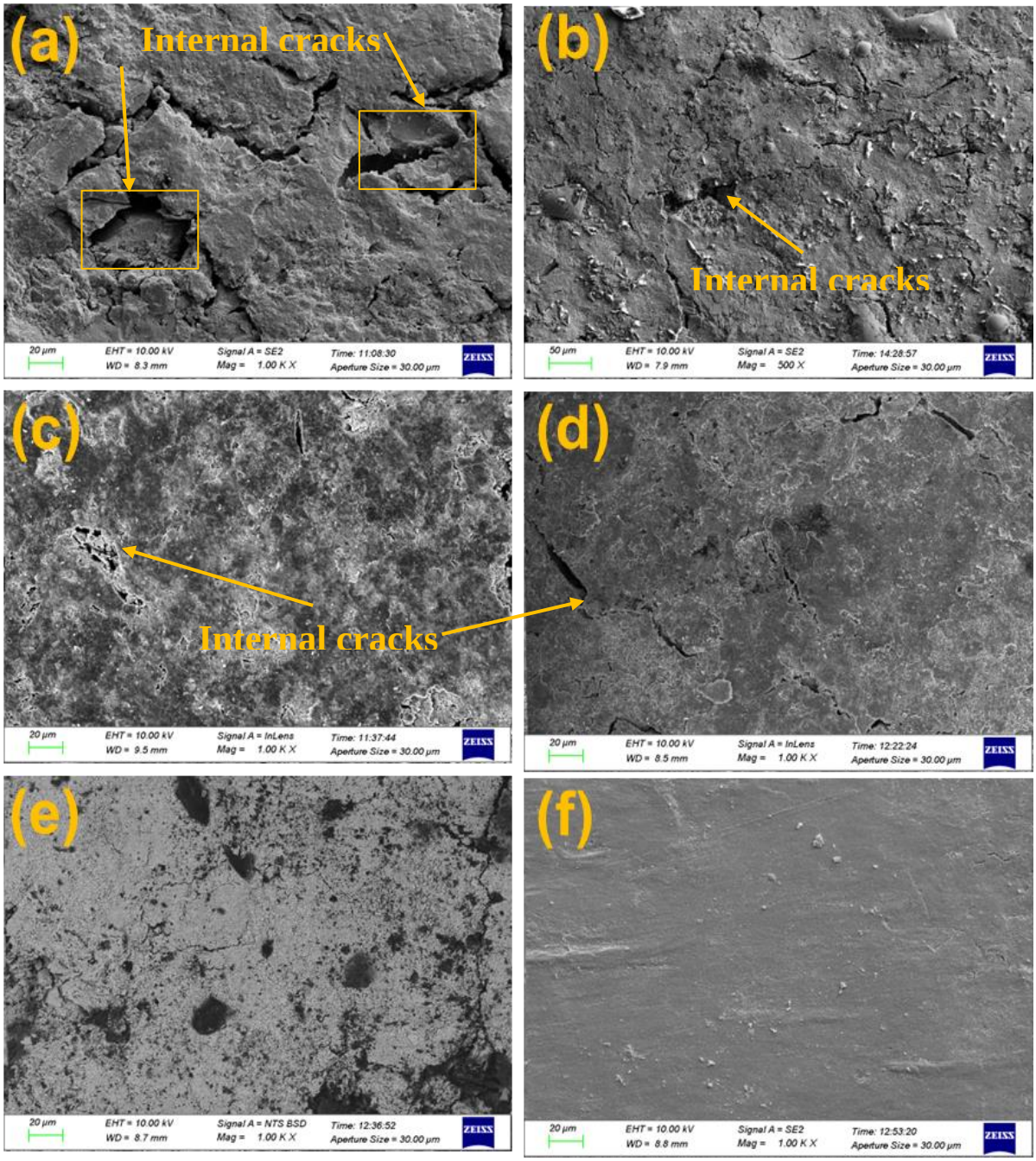

Figure 4.13: Scanning electron microscopy analysis at 1000X magnification of a) GS/10 CTP, b) GS/30 CTP, c) GG1/10 CTP, d) GG1/20 CTP, e) GS/20 DMPS, and f) GG1/20 DMPS

4.2.5 Compressive strength

Compressive strength is the most important parameter for building materials as it determines the ability of the material to withstand crushing loads. The compressive strength for all the composites produced is depicted in Figure 4.14 (see Table A.10). The composites' compressive strength values ranged from 106.58 to 344.71 MPa, with the GG1 80/20 DMPS composite having the lowest strength value and GG1 70/30 CTP having the highest strength value. The

CTP binder composites exhibited superior compressive resistance compared to the DMPS binder composites. All the composites produced withstood very high compressive stress compared to the data reported by X-MAT on their coal core composite roof shingles at 40 MPa (X-MAT, 2020; Eterigho-Ikelegbe *et al*., 2021a). It was observed in the current study that the coal (GG1) with a higher and more intense O-H group produced better compressive strength when blended with CTP at 10 and 30% compared to GS (Guang-Heng *et al*., 2006; Hu *et al*., 2017).

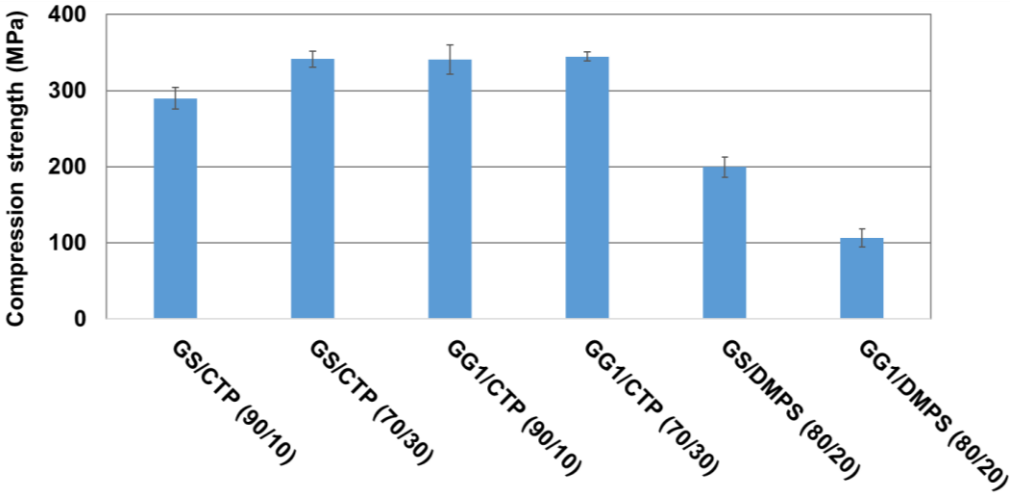

Figure 4.14: Compressive strength of the coal composites produced from CTP and DMPS

4.2.6 Flexural strength

Flexural strength is the ultimate strength of a material to withstand a bending load (Eliche-Quesada *et al*., 2011). Table 4.4 lists the bending properties of the composites, and Figure 4.15 depicts the flexural strength test procedure and samples tested. The table shows that the flexural modulus, yield force, yield stress, and yield strain for the GS/20% DMPS, GG1/20% DMPS, and GG1/10% CTP composites could not be determined. The composites that were able to withstand bending loads were GS/10% CTP, GS/30% CTP, and GG1/30% CTP, with flexural strengths of 48.75, 159.30, and 63.80 MPa, respectively. The flexural strength of these coal composites is greater than the flexural strength of the concrete roof tiles, which ranges from 14 to 41 MPa (Thasneem and Reddy, 2018). However, the GG1/30% CTP composite had a maximum modulus of 140 8333 MPa, showing that it has the highest resistance to deformation under bending loads. The higher concentration of the O-H group in the coal composite might be responsible; according to Guang-Heng *et al*. (2006), the O-H group leads to a high modulus.

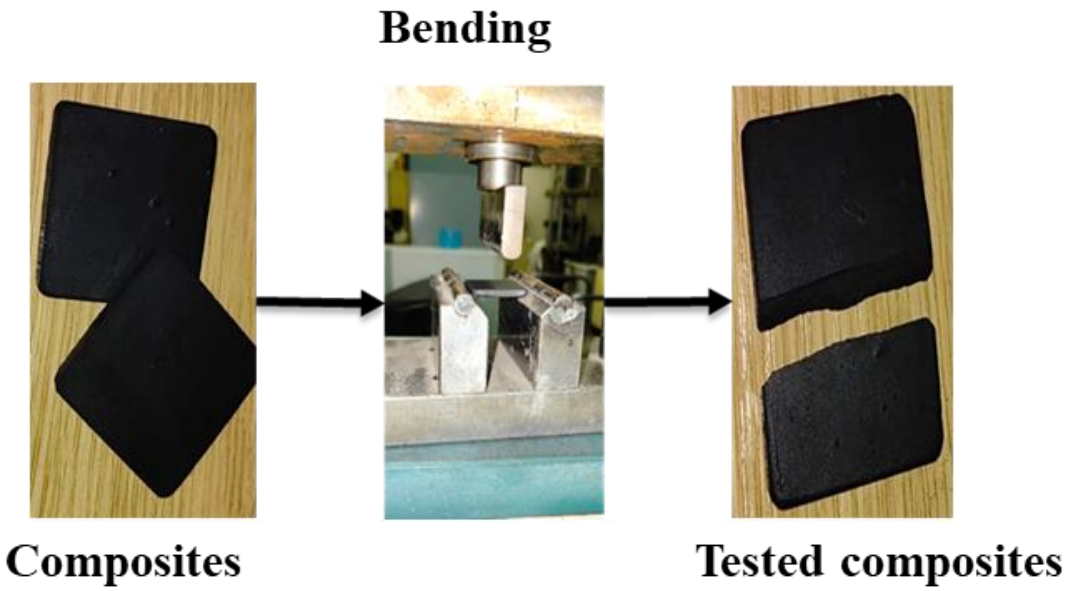

Figure 4.15: Procedure used to test flexural strength

Composite GS/30% CTP had the highest yield stress. The yield force, causing the composites to fracture, is directly proportional to yield stress. The GS/30% CTP composite withstood high stress up to 284.3 MPa and was the top composite in terms of yield and flexural strength. Thus, only GS/10% CTP, GS/30% CTP, and GG1/30% CTP composites are suitable for building applications.

Table 4.4: Flexural strength of the coal composites

Sample name	Modulus (MPa)	Yield force (N)	Yield stress (MPa)	Yield strain (%)	Flexural strength (MPa)
GS/20% DMPS	N/A	N/A	N/A	N/A	-
GG1/20% DMPS	N/A	N/A	N/A	N/A	-
GS/10% CTP	1030500±500	97.5±0.721	85.2±0.681	0.00830±0.0005	48.75±0.361
GS/30% CTP	1270000±264.6	318.7±1.528	284.3±6.429	0.0148±0.000306	159.3±0.764
GG1/10% CTP	N/A	N/A	N/A	N/A	N/A
GG1/30% CTP	1408333±288.7	127.5±0.5	113±2	0.00261±0.000458	63.8±0.25

CTP: coal tar pitch; DMPS: dimethylpolysiloxane; GG1: coal discard; GS: greenside coal; MPa: megapascals; N: newtons; N/A: not applicable

4.2.7 Flammability test

A flammability test was conducted on the composites produced to determine if they were fire resistant. The test was conducted using a butane acetylene torch at various exposure times, as shown in Figure 4.16. The linear ablation rate (LAR), which is the ratio of the heat flux to the enthalpy needed to heat and melt a unit volume of concrete, was applied to the composites. This provides information on the change in thickness (mm) of the composites over exposure time (seconds). The thickness of the composites after different flame exposure times are provided in Table A.14.

Figure 4.17 demonstrates that the LAR decreased slightly when the CTP content in the composites increased from 10% to 30% for 30- and 40-seconds exposure time. For the 30% CTP-GS composite, the LAR was 0.00367, 0.00983, 0.00311, and 0.00275 mm/sec for exposure times of 10, 20, 30, and 40 seconds, respectively. The 30% CTP-GG1 composites had LAR values of 0.00400, 0.0286, 0.00811, and 0.00650 mm/sec for the same exposure times, respectively. The decline in LAR post 20 s of exposure time suggests the formation of a char-like substance resistant to the butane acetylene torch flame. In general, the GS/CTP composites exhibited better resistance to substantial volume/thickness changes under intense heat compared to the GG1/CTP composites.

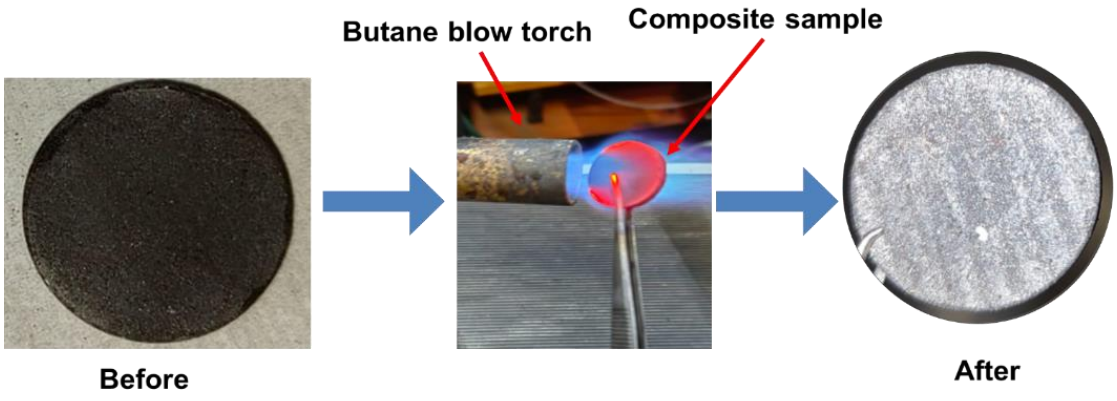

Figure 4.16: Flammability test of coal composites

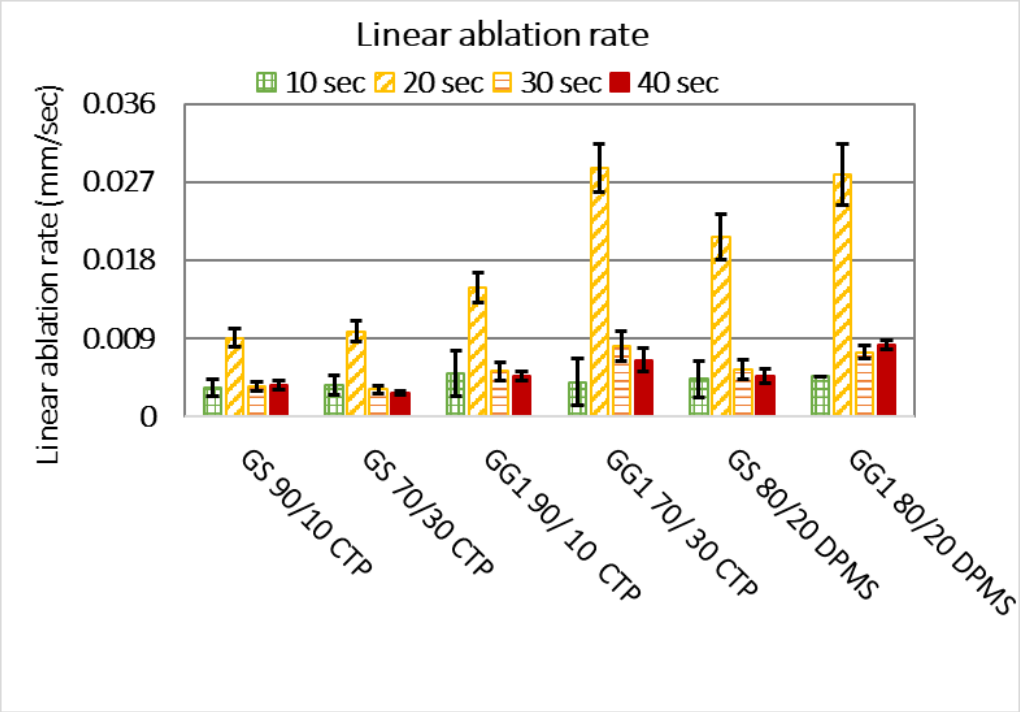

Figure 4.17: Linear ablation rate

Figure 4.18 displays the mass ablation rate (MAR) results for all composites, and there was no correlation between LAR and MAR (see Table A.12 for mass residual after different flame exposure times). For most composites, the MAR was high within the first ten seconds, which signifies the mass loss for this flame exposure time. As the exposure times increased, lower MAR values, indicating a slower rate of mass change over time, were noted. The 10% CTP-GG1 and 10% CTP-GS coal-based composites had similar MARs, while there was a significant difference between 30% CTP-GG1 and GS composites. The 30% CTP-GS composite had a higher MAR than 30% CTP-GG1. The high H/C ratio in GS might have made it less thermally stable than GG1 samples (Marcovich *et al*., 2001; Rimdusit *et al*., 2005; Sliwa *et al*., 2012). In addition, the higher volatile matter content in GS coal might also lead to the composite's higher MAR. The MAR for all composites produced was less than 0.008 g/sec, which is lower than the 0.1 g/sec flammability criterion for mesophase pitch-phenolic composites applicable as thermal protection systems for spacecraft, as reported by Huang *et al*. (2022).

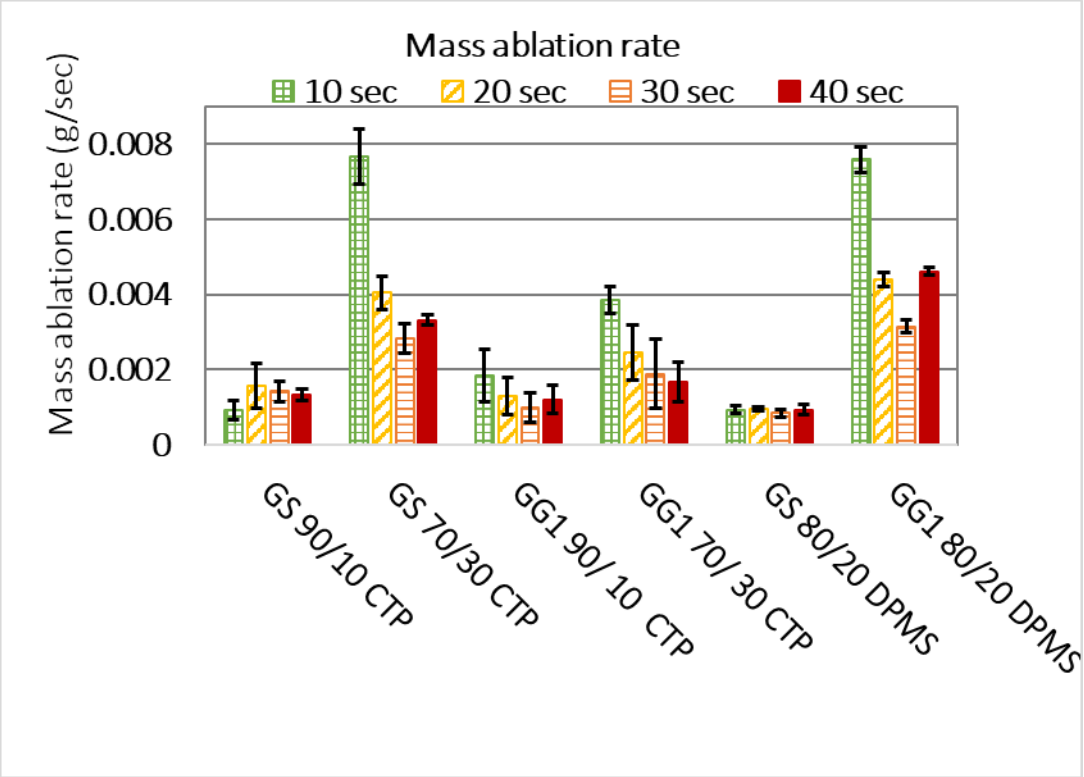

Figure 4.18: Mass ablation rate of coal composites

4.2.8 Corrosion resistance

Corrosion is one of the factors that contribute to composite failure, either directly or indirectly. The corrosion rates gauge the corrosion resistance of the composite and hence the durability of the composite. These rates reflect how swiftly composite degradation could occur due to chemical reactions upon exposure to corrosive environments, particularly in extreme or low pH levels. For this study, the composites were subjected to short-term laboratory tests by exposing them to an alkaline solution for seven days. As depicted in Figure 4.19, GS-based composites corroded faster than those of GG1-based composites. The corrosion rate increased as the CTP content of the composites increased. The high corrosion rate achieved from GS coal composites may be due to the high carbon content of GS. The highest corrosion rate of 0.081 µmpy achieved for the GS 80%/20% DMPS composites is minimal compared to commercial glaze ceramic floor tiles at 0.2427 µmpy reported by Ali *et al*. (2019). The full analysis is provided in Table A.11.

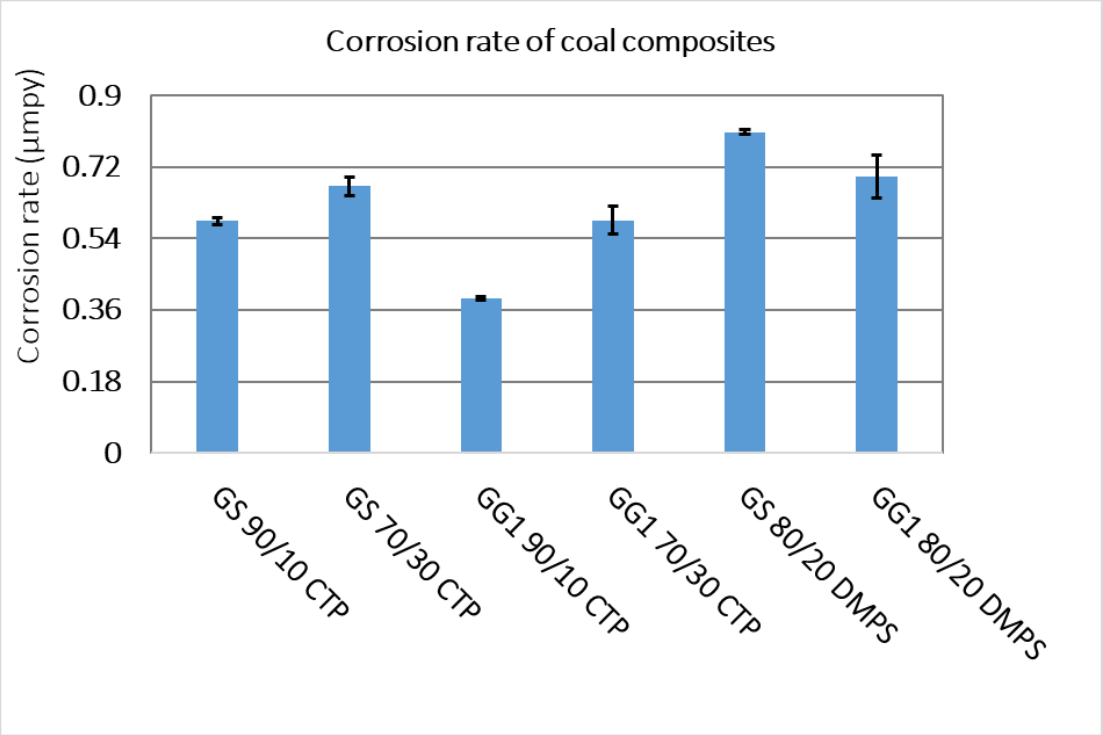

Figure 4.19: Corrosion resistance of coal composites

4.2.9 Environmental friendliness

Coal is known to contain a diverse array of heavy and trace metal elements, which have the potential to react with the surrounding environment. Additionally, composites derived from coal may release soluble constituents upon interaction with various substances, which may pose potential environmental hazards during their use. To mitigate any adverse environmental impacts associated with the use of coal composites, it is essential to carefully consider and manage these factors. Understanding the risks and properties of disposing and using coal composites in the environment is crucial. Leaching tests were conducted on the composites at pH 2.9, 4.9, and 9.2 to assess the release of trace elements. Additionally, the solution's concentrations of heavy and toxic elements were examined against the leachable concentration threshold (LCT) established by waste management standards (NEM WA, 2008).

The composites' concentrates were evaluated and compared with three types of waste management risk assessment data, i.e. LCT 0, LCT 1, LCT 2, and LCT 3 as shown in Table 4.5. From the standard, green indicates low risk (LCT 0), blue indicates moderate risk (LCT 1), yellow indicates high risk (LCT 2), and red indicates extreme high risk (LCT 3). As, Cr, Cu, Zn, Hg, Se, Cd, and Pb from the composites are low and moderate risk, mostly in pH 2.9 (acidic environment). Mn in GG1/30 CTP and GS/20 DMPS exhibited high risk at pH 2.9 and

4.9, respectively. The low risk posed by the trace elements in the eluate can be attributed to the stable phase obtained by the composite during pyrolysis. Variations in the pH level do not affect the release of these trace elements into the solution, as shown in Table 4.5. According to the results, the composites produced in this study are unlikely to pose any environmental risks, which makes them suitable for building applications. However, further environmental analyses are necessary to fully assess the eco-friendliness of these composites when used in large quantities.

Table 4.5: Leaching behaviour of the coal composites

Metal ion contaminants	Concentration (mg/L)															
	pH= 2.9				pH= 4.9				pH= 9.2				LCT 0 Low risk	LCT 1 Moderate risk	LCT 2 High risk	LCT 3 Extreme risk
	GG1/ 30 CTP	GG1/ DMPS	GS/ DMPS	GS/ 30 CTP	GG1/ 30 CTP	GG1/ DMPS	GS/ DMPS	GS/ 30 CTP	GG1/ 30 CTP	GG1/ DMPS	GS/ DMPS	GS/ 30 CTP				
As	0.0085	0.161	0.0702	0.156	0.211	0.0168	0.0243	0.233	0.0026	0.0031	0.0033	0.0016	0.01	0.5	1	4
Cr	0.0416	0.105	0.144	0.418	0.353	0.0286	0.0292	0.725	0.0260	0.0052	0.0084	0.0228	0.1	5.0	10	40
Cu	0.0859	0.0856	0.195	0.0822	0.312	0.0948	0.255	0.144	0.0257	0.0474	0.0324	0.0513	2.0	100	200	800
Hg	<0.00 1	<0.00 1	<0.00 1	<0.00 1	0.0015	<0.00 1	<0.00 1	<0.00 1	<0.00 1	<0.00 1	0.0014	<0.00 1	0.006	0.3	0.6	2.4
Se	0.0178	0.0378	0.0233	0.0275	0.0256	0.0284	0.0223	0.0467	0.0108	0.0104	0.0085	0.0209	0.01	0.5	2.0	8
Cd	0.00434	0.00213	0.00165	0.00093	0.00077	0.00086	0.00076	0.00175	0.00040	0.00081	0.00052	0.00046	0.003	0.15	0.3	1.2
Zn	0.0574	1.068	0.514	1.352	1.923	0.646	1.276	1.808	0.0163	0.309	0.0285	0.0163	5.0	250	500	2000
Pb	0.0123	0.0851	0.0349	0.119	0.0125	0.088	0.005	0.122	0.001	0.0029	0.0014	0.0011	0.01	0.5	1	4
Mn	25.2	13.0	17.3	19.8	9.4	2.6	45.2	17.4	< 0.1	1.1	< 0.1	< 0.1	0.5	25	50	200

GG1: GG1 coal discard; GS: greenside coal fines; CTP: coal tar pitch; DMPS: dimethylpolysiloxane; LCT: leaching concentration threshold; As: arsenic; Cr: chromium; Cu: copper; Hg: mercury; Se: selenium; Cd: caladium; Zn: zinc; Pb: lead; Mn: manganese

Color codes for risk management

- Low risk
- Moderate risk
- High risk
- Extreme risk

Chapter 5

Conclusion and Recommendations

This chapter provides the comprehensive conclusions drawn from the results obtained from this research. It shows the relationship between the physicochemical, mechanical, structural, and thermal properties of coal, coal tar, CTP, and coal composites produced. It also provides recommendations for future research.

5.1 Conclusion

This study analysed fine coal and coal tar samples, air-blowing coal tar to produce CTP, as well as the fabrication and characterisation of coal composites produced from the blend of CTP and DMPS with fine coals. From the characterisation of the raw samples, coal composites, and both binders, the following conclusions have been drawn:

I. Increasing the air-blowing residence time and temperature increased the total carbon content and low volatile matter in the CTP produced at 400°C for nine hours and at 450°C for six hours, respectively. The CTP produced exhibited a low H/C atomic ratio and high aromatic ratio (f_a), which shows that increasing the air-blowing pretreatment temperature and time increased the aromaticity of the CTP. In addition, with an increasing air-blowing temperature, anisotropic spherules in the resulting CTP become coarser.

II. The FTIR results showed that DMPS was more aliphatic (2962 cm^{-1} wave number) than coal tar. The aliphatic CH stretch that appeared at 3054-2895 cm^{-1} for coal tar was not visible in the CTP produced (all residence times and temperatures), and more aromatic groups were formed as the air-blowing time and temperature increased.

III. The XRD analysis results revealed that the coal fines had more inorganic minerals than organic components, which is consistent with the presence of more than 60% ash in both coals. Coal tar and CTP are organic substances with little or no mineral content, as they both have over 80% total carbon content. The resulting composites made from CTP and coal fines had amorphous humps due to the carbon from CTP present in the composites.

IV. The Raman spectroscopic data revealed the decrease in the I_D/I_G ratio results in a high L_a, which is evidence of an amorphous carbon structure in the composites with low I_D/I_G ratio.

V. The thermal stability of composites containing high CTP content was superior, with all exhibiting low mass degradation at 600°C. The thermal stability of the GS composites was lower than that of the GG1 composites. The fusibility and surface homogeneity of the GS/CTP composites in micrographs are the reason for this difference.

VI. The water absorption behaviour of the composites had an inverse relationship with the concentration of CTP, due to the lower H/C atomic ratio of CTP. This characteristic contributed to the high aromaticity and densification of the composites, which reduced their porosity. Conversely, DMPS-based composites showed high water absorption due to their relatively higher aliphatic nature compared to CTP. Additionally, microscopic examination revealed a decrease in surface cracks as the CTP content increased. This phenomenon was attributed to the enhanced fusibility and compaction of composites rich in aromatic constituents.

VII. As the binder proportion increased, the compressive strength of the composite increased. GG1 coal with a more intense O-H group produced higher compressive strength composites when mixed with CTP at 10 and 30% compared to GS-based composites.

VIII. The only composites that exhibit flexural strength were GS/10% CTP, GS/30% CTP, and GG1/30% CTP, with strengths of 48.75, 159.30, and 63.80 MPa, respectively. The composite with the highest modulus was GG1/30% CTP due to its high O-H group concentration.

IX. This study confirmed that composites with high CTP content have lower flammability. Furthermore, the CTP-GS composites are more aromatic and could sustain high temperatures without significant volume changes than the CTP-GG1 composites.

X. All composites had leachable concentrations below the moderate risk threshold, as shown in the context of managing heavy and trace element waste. These composites showed low risks across a wide pH range, including acidic, neutral, and alkaline conditions. The findings indicate that the coal composites that were produced are environmentally friendly and can be used safely in typical conditions. Furthermore, their ability to maintain low risk levels in harsh environmental conditions shows their potential for use without causing harm to the environment.

5.2 Recommendations

This study has unequivocally demonstrated that CTP can be used as a binder to produce composites suitable for construction applications. Based on the finding in this study, it is necessary to make composite materials that are similar in size to standard building materials like bricks and tiles and then subject them to the same standards as these building materials. In addition, this study recommends an optimisation study for coal composites to determine the following:

I. A pilot scale of coal composite manufacturing should be conducted.
II. Tank leaching experiments on coal composites should be conducted to assess the concentration of heavy metal elements leached over a long period.
III. Assessing the economic viability of the composites is necessary to determine the feasibility of using coal composites in comparison to conventional building materials.

References

Abali, F., Shivakumar, K., Hamidi, N. and Sadler, R. (2003). An RTM densification method of manufacturing carbon–carbon composites using Primaset PT-30 resin. *Carbon*, 41(5), pp.893-901.

Abdulsalam, J., Mulopo, J., Bada, S. and Oboirien, B. (2020). Natural gas storage properties of adsorbents synthesised from three different coal waste in South Africa. *Fuel*, 267, 117157.

Alcañiz-Monge, J., Cazorla-Amorós, D. and Linares-Solano, A. (2001). Characterisation of coal tar pitches by thermal analysis, infrared spectroscopy and solvent fractionation. *Fuel*, 80(1), pp.41-48.

Alcañiz-Monge, J., Cazorla-Amorós, D., Linares-Solano, A., Oya, A., Sakamoto, A. and Hosm, K. (1997). Preparation of general purpose carbon fibers from coal tar pitches with low softening point. *Carbon*, 35(8), pp.1079-1087.

Ali, N., Putra, T.E., Husaini, Iskandar, V.Z. and Thalib, S. (2019). Corrosion rate of low carbon steel for construction materials in various *NaCl* concentrations. *IOP Conference Series: Materials Science and Engineering*, 536, 012015.

Al-Majali, Y.A., Chirume, C.T., Marcum, E.P., Daramola, D.A., Kappagantula, K.S. and Trembly, J.P. (2019). Coal-filler-based thermoplastic composites as construction materials: A new sustainable end-use application. A*CS Sustainable Chemistry & Engineering*, 7(19), pp. 16870-16878.

Al-Majali, Y.T. et al. (2023) 'Mechanical performance assessment of sustainable coal plastic composite building materials', Journal of Building Engineering, 80, p. 108089.

Alonso-Santurde, R., Coz, A., Viguri, J.R. and Andrés, A. (2012). Recycling of foundry by-products in the ceramic industry: Green and core sand in clay bricks. *Construction and Building Materials*, 27(1), pp. 97-106.

American Elements. (2023) *Poly(dimethylsiloxane)*. Available at: https://www.americanelements.com/poly-dimethylsiloxane-63148-62-9 (Accessed: 15 September 2023).

Ancheyta, J., Rana, M.S. and Furimsky, E. (2005). Hydroprocessing of heavy petroleum feeds: Arai, Y. (2016). Pitch-based carbon fibers, In: The Society of Fibre Science and Technology (Ed.), *High-performance and specialty fibers*, pp.343-354. Springer.

ASTM C373-18, Standard test methods for determination of water absorption and associated properties by vacuum method for pressed ceramic tiles and glass tiles and boil method for extruded ceramic tiles and non-tile fired ceramic whiteware products, ASTM International, West Conshohocken, PA, 2018, www.astm.org.

ASTM C67-05. Standard test methods for sampling and testing brick and structural clay tile, ASTM International, West Conshohocken, PA, 2003. https://www.astm.org/

Bai, Y.F., Cao, X.X., Xu, M.L., He, X.F. and Cai, G.H. (2019). Coal powder and ethylene-propylene-diene monomer reinforced hybrid polypropylene composites. *Materials Science Forum*, 956, pp.192-200.

Banerjee, C., Chandaliya, V.K. and Dash, P.S. (2021). Recent advancement in coal tar pitch-based carbon fiber precursor development and fiber manufacturing process. *Journal of Analytical and Applied Pyrolysis*, 158, 105272.

Banerjee, C., Chandaliya, V.K., Dash, P.S. and Meikap, B.C. (2019). Effect of different parameters on porosity and compressive strength of coal tar pitch derived carbon foam. *Diamond and Related Materials*, 95, pp.83-90.

Bardají Luna, M. and Coco Cea, S. (2022). Organometallic mesogens, In: G. Parkin, K. Meyer and D. O'Hare (Eds.), *Comprehensive organometallic chemistry IV*, pp.285-338. Elsevier.

Bartolomei, S.S. and Wiebeck, H. (2019). Characterization of gypsum waste from civil construction to obtain polymer composites. Materials Science Forum, 958, pp. 47–51.

Bermudez, V., Lukubira, S. and Ogale, A.A. (2018). 1.3 Pitch precursor-based carbon fibers. *Comprehensive Composite Materials II*, 1, pp.41-65.

Berrueco, C., Álvarez, P., Díez, N., Granda, M., Menéndez, R., Blanco, C., et al. (2012). Characterisation and feasibility as carbon fibre precursors of isotropic pitches derived from anthracene oil. *Fuel*, 101, pp.9-15.

Bi, H., Ziaojun, H., Zhang, H., Li, H., Xiao, N. and Qiu, J. (2021). N, P co-doped hierarchical porous carbon from rapeseed cake with enhanced supercapacitance. *Renewable Energy*, 170, pp.188-196.

Blanco, C., Santamaría, R., Bermejo, J. and Menéndez, R. (2000). A comparative study of air-blown and thermally treated coal-tar pitches. *Carbon*, 38(4), pp.517-523.

Britannica Kids (2022). *Coal-tar product*. Available at: https://kids.britannica.com/students/article/coaltarproduct/273711#:~:text=About%20one%20fourth%20of%20the,a%20tower%20called%20a%20scrubber (Accessed: 5 August 2022).

Bureau of Indian Standards. 1992. IS: 3495 (Part 1, 2 and 3) (1992). Methods of tests of burnt clay building bricks — Specification. New Delhi: Bureau of Indian Standards

Cha, J., Seo, J. and Kim, S. (2011) 'Building materials thermal conductivity measurement and correlation with heat flow meter, laser flash analysis and TCI', Journal of Thermal Analysis and Calorimetry, 109(1), pp. 295–300.

Chai, L., Lou, B., Yu, R., Wen, F., Yuan, H., Li, Z., et al. (2021). Study on structures and properties of isotropic pitches and carbon fibers from co-carbonization of aromatic-rich distillate oil and polyethylene glycol. *Journal of Analytical and Applied Pyrolysis*, 158, 105260.

Chawla, K.K. (2012). Ceramic matrix composites. *Composite Materials*, pp. 249–292.

Chelgani, S.C. and Matin, S.S. (2018). Study the relationship between coal properties with Gieseler plasticity parameters by random forest. *International Journal of Oil, Gas and Coal Technology*, 17(1), pp.113-127.

Chen, A., Fu, X., Liu, L., Wang, W., Yu, Y. and Zhang, Y. (2018). Synthesis of nitrogen-doped porous carbon monolith for binder-free all-carbon supercapacitors. *ChemElectroChem*, 6(2), pp.535-542.

Chen, C., et al. (2017). Carbon-carbon composites for heat exchanger applications: a review. *Journal of Materials Science*, 52(13), pp.7641-7659.

Choi, D., Kil, H.-S. and Lee, S. (2019). Fabrication of low-cost carbon fibers using economical precursors and advanced processing technologies. *Carbon*, 142, pp.610-649.

Chowdhury, P., Sehitoglu, H. and Rateick, R. (2018). Damage tolerance of carbon-carbon composites in aerospace application. *Carbon*, 126, pp.382-393.

Clough, H. (1957). Gasoline production from coal tar oils. *Industrial & Engineering Chemistry*, 49(4), pp.673-678.

Collett, G.W. and Rand, B. (1978). Thixotropic changes occurring on reheating a coal tar pitch containing mesophase. *Carbon*, 16(6), pp. 477–479.

Cuesta, A., Dhamelincourt, P., Laureyns, J., Martínez-Alonso, A. and Tascón, J.M. (1998). Comparative performance of X-ray diffraction and Raman microprobe techniques for the study of carbon materials. *Journal of Materials Chemistry*, 8(12), pp.2875-2879.

Daguerre, E., Nauguier, F. and Py, X. (1998). Alpha-relaxation of a coal tar pitch and temperature-density effects on the viscoelastic parameters analysis. *Carbon*, 36(7-8), pp.1099-1105.

Das Lala, S., Deoghare, A. and Chatterjee, S. (2018). Effect of reinforcements on polymer matrix bio-composites – an overview. *Science and Engineering of Composite Materials*, 25(6), pp.1039-1058.

Daulbayev, C. Kaidar, B., Sultanov, F., Bakbolat, B., Smagulova, G. and Mansurov, Z. (2021). The recent progress in pitch derived carbon fibers applications. A review. *South African Journal of Chemical Engineering*, 38, pp.9-20.

De Araújo, M. (2011). Natural and man-made fibres: Physical and mechanical properties, In: R. Fangueiro (Ed.), *Fibrous and composite materials for civil engineering applications*, pp.3-28. Woodhead Publishing.

Department of Economic and Social Affairs (2021). *2019 Energy statistics yearbook*. United Nations.

Dresselhaus, M.S., Jorio, A., Souza Filho, A.G. and Saito, R. (2010). Defect characterization in graphene and carbon nanotubes using Raman spectroscopy. *Philosophical Transactions of the Royal Society A: Mathematical, Physical and Engineering Sciences*, 368(1932), pp.5355-5377.

Dun, W., Guijian, L., Ruoyu, S. and Xiang, F. (2013). Investigation of structural characteristics of thermally metamorphosed coal by FTIR spectroscopy and X-ray diffraction. *Energy & Fuels*, 27(10), pp.5823-5830.

Eckel, Z.C. Zhou, C., Martin, J.H., Jacobsen, A.J., Carter, W.B. and Schaedler, T.A. (2016). Additive Manufacturing of polymer-derived ceramics. *Science*, 351(6268), pp.58-62.

Eliche-Quesada, D., Martínez-García, C., Martínez-Cartas, M.L., Cotes-Palomino, M.T., Pérez-Villarejo, L., Cruz-Pérez, N. and Corpas-Iglesias, F.A. (2011). The use of different forms of waste in the manufacture of ceramic bricks. *Applied Clay Science*, 52(3), pp.270-276.

Enerdata. (2022). *Coal and lignite production data*. Available at: https://yearbook.enerdata.net/coal-lignite/coal-production-data.html (Accessed: 13 August 2022).

Eterigho-Ikelegbe, O., Ricohermoso III, E., Harrar, H., Riedel, R. and Bada, S. (2023a). Correction: Strong, lightweight, thermally stable, and hydrophobic sustainable structural composites produced from coal-based waste and polymer-derived SiOC ceramics. *Clean Technologies and Environmental Policy*, 25, pp.2885-2887.

Eterigho-Ikelegbe, O., Ricohermoso III, E., Harrar, H., Riedel, R. and Bada, S. (2023b). Strong, lightweight, thermally stable, and hydrophobic sustainable structural composites produced from coal-based waste and polymer-derived SiOC ceramics. *Clean Technologies and Environmental Policy*, 25, pp.2865-2884.

Eterigho-Ikelegbe, O., Trammell, R. and Bada, S. (2021a). Preparation and characterization of ceramic composites from South Africa coal discard. *Construction and Building Materials*, 302, 124164.

Eterigho-Ikelegbe, O., Trammell, R. and Bada, S.O. (2022). Novel ceramic composites produced from coal discards with potential application in the building and construction sectors. *Journal of the Southern African Institute of Mining and Metallurgy*, 122(8), pp.421-428.

Eterigho-Ikelegbe, O., Trammell, R., Ricohermoso III, E. and Bada, S. (2023c). Mechanism of bonding, surface property, electrical behaviour, and environmental friendliness of carbon/ceramic composites produced via the pyrolysis of coal waste with polysiloxane polymer. *Environmental Science and Pollution Research*, 30, 93786-93799.

Eterigho-Ikelegbe, O., Yoro, K.O. and Bada, S. (2021b). Coal as a filler in polymer composites: A review. *Resources, Conservation and Recycling*, 174, 105756.

Fan, X. Fe, Y., Chen, L. and Li, W. (2017). Distribution and structural analysis of polycyclic aromatic hydrocarbons abundant in coal tar pitch. *Energy & Fuels*, 31(5), pp.4694-4704.

Fang, R., Zhao, S., Hou, P., Cheng, M., Wang, S., Cheng, H.-M., et al. (2016). 3D interconnected electrode materials with ultrahigh areal sulfur loading for Li-S batteries. *Advanced Materials*, 28(17), pp.3374-3382.

Fernández, J.J, Figueiras, A., Granda, M., Bermejo, J. and Menéndez, R. (1995). Modification of coal-tar pitch by air-blowing. Variation of pitch composition and properties. *Carbon*, 33(3), pp.295-307.

Ferrari, A.C. (2007). Raman spectroscopy of graphene and graphite: Disorder, electron-phonon coupling, doping and nonadiabatic effects. *Solid State Communications*, 143(1–2), pp.47-57.

Fitzer, E., Kompalik, D. and Yudatet, K. (1987). Rheological characteristics of coal-tar pitches. *Fuel*, 66(11), pp.1504-1511.

Fraga, M., Flores, B., Osório, E. and Vilela, A. (2020). Evaluation of the thermoplastic behavior of charcoal, coal tar and coking coal blends. *Journal of Materials Research and Technology*, 9(3), pp.3406-3410.

Future Market Insights. (2022). *Coal tar pitch market*. Available at: https://www.futuremarketinsights.com/reports/coal-tar-pitch-market (Accessed: 13 August 2022).

Gagarin, H., Sridhar, S., Lange, I. and Bazilian, M. (2020). Considering non-power generation uses of coal in the United States. *Renewable and Sustainable Energy Reviews*, 124, 109790.

Galande, P. (2016). Effect of various fillers on mechanical properties of glass fiber reinforced polymer composites: A review. *International Journal of Emerging Trends in Science and Technology*, 3(04), 3778-3782.

Gan, Y.X., Solomon, D. and Reinbolt, M. (2010). Friction stir processing of particle reinforced composite materials. *Materials*, 3(1), pp.329-350.

Gao, B., Zhang, R., He, M., Sun, L., Wang, C., Liu, L., et al. (2016). Effect of a multiscale reinforcement by carbon fiber surface treatment with graphene oxide/carbon nanotubes on the mechanical properties of reinforced carbon/carbon composites. *Composites Part A: Applied Science and Manufacturing*, 90, pp.433-440.

Gao, F. (2004). Clay/polymer composites: The story. *Materials Today*, 7(11), pp.50-55.

George, W. K. & Beuther, P. D. (1977). Pressure spectra in a homogeneous isotropic turbulent flow. *Bull. Am. Phys. Soc*. 22, 1285

Globe Newswire. (2022). *Coal tar pitch market to reach US$ 5,145.5 Mn by 2028 - Comprehensive research report by FMI.* Available at: https://www.globenewswire.com/en/news-release/2022/02/10/2382366/0/en/Coal-Tar-Pitch-Market-to-reach-US-5-145-5-Mn-by-2028-Comprehensive-Research-Report-by-FMI.html (Accessed: 13 August 2022).

Gopalakrishnan, S. and Murugan, N. (2012). Production and wear characterisation of AA 6061 matrix titanium carbide particulate reinforced composite by enhanced stir casting method. *Composites Part B: Engineering*, 43(2), pp.302-308.

Granda Ferreira, M., Blanco Rodríguez, C., Álvarez Rodríguez, P., Patrick, J. W., Menéndez López, R. M. (2013). Chemicals from coal coking. *Chemical Reviews*, 114(3), pp.1608-1636.

Greene, J.P. (2021). *Automotive plastics and composites*. Elsevier.

Guang-Heng, W., An-ning, Z. and Xiao-Bing, H. (2006). Effect of coal filler on the properties of soy protein plastics. *Journal of Applied Polymer Science*, 102(4), pp.3134-3143.

Guo, X., et al. (2019). Preparation and properties of building materials based on coal gangue and biomass fly ash. *Journal of Materials in Civil Engineering*, 31(9), 04019191

Hafeez, M. (2022). Recent progress and overview of nanocomposites, In: A. Sharma (Ed.), *Nanocomposite materials for biomedical and energy storage applications.* IntechOpen.

Haghshenas, M. (2016). Metal–matrix composites. *Reference Module in Materials Science and Materials Engineering* [online].

He, X., Li, X., Ma, H., Han, J., Zhang, H. Yu, C., et al. (2017). ZnO template strategy for the synthesis of 3D interconnected graphene nanocapsules from coal tar pitch as supercapacitor electrode materials. *Journal of Power Sources,* 340, pp.183-191.

Hegde, R. R., et al. (2013). Carbon-carbon composites from coal tar pitch and carbon fiber precursor for high-temperature applications. *Journal of Composite Materials*, 47(2), pp.155-163.

Hill A., Easter W. (2019). Carbon Ceramic Composites and Methods (Google Patents). *Patent No*: US20190292441A1

Hill A., Easter W. (2021). Carbon ceramic composites and methods. *Patent No: U.S. Patent* 10,988,680. https://patents.google.com/patent/US10988680B2/en. Accessed 23 Sept 2022

Hill A., Sherwood W., Trammell R., Easter W. (2022). High strength, tough, coal and coal by-product based composite ceramics (Google Patents). *Patent No*: US20220144706A1

Hsissou, R., Seghiri, R., Benzekri, Z., Hilali, M., Rafik, M. and Elharfi, A. (2021). Polymer composite materials: A comprehensive review. *Composite Structures,* 262, 113640.

Hu, G., Bian, Z., Xue, R., Huang, W. and Komarneni, S. (2017). Polymer-coal composite as a novel plastic material. *Materials Letters*, 197, pp.31-34.

Huang, X. (2009). Fabrication and properties of carbon fibers. *Materials*, 2(4), pp.2369-2403.

Huang, Y., Zhang, H. Liu, Z., Zhou, C., Yan, L., Zou, H., et al. (2023a). Pre-oxidized mesophase pitch modified phenolic composites with mosaic-structured char layers and excellent ablation resistance. *Composites Part B: Engineering*, 257, 110691.

Huang, Y., Zhang, H., Zhang, X., Yan, L., Ling, Y., Zou, H., et al. (2022). Effect of mesophase pitch incorporation on the ablation behavior and mechanism of phenolic composites. *Industrial & Engineering Chemistry Research*, 61(13), pp.4612-4624.

Huang, Z., Zhou, W. and Wei, J. (2023b). Study on the molecular structure model of tar-rich coal and its pyrolysis process. *Journal of Molecular Structure*, 1286, 135613.

Hunt, W.H. (2000). 6.05 - Metal matrix composites. *Comprehensive composite materials*, 6, pp.57-66.

Husić, S., Javnu, I. and Petrović, Z.S. (2005). Thermal and mechanical properties of glass reinforced soy-based polyurethane composites. *Composites Science and Technology*, 65(1), pp.19-25.

Igisu, M., Ueno, Y., Komiya, T., Awramik, S.M., Ikemoto, Y. and Takai, K. (2022). Spatial distribution of organic functional groups in Ediacaran acritarchs from the Doushantuo Formation in South China as revealed by micro-FTIR spectroscopy. *Precambrian Research*, 373, 106628.

International Energy Agency (2023). Coal market update – July 2023. https://www.iea.org/reports/coal-market-update-july-2023/demand (Accessed: 22 October 2023).

International Energy Agency. (2021). Coal 2021: Analysis and forecast to 2026. Paris, France: IEA Publications.

Ispatguru.com. (2018). *Coal tar and its distillation processes.* Available at:. https://www.ispatguru.com/coal-tar-and-its-distillation-processes/ (Accessed: 29 July 2022).

Jayaseelan, C. et al. (2013). Green synthesis of gold nanoparticles using seed aqueous extract of abelmoschus esculentus and its antifungal activity. *Industrial Crops and Products*, 45, pp. 423–429.

Jayaseelan, D. D., et al. (2012). Processing and characterization of carbon-carbon composites for high temperature aerospace applications. *Journal of Materials Science*, 47(1), pp.38-56.

Jiang, J., Yang, W., Cheng, Y., Liu, Z., Zhang, Q. and Zhao, K. (2019). Molecular structure characterization of middle-high rank coal via XRD, Raman and FTIR spectroscopy: Implications for coalification. *Fuel*, 239, pp.559-572.

Jiang, J., Zhang, S., Longhurst, P., Yang, W. and Zheng, S. (2021). Molecular structure characterization of bituminous coal in northern China via XRD, Raman and FTIR spectroscopy. *Spectrochimica Acta Part A: Molecular and Biomolecular Spectroscopy*, 255, 119724.

Jiang, T. et al. (2019) 'Comprehensive reuse of pyrolysis chars from coals for fabrication of highly insulating building materials', Journal of Cleaner Production, 222, pp. 424–435.

Jurisch, S., Heim, S., Krooss, B. and Littke, R. (2012). Systematics of pyrolytic gas (N_2, CH_4) liberation from sedimentary rocks: Contribution of organic and inorganic rock constituents. *International Journal of Coal Geology*, 89, pp.95-107.

Kelham, S. (1988). A water absorption test for concrete. *Magazine of Concrete Research*, 40(143), pp.106-110.

Kim, J., Ui-Su, I., Byungrok, L., Dong-Hyun, P., Seong-Ho, Y., Doo-Hwan, J., et al. (2016). Pitch-based carbon fibers from coal tar or petroleum residue under the same processing condition. *Carbon Letters*, 19, pp.72-78.

Kim, K. J., et al., (2004). Ceramic composites from coal fly ash: processing, properties and applications. *International Journal of Applied Ceramic Technology*, 1(5), pp.402-414.

Kim, M. H. and Pandey, A. (2019). Utilization of coal bottom ash as fine aggregate in colored tiles. *Sustainability*, 11(7), 2141.

Krenkel, W. (2018). *Ceramic matrix composites*. Springer

Kumar, A., et al. (2019). Ceramic materials for construction industry: a review. *Materials Today: Proceedings* 18, 3471-3476

Kumar, S., et al. (2020). Environmental impact assessment of coal ash disposal: A case study of Singrauli region, India. *Environmental Science and Pollution Research*, 27(8), 7927-7944

Kwon, S. J., et al. (2005). Ceramic composites using coal fly ash for concrete reinforcement. *Journal of the American Ceramic Society*, 88(2), 311-313

Letcher, T. (Ed.) (2008). *Future energy* (1st ed.). Elsevier.

Li, C., & Wang, Y. (2020). A review of the potential application of coal mine tailings in building materials. Environmental Science and Pollution Research, 27(29), 36497-36508.

Li, D., Li, Z., Li, W., Liu, Q., Feng, Z. and Fan, Z. (2013). Hydrotreating of low temperature coal tar to produce clean liquid fuels. *Journal of Analytical and Applied Pyrolysis*, 100, pp.245-252.

Li, H. et al. (2012). Carbon nanodots: synthesis, properties and applications. *Journal of Materials Chemistry*, 22(46), p. 24230.

Li, J., Duan, Q., Xia, G., Wan, Z., Yin, G. and Xie, J., et al. (2022). Enhancing surface insulation of glass fiber reinforced polymer composites by plasma fluorinating glass fiber. *Polymer Composites*, 43(8), pp.5715-5725.

Li, M., Liu, D., Du, H., Li, Q., Hou, X and Ye, J. (2015). Preparation of mesophase pitch by aromatics-rich distillate of naphthenic vacuum gas oil. *Applied Petrochemical Research*, 5(4), pp. 339-346.

Liew, K.B., Goh, C.F., Asghar, S. and Syed, H.K. (2021). Overview of mechanical and physicochemical properties of polymer matrix composites, In: D. Brabazon (Ed.), *Encyclopedia of materials: Composites*, pp. 565-576. Elsevier.

Liu, H., Li, T., Wang, X., Zhang, W. and Zhao, T. (2014). Preparation and characterization of carbon foams with high mechanical strength using modified coal tar pitches. *Journal of Analytical and Applied Pyrolysis*, 110, pp.442-447.

Liu, X., Wang, Y. and Zhan, L. (2018). Carbon foams prepared from coal tar pitch for building thermal insulation material with low cost. *Chinese Journal of Chemical Engineering*, 26(2), pp.415-420.

Liu, Y., et al. (2019). Carbon-carbon composite heat exchanger: a review. *Journal of Thermal Science and Engineering Applications*, 11(4), 041011.

Longwell, J., Rubin, E.S. and Wilson, J. (1995). Coal: Energy for the future. *Progress in Energy and Combustion Science*, 21(4), pp.269-360.

Lu, Y., Hussein, A., Li, D., Huang, X., Mollaabbasi, R., Picard, D., et al. (2020). Properties of bio-pitch and its wettability on coke. *ACS Sustainable Chemistry & Engineering*, 8(40), pp.15366-15374.

Lu, Y., Kocaefe, D., Kocaefe, Y., Huang, X.-A., Bhattacharyay, D. and Coulombe, P. (2016). Study of the wettability of coke by different pitches and their blends. *Energy & Fuels*, 30(11), pp.9210-9216.

Ma, Z.-H., Wei, X.-Y., Liu, G.-H., Liu, F.-J. and Zong, Z.-M. (2021). Value-added utilization of high-temperature coal tar: A review. *Fuel*, 292, 119954.

Maeda, T., Zeng, S.M., Tokumitsu, K., Mondori, J. and Mochida, I. (1993). Preparation of isotropic pitch precursors for general purpose carbon fibers (GPCF) by air blowing—I. Preparation of spinnable isotropic pitch precursor from coal tar by air blowing. *Carbon*, 31(3), pp.407-412.

Magazzino, C., Bekun, F., Etokakpan, M. and Uzuner, G. (2020). Modeling the dynamic Nexus among coal consumption, pollutant emissions and real income: empirical evidence from South Africa. *Environmental Science and Pollution Research*, 27(8), pp.8772-8782.

Mallick, P.K. (2012). Advanced materials for automotive applications: An overview, In: J, Rowe (Ed.), *Advanced materials in automotive engineering*, pp.5-27. Woodhead Publishing Limited.

Mandal, A.K., Verma, H.R. and Sinha, O.P. (2017). Utilization of aluminum plant's waste for production of insulation bricks. *Journal of Cleaner Production*, 162, pp. 949–957.

Manjarekar, P., Gulpatil, R.D., Patil, V.P., Nikam, R.S. and Jeur, C.M. (2017). Utilization of plastic waste in foundry sand bricks. *International Journal for Research in Applied Science and Engineering Technology*, 5(III), pp.1114-1119.

Manocha, L.M. (2003). High performance carbon-carbon composites. *Sadhana*, 28(1-2), pp.349-358.

Marafi, A., Hauser, A. and Stanislaus, A. (2006). Atmospheric residue desulfurization process for residual oil upgrading: an investigation of the effect of catalyst type and operating severity on product oil quality. *Energy & Fuels*, 20(3), pp.1145-1149.

Marcovich, N.E., Reboredo, M.M. and Aranguren, M.I. (2001). Modified woodflour as thermoset fillers. *Thermochimica Acta*, 372(1–2), pp.45-57.

Mazumder, S., Saha, P. and Reza, M. (2020). Co-hydrothermal carbonization of coal waste and food waste: fuel characteristics. *Biomass Conversion and Biorefinery*, 12(1), pp.3-13.

Mehmandoust, M., Li, G. and Erk, N. (2022). Biomass-derived carbon materials as an emerging platform for advanced electrochemical sensors: Recent advances and future perspectives. *Industrial & Engineering Chemistry Research*, 62(11), pp.4628-4635.

Miller, B.G. (2005). *Coal energy systems*. Elsevier.

Miyajima, N., Akatsu, T., Ikoma, T., Ito, O., Rand, B. Tanabe, Y., et al. (2000). A role of charge-transfer complex with iodine in the modification of coal tar pitch. *Carbon*, 38(13), pp.1831-1838.

Mochida, I., Korai, Y., Ku, C., Watanabe, F. and Sakai, Y. (2000). Chemistry of synthesis, structure, preparation and application of aromatic-derived mesophase pitch. *Carbon*, 38(2), pp.305-328.

Mochida, I., Shimizu, K., Korai, Y., Otsuka, H., Sakai, Y. and Fujiyama, S. (1990). Preparation of mesophase pitch from aromatic hydrocarbons by the aid of HFBF3. *Carbon*, 28(2-3), pp.311-319.

Molewa BEE (2013) National environmental management: waste act, 2008 (act no.59 of 2008) national norms and standards for the assessment of waste for landfill disposal. http://sawic.environment.gov.za/documents/2177.pdf. Accessed 21 Apr 2023

Mora, E., Blanco, C., Santamaria, R., Granda, M. and Menéndez, R. (2003). A novel method to obtain a petroleum-derived mesophase pitch suitable as carbon fibre precursor. *Carbon*, 41(3), pp.445-452.

Mouzakis, D.E. (2013). Biomedical polymer composites and applications, In: S. Thomas, K. Joseph, S.K. Malhotra, K. Goda and M.S. Sreekala (Eds.), *Polymer composites*, pp.483-514. Wiley-VCH.

Muangwaeng, B., Rojananan, S. and Rojananan, S. (2013). The effect of injection parameters on morphology in metal injection moulding. *Advanced Materials Research*, 802, pp.174-178.

Nip, M., De Leeuw, J. and Crelling, J. (1992). Chemical structure of bituminous coal and its constituting maceral fractions as revealed by flash pyrolysis. *Energy & Fuels*, 6(2), pp.125-136.

Oh, S.-M., Yoon, S.H., Lee, G.D. and Park, Y.D. (1991). Effects of pressurized pretreatment on the preparation of mesophase pitch. *Carbon*, 29(7), pp.1009-1014.

Onifade, M. and Genc, B. (2018). Prediction of the spontaneous combustion liability of coals and coal shales using statistical analysis. *Journal of the Southern African Institute of Mining and Metallurgy*, 118(8).

Otani, S., Kokubo, Y. and Koitabashi, T. (1970). The preparation of highly-oriented carbon fiber from pitch material. *Bulletin of the Chemical Society of Japan*, 43(10), pp.3291-3292.

Ozbayoglu, G. (2018). 3.19 Energy production from coal. *Comprehensive Energy Systems*, 3, pp.788-821.

Papole, G., Focke, W.W. and Manyala, N. (2012). Characterization of medium-temperature Sasol–Lurgi gasifier coal tar pitch. *Fuel*, 98, pp.243-248.

Patel, A.B., Shaikh, S., Jain, K., Desai, C., Madamwar D. (2020). Polycyclic aromatic hydrocarbons: Sources, toxicity, and remediation approaches. *Frontiers in Microbiology*, 11.

Patel, R.H., Sharma, S., Prajapati, K.K., Vyas, M.M. and Batra, N.M. (2016). Studies on non-oxide coating on carbon fibers using plasma enhanced chemical vapor deposition technique. *AIP Conference Proceedings*, 1728, 020480.

Pavlova, I., Kutasheva, S.S. and Farafontova, E. (2019). Production technology of ceramic roof tiles based on raw materials of ural region. *IOP Conference Series: Materials Science and Engineering*, 687(2), 022022.

Peijs, T., Kirschbaum, R. and Lemstra, P.J. (2022). Chapter 5: A critical review of carbon fiber and related products from an industrial perspective. *Advanced Industrial and Engineering Polymer Research*, 5(2), pp.90-106.

Pendhari, S.S., Kant, T. and Desai, Y.M. (2008). Application of polymer composites in civil construction: A general review. *Composite Structures*, 84(2), pp.114-124.

Peng, Y., Yang, J., Shi, K., Guo, J. and Zhu, H. (2020). Effects of the degree of oxidation of pitch fibers on their stabilization and carbonization behaviors. *New Carbon Materials*, 35(6), pp.722-730.

Petrova, B., Tsyntsarski, B., Budinova, T., Petrov, N. Velasco, L.F. and Ania, C.O. (2011). Activated carbon from coal tar pitch and furfural for the removal of P-nitrophenol and m-aminophenol. *Chemical Engineering Journal*, 172(1), pp.102-108.

Phillips, L.N., Kappagantula, K.S. and Trembly, J.P. (2019). Mechanical performance of thermoplastic composites using bituminous coal as filler. Study of a potentially sustainable end-use application for Appalachian coal. *Polymer Composites*, 40, pp.591-599.

Poot, M. and Everson, R.C. (1999). Extraction of coal-tar pitches with toluene near the critical point: Gasification and coal hydrogenated pitches. *Fuel*, 78(9), pp.1017-1025.

Prada, V. et al. (1999). Preparation of novel pitches by Tar Air-blowing. *Carbon*, 37(1), pp. 97–106.

Prauchner, M., Pasa, V., Otani, C. and Otani, S. (2001). Characterization and thermal polymerization of *Eucalyptus* tar pitches. *Energy & Fuels*, 15(2), pp.449-454.

Prauchner, M., Pasa, V., Otani, C., Otani, S. and de Menezes, S. (2003). Eucalyptus tar pitch pretreatment for carbon material processing. *Journal of Applied Polymer Science*, 91(3), pp.1604-1611.

Rafikullah-Deraman., Nawi, M.N., Yasin, M.N., Ismail, M.H. and Ahmed, R.S. (2021). Polyethylene terephthalate waste utilisation for production of low thermal conductivity cement sand bricks. *Journal of Advanced Research in Fluid Mechanics and Thermal Sciences*, 88(3), pp.117-136.

Rahman, A., Ali, I., Zahrani, S.M. and Eleithy, R.H. (2011). A review of the applications of nanocarbon polymer composites. *Nano*, 06(03), pp.185-203.

Rajak, D.K., Pagar, D., Kumar, R. and Pruncu, C.I. (2019). Recent progress of reinforcement materials: A comprehensive overview of composite materials. *Journal of Materials Research and Technology*, 8(6), pp.6354-6374.

Ramakrishna, S., Mayer, J., Wintermantel, E. and Leong, K.W. (2001). Biomedical applications of polymer-composite materials: A review. *Composites Science and Technology*, 61(9), pp.1189-1224.

Restuccia, L. and Ferro, G.A. (2016) 'Promising low cost carbon-based materials to improve strength and toughness in cement composites', Construction and Building Materials, 126, pp. 1034–1043.

Rimdusit, S., Tanthapanichakoon, W. and Jubsilp, C. (2005). High performance wood composites from highly filled polybenzoxazine. *Journal of Applied Polymer Science*, 99(3), pp.1240-1253.

Roberts, L. (2014). Coal tar. *Encyclopedia of Toxicology*, pp. 993–995.

Romadhon, R.N. (2021). Kajian kuat lekat pada beton self compacting concrete, fly ash concrete dengan kadar fly ash 15%, high volume fly ash concrete dengan kadar fly ash 50% dan high volume fly ash-self compacting concrete dengan kadar fly ash 50% dari berat binder. *Matriks Teknik Sipil*, 9(3), 192.

Ruz, P., Banerjee, S., Pandey, M., Sudarsan, V., Sastry, P.U. and Kshirsagar, R.J. (2016). Structural evolution of turbostratic carbon: Implications in H_2 storage. *Solid State Sciences*, 62, pp.105-111.

Šafářová, M., Kusý, J., and Anděl, L. (2010). Brown coal tar hydrotreatment. *Journal of Analytical and Applied Pyrolysis*, 89(2), pp.265-270.

Santa, A.C., Gómez. M.A., Castaño, J.G., Tamayo. J.A. and Baena, L.M. (2023). Atmospheric deterioration of ceramic building materials and future trends in the field: A review. *Heliyon*, 9(4), e15028.

Savage, G. (2016). *Carbon-carbon composites*. Springer.

Sazali, N., Deraman, M., Omar, R., Othman, M.A., Suleman, M., Shamsudin, S.A., et al. (2016). Preparation and structural characterization of turbostratic-carbon/graphene derived from amylose film. *AIP Conference Proceedings*, *1784*, 040009.

Sekhohola, L. and Cowan, A.K. (2017). Biological conversion of low-grade coal discard to a humic substance-enriched soil-like material. *International Journal of Coal Science & Technology*, 4(2), pp.183-190.

Shamsol, A. 'lia S. et al. (2024) 'Graphene oxide as carbon-based materials: A review of geopolymer with addition of graphene oxide towards sustainable construction materials', Construction and Building Materials, 411, p. 134410.

Sharma, S., Malik, A. and Gupta, P. (2021). Bionanocomposites in tissue engineering and regenerative medicine, In: S. Ahmed and Annu (Eds.), *Bionanocomposites in tissue engineering and regenerative medicine*, pp.507-532. Woodhead Publishing.

Sharma, S., Patel, R.H. and Patel, B.K. (2020). Comparative study on the carbon–carbon composites developed from petroleum pitch, coal tar pitch, and their mixture. *Journal of Composite Materials*, 54(23), pp.3395-3404.

Sheikh-Ahmad, J. (2009). *Machining of polymer composites*. Springer.

Shindo, A. (1961). Studies on graphite fiber. J. Cerem. Assoc. Japan, pp. 195e199.

Shirvanimoghaddam, K., Hamim, S.U., Akbari, M.K., Fakhrhoseini, S.M., Khayyam, H., Pakseresht, A.M., et al. (2017). Carbon fiber reinforced metal matrix composites: Fabrication Processes and properties. *Composites Part A: Applied Science and Manufacturing*, 92, pp.70-96.

Singh, M., et al. (2018). *Carbon-carbon composites: Properties, preparation and applications*. Elsevier.

Sliwa, F., El Bounia, N., Martin, G., Charrier, F. and Malet, F. (2012). A new generation of wood polymer composite with improved thermal stability. *Polymer Degradation and Stability*, 97(4), pp.496-503.

Song, Q., Li, K., Li, H., Li, H. and Ren, C. (2012). Grafting straight carbon nanotubes radially onto carbon fibers and their effect on the mechanical properties of carbon/carbon composites. *Carbon*, 50(10), pp.3949-3952.

Soni, N., Shah, R.K., Shrivastava, R. and Datar, M. (2013). A study on the effect of heat treatment temperature on mesophase development in coal tar pitch. *AIP Conference Proceedings*, 1538, pp.141-145.

Standard Specification for Building Brick (Solid Masonry Units Made from Clay or Shale) ASTM C62, ASTM International, West Conshohocken, PA (2017)

SteelMintEvents (2023) Global coking coal demand likely to rise over 2% in 2023, SteelMint Events. Available at: https://www.steelmintevents.com/global-coking-coal-demand-likely-to-rise-over-2-in-2023/ (Accessed: 03 May 2024).

Stolboushkin A, Yu., Ivanov A.I. and Fomina O.A. (2016). Use of coal-mining and processing wastes in production of bricks and fuel for their burning. *Procedia Engineering,* 150, pp.1496-1502.

Sutcu, M. and Akkurt, S. (2009) 'The use of recycled paper processing residues in making porous brick with reduced thermal conductivity', Ceramics International, 35(7), pp. 2625–2631.

Swain, S.K. (2014). The use of nano-boron nitride reinforcements in composites for packaging applications, In: I.M. Low (Ed.), *Advances in Ceramic Matrix Composites*, pp.678-689. Woodhead Publishing.

Swapna, M.N.S., Saritha Devi, H.V., Vimal, R and Sankararaman, S. (2018). Fractal and spectroscopic analysis of soot from internal combustion engines. *The European Physical Journal Plus*, 3(133).

Taha, Y., Benzaazoua, M., Hakkou, R. and Mansori, M. (2017). Coal mine wastes recycling for coal recovery and eco-friendly bricks production. *Minerals Engineering*, 107, pp.123-138.

Thakur, M., Chandel, M., Rani, A. and Sharma, A. (2022). Introduction to biorenewable nanocomposite materials: Methods of preparation, current developments, and future perspectives, In: D. Pranthania and L. Singh (Eds.), *Biorenewable nanocomposite materials, Vol. 2: Desalination and wastewater remediation*, pp.1-24. American Chemical Society.

Thasneem, S.A. and Reddy, B.M. (2018). A study on strength and durability of cement concrete made with industrial waste water containing iron heavy metal. *International Journal for Research in Applied Science and Engineering Technology*, 6(2), pp.604-612.

Tishmack, J.K. and Burns, P.E., (2004). The chemistry and mineralogy of coal and coal combustion products. *Geological Society, London, Special Publications*, 236(1), pp.223-246.

Tschierske, C. (2002). Liquid crystalline materials with complex mesophase morphologies. *Current Opinion in Colloid & Interface Science*, 7(1-2), pp.69-80.

Turvey, G.J. (2023). Testing of pultruded glass fiber-reinforced polymer (GFRP) composite materials and structures, In: J Bai, (Ed.), *Advanced fiber-reinforced polymer(FRP) composites for structural applications*, pp. 343-441. Woodhead Publishing.

U.S. EPA (1992) Method 1311 Toxicity characteristic leaching procedure SW-846. United States Environmental Protection Agency. https://www.epa.gov/sites/default/files/2015-12/documents/1311.pdf; https://www.epa.gov/sitesdefault/files/2020-04/documents/sw_846_ch7.pdf. Accessed 21 Apr 2023

Vasić, M.V., Goel, G., Vasić, M. and Radojević, Z. (2021). Recycling of waste coal dust for the energy-efficient fabrication of bricks: A laboratory to industrial-scale study. *Environmental Technology & Innovation*, 21, 101350.

Vassilev, S. and Vassileva, C. (2009). A new approach for the combined chemical and mineral classification of the inorganic matter in coal. 1. Chemical and mineral classification systems. *Fuel*, 88(2), pp.235-245.

Vidhya, K. and Kandasamy, S. (2016) 'Experimental investigations on the properties of coal-ash brick units as Green Building Materials', International Journal of Coal Preparation and Utilization, 36(6), pp. 318–325.

Wang, J. et al. (2019). Carbon fibers from coal waste for carbon-carbon composites: A review. *Journal of Cleaner Production*, 213, pp.1068-1081.

Wang, L., Wang, J., Jia, F., Wang, C. and Chen, M. (2013). Nanoporous carbon synthesised with coal tar pitch and its capacitive performance. *Journal of Materials Chemistry A*, 1(33), pp.9498-9507.

Wang, Y., Liu, Y., Wang, D., Wang, C., Guo, L. and Yi, T. (2020). Free-standing honeycomb-like N doped carbon foam derived from coal tar pitch for high-performance supercapacitor. *Applied Surface Science*, 506, 145014.

Wang, Y.-G., Niu, Z.-S., Shen, J., Li, P., Niu, Y.-X., Zhao, W. and Wei, X. (2019). Formation of benzene polycarboxylic acids using alkali-oxygen oxidation of coal-tar pitch pre-treated by extraction and air-blowing. *Fuel Processing Technology*, 185, pp.100-105.

Wei, F., He, X., Bi, H., Jiao, S., Xiao, N. and Qiu, J. (2020). 3D hierarchical carbons composed of cross-linked porous carbon nanosheets for supercapacitors. *Journal of Power Sources*, 474, 228698.

Whitehurst, D.D. (1978). A primer on the chemistry and constitution of coal, In: J.W. Larsen, (Ed.), *Organic chemistry of coal*, pp.1-35. American Chemical Society.

Windhorst, T. and Blount, G. (1997). Carbon-carbon composites: A summary of recent developments and applications. *Materials & Design*, 18(1), pp.11-15.

Wong, W.H. (2009). Coal composition in triangular diagram. *Bulletin of the Geological Society of China*, 6(1), pp.65-67.

Wu, Q., Miao, W., Zhang, Y., Gao, H. and Hui, D. (2020). Mechanical properties of nanomaterials: A review. *Nanotechnology Reviews*, 9(1), pp.259-273.

Xie, X., et al. (2014). Synthesis and characterization of coal-based ceramic composites from coal fly ash and kaolin. *Ceramics International*, 40(3), pp.4703-4709.

Xie, Z., Wang, S. and Chen, Z. (2007). Active filler (aluminum–aluminum nitride) controlled polycarbosilane pyrolysis. *Journal of Inorganic and Organometallic Polymers and Materials*, 17(1), pp.307-307.

X-MAT. (2020). *Introducing* X-*Tiles.* Available at: https://x-materials.com/rooftiles/ (Accessed: 17 September 2023).

Xu, H., Song, W., Cao, W., Shao, G., Lu, H., Yang, D., et al. (2017). Utilization of coal gangue for the production of brick. *Journal of Materials Cycles and Waste Management*, 19, pp.1270-1278.

Yang, K.S., Choi, Y.O., Kim, Y.M., Park, S.H., Yang, C.M., Kim, Y.J., et al. (2000a). Preparations of carbon fibers from precursor pitches synthesized with coal tar or petroleum residue oil. *Fibers and Polymers*, 1(2), pp.97-102.

Yang, K.S., Kim, B.-H. and Yoon, S.-H. (2014). Pitch based carbon fibers for automotive body and electrodes. *Carbon Letters*, 15(3), pp.162-170.

Yang, Y., Niu, H., Qin, F., Guo, Z., Wang, J., Ni, G., et al. (2020b). MnO_2 doped carbon nanosheets prepared from coal tar pitch for advanced asymmetric supercapacitor. *Electrochimica Acta*, 354, 136667.

Yang, Y., Zuo, P. and Qu, S. (2022). Adjusting hydrophily and aromaticity strategy for pitch-based hierarchical porous carbon and its application in flexible supercapacitor. *Fuel*, 311, 122514.

Yang, Z., Jia, Y., Niu, Y., Zhang, Y., Zhang, C., Li, P., et al. (2020c). One-step wet-spinning assembly of twisting-structured graphene/carbon nanotube fiber supercapacitor. *Journal of Energy Chemistry*, 51, pp.434-441.

Yao, Y., Wu, H., Huang, L., Li, X., Yu, L., Zeng, S., et al. (2017). Nitrogen-enriched hierarchically porous carbon nanofiber network as a binder-free electrode for high-performance supercapacitors. *Electrochimica Acta*, 246, pp.606-614.

Yu, H. et al. (2023) 'Development of high-strength and durable coal char-based building bricks', Journal of Building Engineering, 74, p. 106908.

Yuan, G., Xue, Z., Cui, Z., Westwood, A., Dong, Z., Cong, Y. et al. (2020). Constructing the bridge from isotropic to anisotropic pitches for preparing pitch-based carbon fibers with tunable structures and properties. *ACS Omega*, 5(34), pp.21948–21960.

Yuan, Y., Li, D., Zhang, L., Zhu, Y., Wang, L. and Li, W. (2016). Development, status, and prospects of coal tar hydrogenation technology. *Energy Technology*, 4(11), pp.1338-1348.

Zander, M. (1987). On the composition of pitches. *Fuel*, 66(11), pp.1536-1539.

Zhai, X., Liu, J., Zhang, Y., Fan, Q., Li, Z. and Zhou, Y. (2019). Microcrystal structure evolution of mesophase pitch-based carbon fibers with enhanced oxidation resistance and tensile strength induced by boron doping. *Ceramics International*, 45(9), pp.11734-11738.

Zhang, L., et al. (2015). Development of coal-based carbon-carbon composites for structural applications. *Carbon*, 94, pp.22-29.

Zhang, W., Jiang, S., Wang, K., Wang, L., Xu, Y., Wu, Z. et al. (2014). Thermogravimetric dynamics and FTIR analysis on oxidation properties of low-rank coal at low and moderate temperatures. *International Journal of Coal Preparation and Utilization*, 35(1), pp.39-50.

Zhang, Y., et al. (2019). Ceramic matrix composites for building materials. *Journal of the American Ceramic Society*, 102(7), pp.3661-3680

Zhang, Z. and Zhang, S. (2020). A new coking coal charging method for 6 m top-charged coke oven: System design and experiment. *Applied Sciences*, 11(1), 33.

Appendices

Appendix A: Tables of physicochemical and mechanical properties of the composites

Table A.1: Proximate analysis results as obtained

Sample	Inherent moisture (%)	Volatile matter (%)	Ash (%)	Fixed carbon (%)
GG1	3.280	10.000	81.260	5.440
GS	1.710	20.370	61.650	16.270
CT	25.300	48.180	0.210	26.320
PP	1.470	55.280	0.450	42.800
CTP 350°C 3h	0.400	28.680	0.280	70.640
CTP 350°C 6h	0.240	26.040	0.240	73.480
CTP 350°C 9h	0.330	22.660	0.330	76.680
CTP 400°C 3h	0.330	22.270	0.290	77.100
CTP 400°C 6h	1.070	16.560	0.830	81.540
CTP 400°C 9h	0.560	11.270	0.490	87.680
CTP 450°C 3h	0.720	12.020	0.550	86.710
CTP 450°C 6h	0.580	11.130	0.490	87.800

GG1: coal fines; GS: Greenside coal fines; CT: as-received coal tar; CTP: coal tar pitch produced at different conditions

Table A.2: Coal tar air blowing results for initial and final weight

Temperature (°C)	Time (h)	Initial mass (g)	Final mass (g)
350	3	250	125
	6	250	85
	9	250	75
400	3	250	90
	6	100	40
	9	250	85
450	3	100	40
	6	100	40

Table A.3: Proximate analysis of the composites

Sample	Inherent moisture (%)	Volatile matter (%)	Ash (%)	Fixed carbon (%)
GG1/10 CTP	1.2	6.97	78.46	13.36
GG1/30 CTP	1.57	6.8	56.51	35.11
GG1/50 CTP	0.52	3.62	49.76	46.09
GG1/DMPS	2.64	7.46	85.23	4.68
GS/10 CTP	2.92	7.35	51.24	38.49
GS/30 CTP	3.16	8.91	40.38	47.55
GS/50 CTP	2.12	9.32	34.84	53.71
GS/DMPS	1.73	3.92	88.32	6.03

Table A.4: Weight loss of the composites after pyrolysis

Sample	Mg (g)	Mp (g)	Weight loss (%)
GS 10 CTP 400	1.990	1.670	16.080
GS 30 CTP 400	1.970	1.710	13.198
GS 50 CTP 400	1.990	1.760	11.558
GG1 10 CTP 400	1.990	1.670	16.080
GG1 30 CTP 400	2.000	1.670	16.500
GG1 50 CTP 400	1.970	1.690	14.213
GS 20 DMPS	1.439	1.178	18.109
GG1 20 DMPS	1.407	1.256	10.716

Mg: mass of the green bodies; Mp: mass of the composites after pyrolysis

Table A.5: Linear shrinkage of the composites after pyrolysis

Sample	L_G (mm)	L_P (mm)	Linear shrinkage (%)
GS 10 CTP 400	3.52	3.33	5.397727
GS 30 CTP 400	3.64	3.53	3.021978
GS 50 CTP 400	3.85	4.47	-16.1039
GG1 10 CTP 400	3.08	2.96	3.896104
GG1 30 CTP 400	3.35	3.22	3.880597
GG1 50 CTP 400	3.5	5.28	-50.8571
GS 20 DMPS	2.58	2.54	1.550388
GG1 20 DMPS	2.09	2.04	2.392344

L_G: thickness of the green bodies; L_P: thickness of the pyrolysed composites

Table A.6: 5-hour cold water absorption test of the composites

	Five-hour cold water test								
Sample	D (g)	M (g)	S (g)	V (cm^3)	Vop (cm^3)	P (%)	WA (%)	T	B (g/cm^3)
GS 10 CTP 400	1.670	1.810	0.790	1.021	0.153	15.062	9.292	1.912	1.622
GS 30 CTP 400	1.710	1.790	0.713	1.074	0.080	7.451	4.678	1.721	1.593
GS 50 CTP 400	1.760	1.790	0.582	1.202	0.027	2.211	1.518	1.497	1.464
GG1 10 CTP 400	1.670	1.790	0.961	0.830	0.140	16.873	8.456	2.403	1.997
GG1 30 CTP 400	1.670	1.710	0.771	0.933	0.027	2.854	1.594	1.850	1.798
GG1 50 CTP 400	1.690	1.800	0.536	1.270	0.127	9.969	7.543	1.469	1.323
GS 20 DMPS	1.178	1.373	0.621	0.766	0.205	26.694	17.292	2.106	1.544
GG1 20 DMPS	1.256	1.270	0.655	0.640	0.016	2.505	1.260	2.029	1.978

D: mass of dry composites; M: mass of wet composites after immersion in water; S: mass of suspended composites in water; V: exterior volume of the composites; Vop: volume of pores; P: porosity; WA: water absorption; T: apparent specific gravity; B: bulk density

Table A.7: 24-hour cold water absorption test of the composites

	24-hour cold test								
Sample	**D (g)**	**M (g)**	**S (g)**	**V (cm^3)**	**Vop (cm^3)**	**P (%)**	**WA (%)**	**T**	**B (g/cm^3)**
GS 10 CTP 400	1.670	1.847	0.854	0.995	0.686	18.783	11.409	2.056	1.666
GS 30 CTP 400	1.710	1.834	0.784	1.049	0.651	11.567	7.161	1.845	1.630
GS 50 CTP 400	1.760	1.823	0.608	1.212	0.629	5.247	3.615	1.533	1.453
GG1 10 CTP 400	1.670	1.805	0.925	0.881	0.660	17.135	8.944	2.262	1.881
GG1 30 CTP 400	1.670	1.752	0.830	0.922	0.607	8.398	4.650	1.986	1.818
GG1 50 CTP 400	1.690	1.747	0.509	1.238	0.612	5.451	4.040	1.436	1.357
GS 20 DMPS	1.178	1.378	0.621	0.735	0.508	24.902	15.429	2.146	1.613
GG1 20 DMPS	1.256	1.281	0.672	0.622	0.437	4.240	2.088	2.123	2.033

D: mass of dry composites; M: mass of wet composites after immersion in water; S: mass of suspended composites in water; V: exterior volume of the composites; Vop: volume of pores; P: porosity; WA: water absorption; T: apparent specific gravity; B: bulk density

Table A.8: Five-hour boiling water absorption test of the composites

	Five-hour boiling test								
Sample	**D (g)**	**M (g)**	**S (g)**	**V (cm^3)**	**Vop (cm^3)**	**P (%)**	**WA (%)**	**T**	**B (g/cm^3)**
GS 10 CTP 400	1.670	1.851	0.854	0.985	0.194	19.642	11.741	2.095	1.683
GS 30 CTP 400	1.710	1.854	0.797	1.064	0.152	14.275	8.887	1.875	1.607
GS 50 CTP 400	1.760	1.936	0.730	1.193	0.170	14.235	9.655	1.720	1.475
GG1 10 CTP 400	1.670	1.826	0.943	0.880	0.172	19.518	10.373	2.339	1.882
GG1 30 CTP 400	1.670	1.796	0.855	0.932	0.126	13.503	7.511	2.079	1.798
GG1 50 CTP 400	1.690	2.000	0.721	1.282	0.320	24.922	19.023	1.745	1.310
GS 20 DMPS	1.178	1.387	0.630	0.763	0.210	27.676	17.801	2.150	1.553
GG1 20 DMPS	1.256	1.282	0.666	0.630	0.030	4.666	2.369	2.107	2.008

D: mass of dry composites; M: mass of wet composites after immersion in water; S: mass of suspended composites in water; V: exterior volume of the composites; Vop: volume of pores; P: porosity; WA: water absorption; T: apparent specific gravity; B: bulk density

Table A.9: Exterior volume (cm^3) results of the composites

Samples	**Five-hour cold test**	**24-hour cold test**	**Five-hour boiling test**
GS 90/10 CTP 400	1.021	0.995	0.985
GS 70/30 CTP 400	1.074	1.049	1.064
GS 50/50 CTP 400	1.202	1.212	1.193
GG1 90/10 CTP 400	0.830	0.881	0.880
GG1 70/30 CTP 400	0.933	0.922	0.932
GG1 50/50 CTP 400	1.255	1.238	1.282
GS 80/20 DMPS	0.766	0.735	0.763
GG1 80/20 DMPS	0.640	0.622	0.630

Table A.10: Force and compression strength of the composites

Samples	Force (N)	Compression strength (MPa)
GS 90/10 CTP	106885.78	289.76
GS 70/30 CTP	106755.67	341.22
GG1 90/10 CTP	106809.28	340.52
GG1 70/30 CTP	106868.37	344.71
GS 80/20 DMPS	106848.3	199.64
GG1 80/20 DMPS	106830.00	106.58

Table A.11: Corrosion rate of the composites

Samples	Initial mass (g)	Final mass (g)	Weight loss (g)	Density (g/cm^3)	Area (cm^2)	Time (h)	Corrosion rate (μmpy)
GS 90/10 CTP	1.77	1.71	0.0058	1.64	3.14	168.00	0.58
GS 70/30 CTP	1.80	1.73	0.0064	1.59	3.14	168.00	0.67
GG1 90/10 CTP	1.86	1.81	0.0047	2.01	3.14	168.00	0.39
GG1 70/30 CTP	1.87	1.80	0.0063	1.78	3.14	168.00	0.59
GS 80/20 DMPS	0.68	0.61	0.0076	1.57	3.14	168.00	0.81
GG1 80/20 DMPS	1.28	1.19	0.0086	2.04	3.14	168.00	0.70

Table A.12: Residual mass at different exposure times

	Residual mass (g)				
Samples	Original	10s	20s	30s	40s
GS/10 CTP	1.689	1.683	1.670	1.653	1.642
GS/30 CTP	1.771	1.703	1.700	1.700	1.642
GG1/10 CTP	1.792	1.775	1.765	1.758	1.737
GG1/30 CTP	1.789	1.772	1.761	1.750	1.739
GS/DPMS	1.130	1.120	1.112	1.108	1.099
GG1/DPMS	1.300	1.224	1.216	1.211	1.119

Table A.13: Mass ablation rate of the composites

	Mass ablation rate (g/sec)			
Samples	10s	20s	30s	40s
GS 90/10 CTP	0.0009	0.0016	0.0014	0.0013
GS 70/30 CTP	0.0077	0.0040	0.0028	0.0033
GG1 90/10 CTP	0.0018	0.0013	0.0010	0.0012
GG1 70/30 CTP	0.0038	0.0025	0.0019	0.0017
GS 80/20 DPMS	0.0009	0.0009	0.0008	0.0009
GG1 80/20 DPMS	0.0076	0.0044	0.0032	0.0046

Table A.14: Change in thickness of the composites at different flame exposure times

	Thickness (mm)				
Samples	**Original**	**10s**	**20s**	**30s**	**40s**
GS/10 CTP	3.42	3.39	3.36	3.33	3.29
GS/30 CTP	3.55	3.52	3.49	3.47	3.45
GG1/10 CTP	2.97	2.94	2.9	2.85	2.81
GG1/30 CTP	3.36	3.33	3.14	3.13	3.12
GS/DPMS	2.45	2.42	2.34	2.29	2.27
GG1/DPMS	2.2	2.16	2.07	1.99	1.87

Table A.15: Linear ablation rate of the composites at different flame exposure times

	Linear ablation rate (mm/s)			
Samples	**10s**	**20s**	**30s**	**40s**
GS 90/10 CTP	0.00333	0.00909	0.00344	0.00367
GS 70/30 CTP	0.00367	0.00983	0.00311	0.00275
GG1 90/10 CTP	0.00500	0.01487	0.00522	0.00467
GG1 70/30 CTP	0.00400	0.02863	0.00811	0.00650
GS 80/20 DPMS	0.00433	0.02069	0.00544	0.00467
GG1 80/20 DPMS	0.00467	0.02793	0.00744	0.00825

Appendix B: Figures of the results

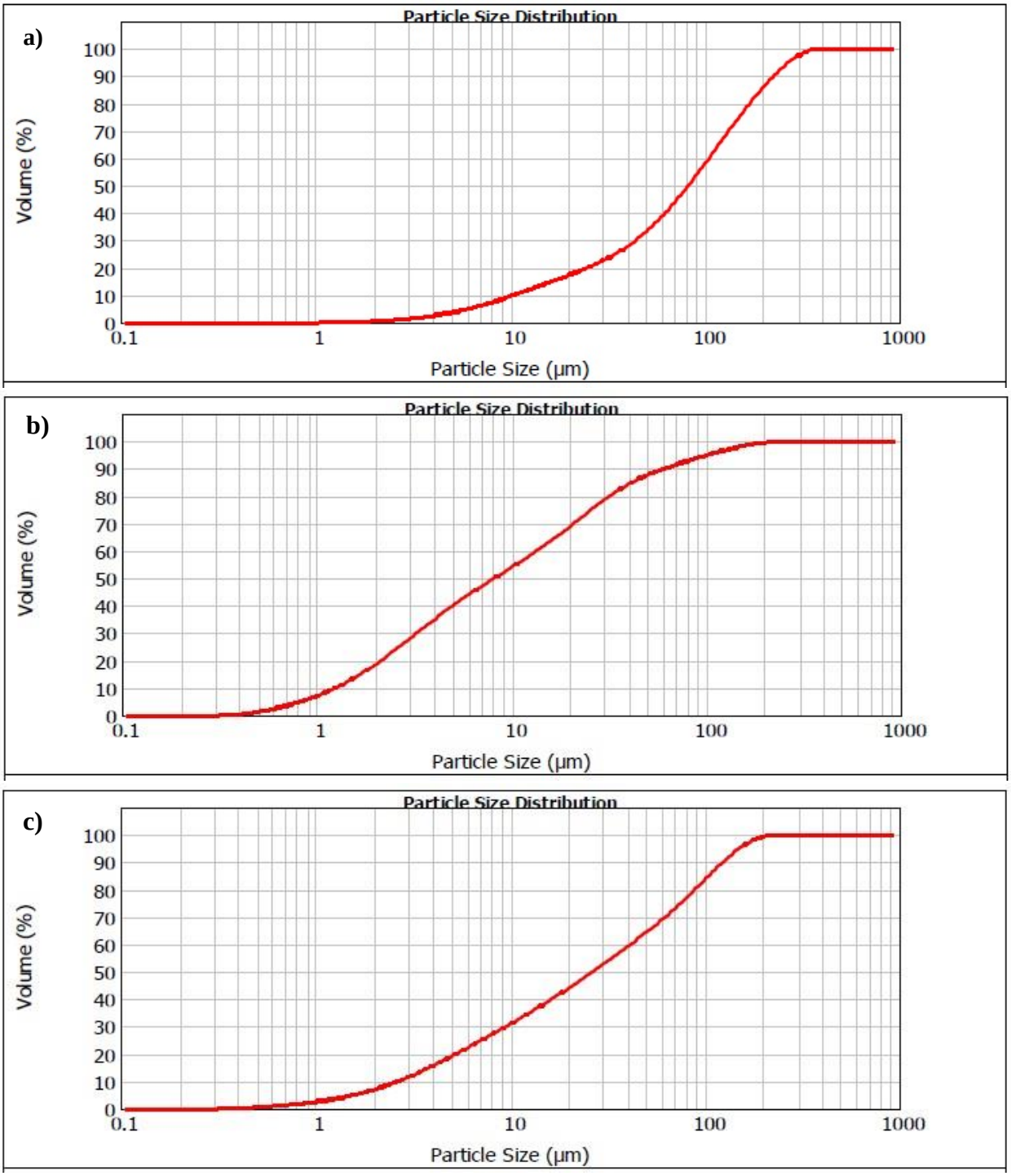

Figure B.1: Malvern Mastersizer 2000 particle size distribution for (a) coal tar pitch, (b) GG1 coal fines, and (c) GS coal fines

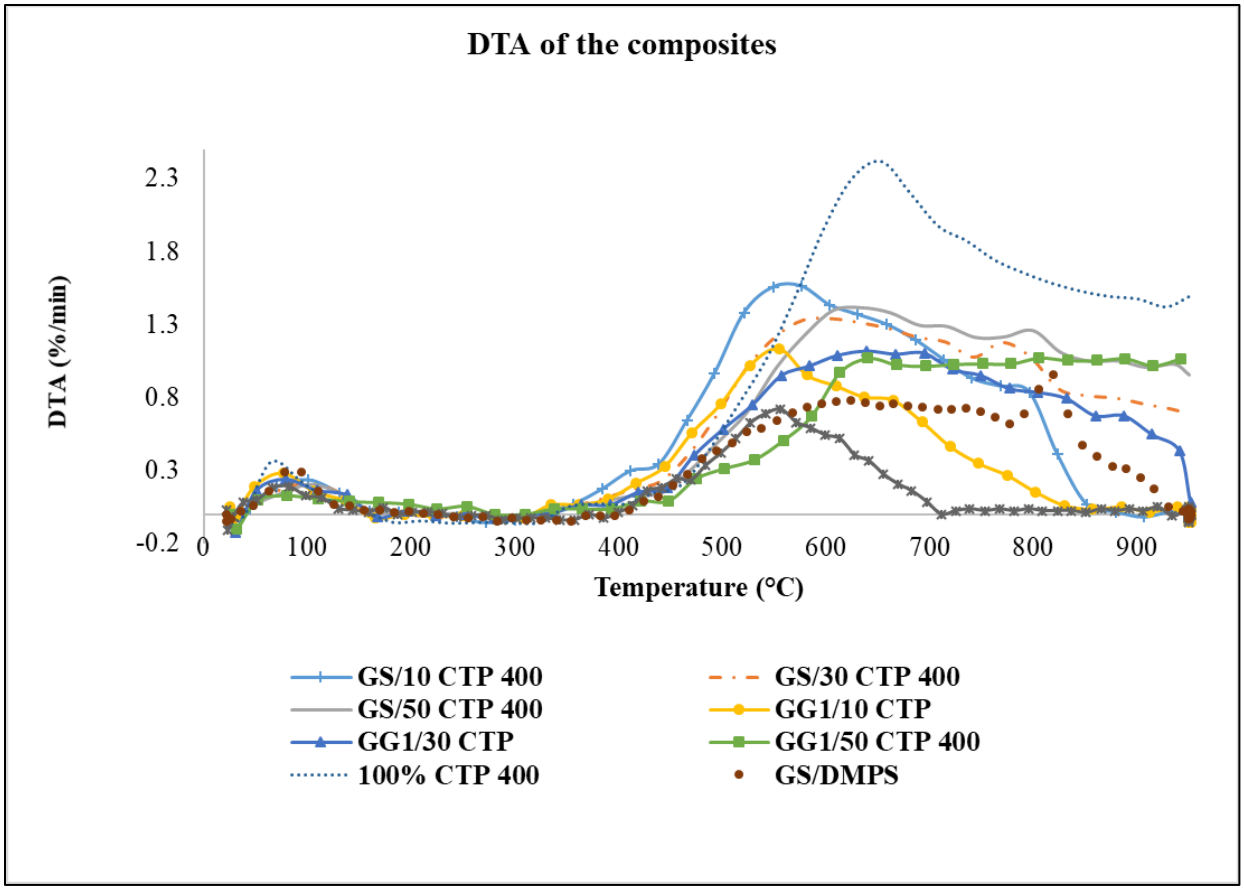

Figure B.2: Differential thermal analysis (DTA) of the coal composites

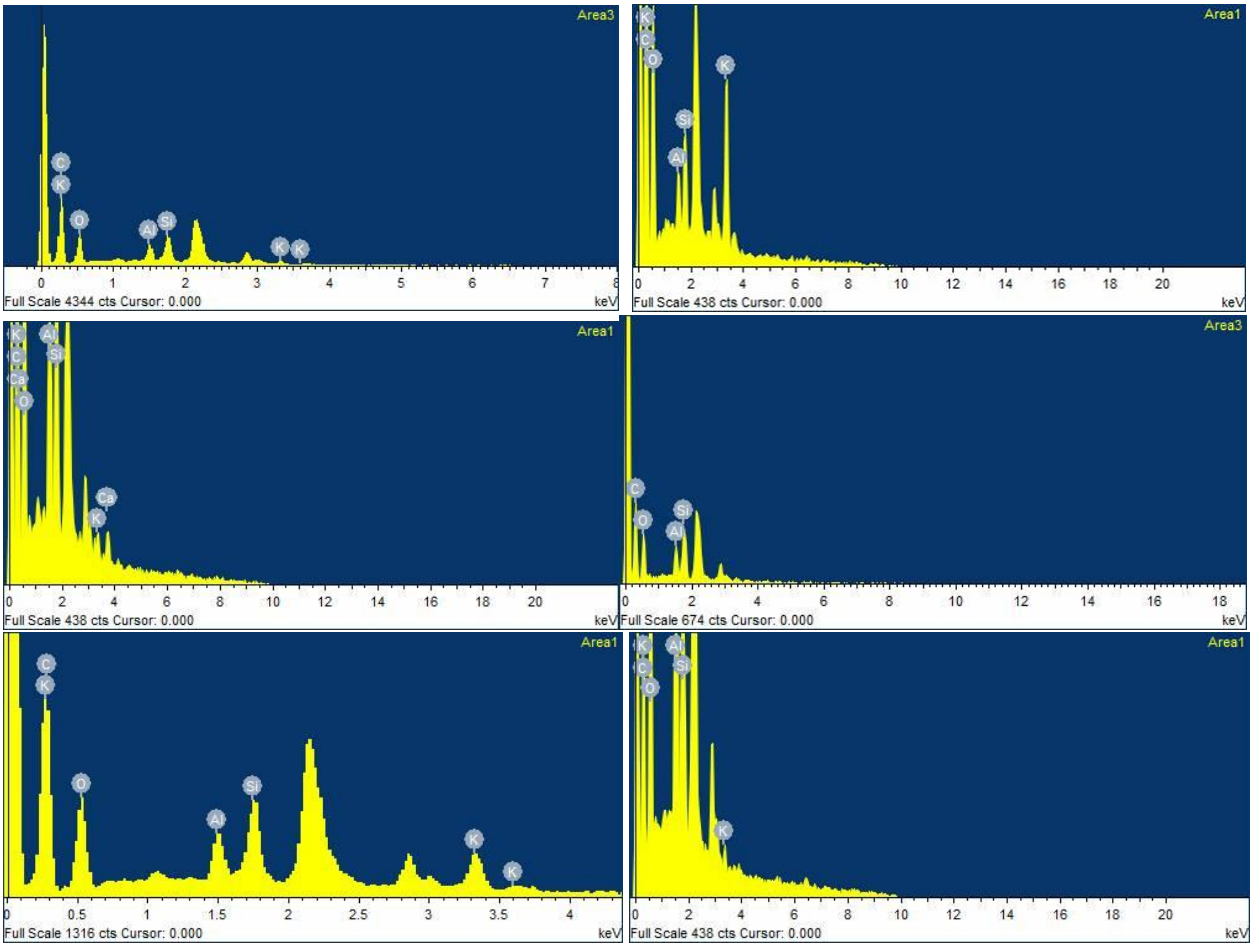

Figure B.3: Energy dispersive X-ray spectroscopy results for (a) GS/10% CTP, (b) GS/30% CTP, (c) GS/20% DMPS, (d) GG1/10% CTP, (e) GG1/30% CTP, and (f) GG1/20% DMPS

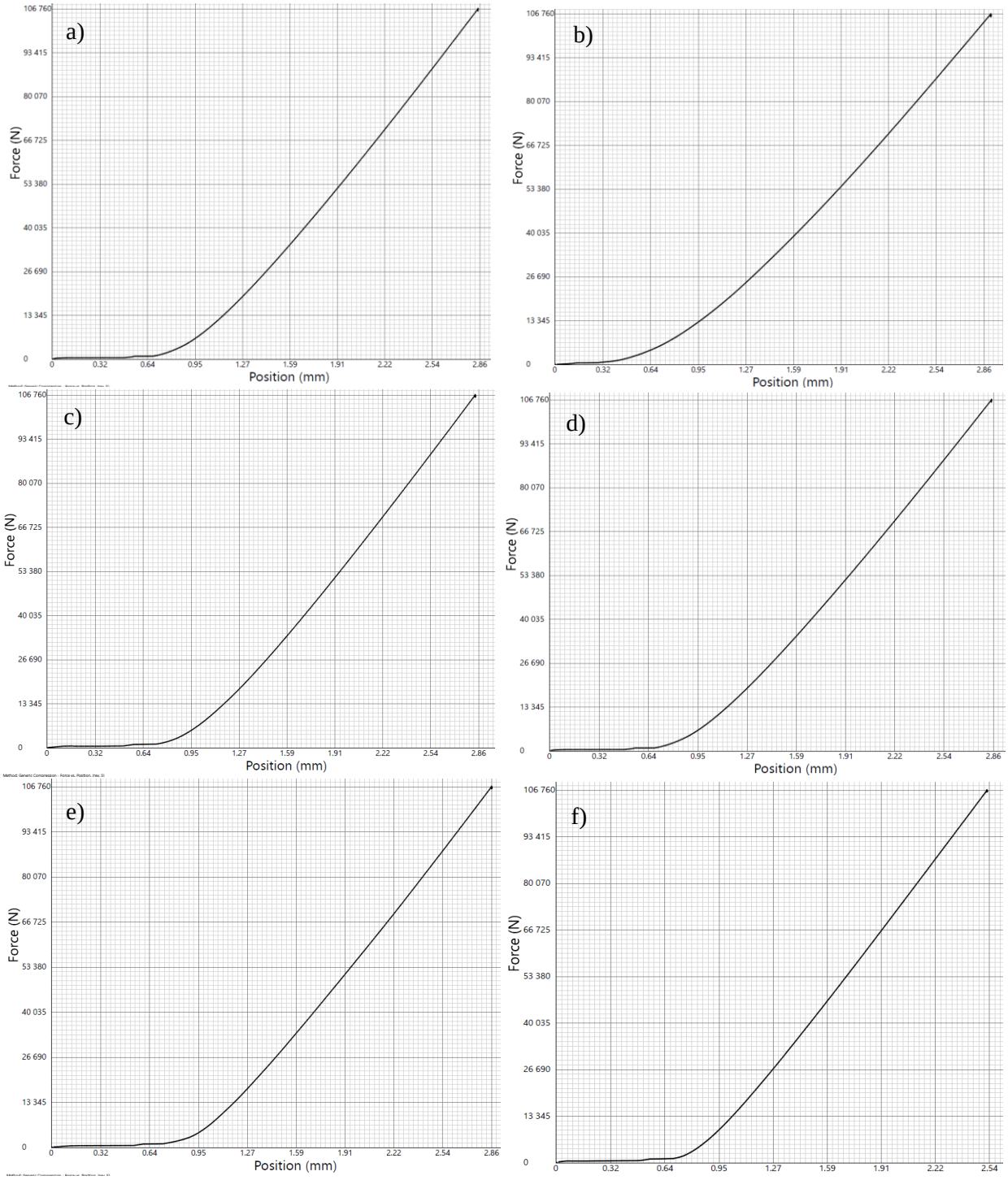

Figure B.4: Compression force of the composites: (a) GS/10% CTP, (b) GS/30% CTP, (c) GS/20% DMPS, (d) GG1/10% CTP, (e) GG1/ 30% CTP, and (f) GG1/20% DMPS

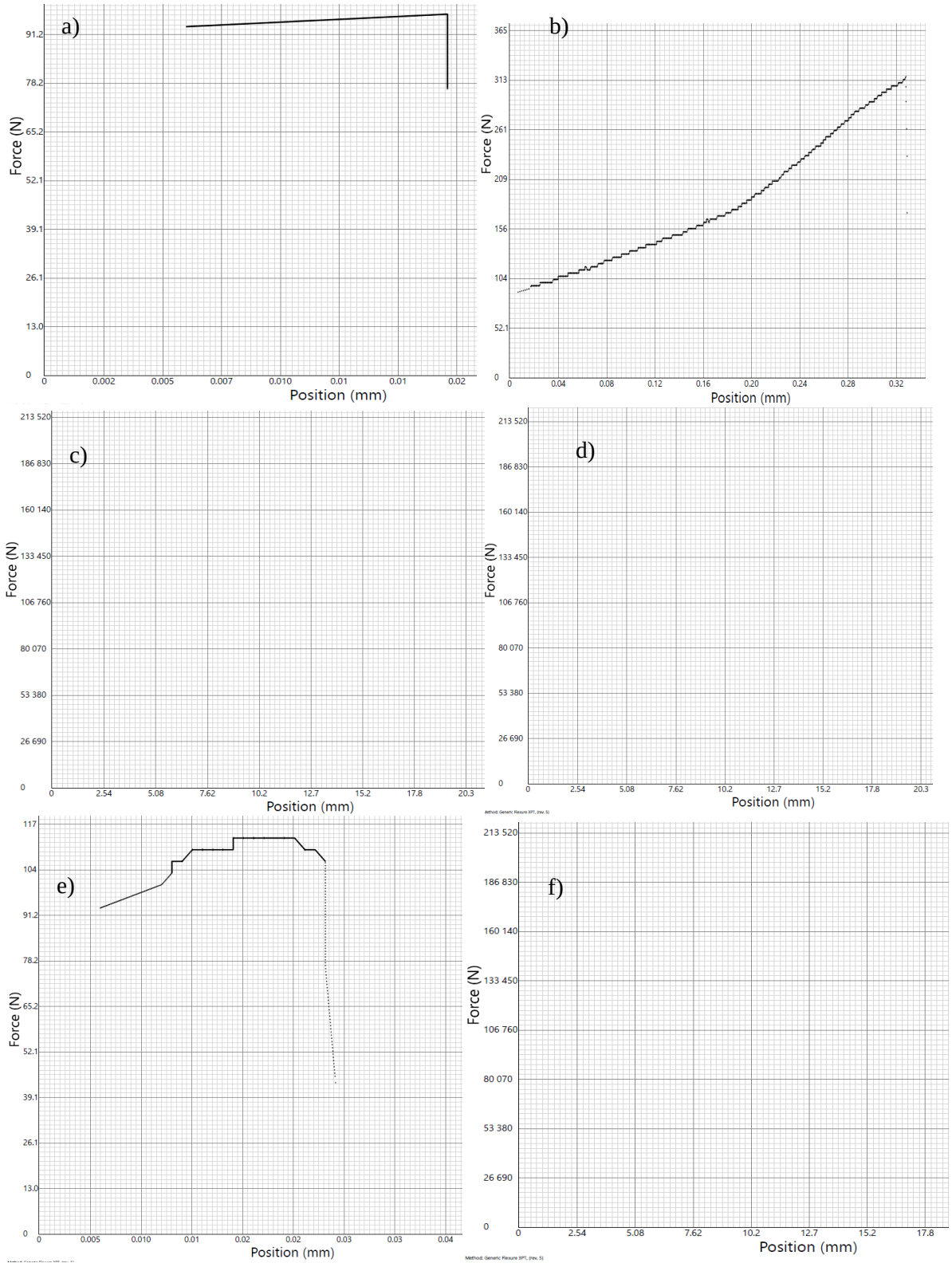

Figure B.5: Bending force of the composites; (a) GS/10% CTP, (b) GS/30% CTP, (c) GS/20% DMPS, (d) GG1/10% CTP, (e) GG1/30% CTP, and (f) GG1/20% DMPS

Appendix C: Composites fabrication

Figure C.1: As received materials: (a) GS coal fines, (b) GG1 coal fines, (c) dimethylpolysiloxane, and (d) coal tar

Figure C.2: Stainless steel thermal reactor used to produce coal tar pitch from coal tar

Figure C.3: Cylindrical mould used to produce small composites

Figure C.4: Method used to mix the coal and binder

Figure C.5: Hydraulic press used to compact the composites

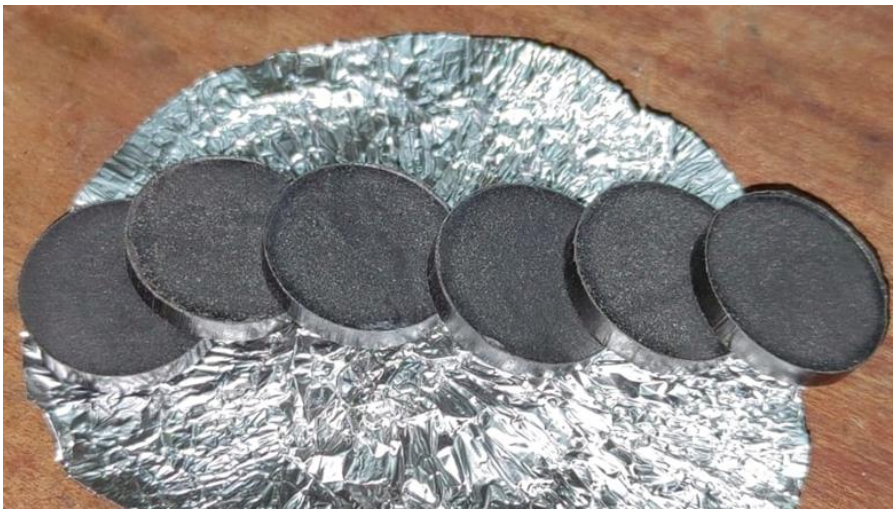

Figure C.6: Green bodies

Figure C.7: The combusted composites that were pyrolysed in air

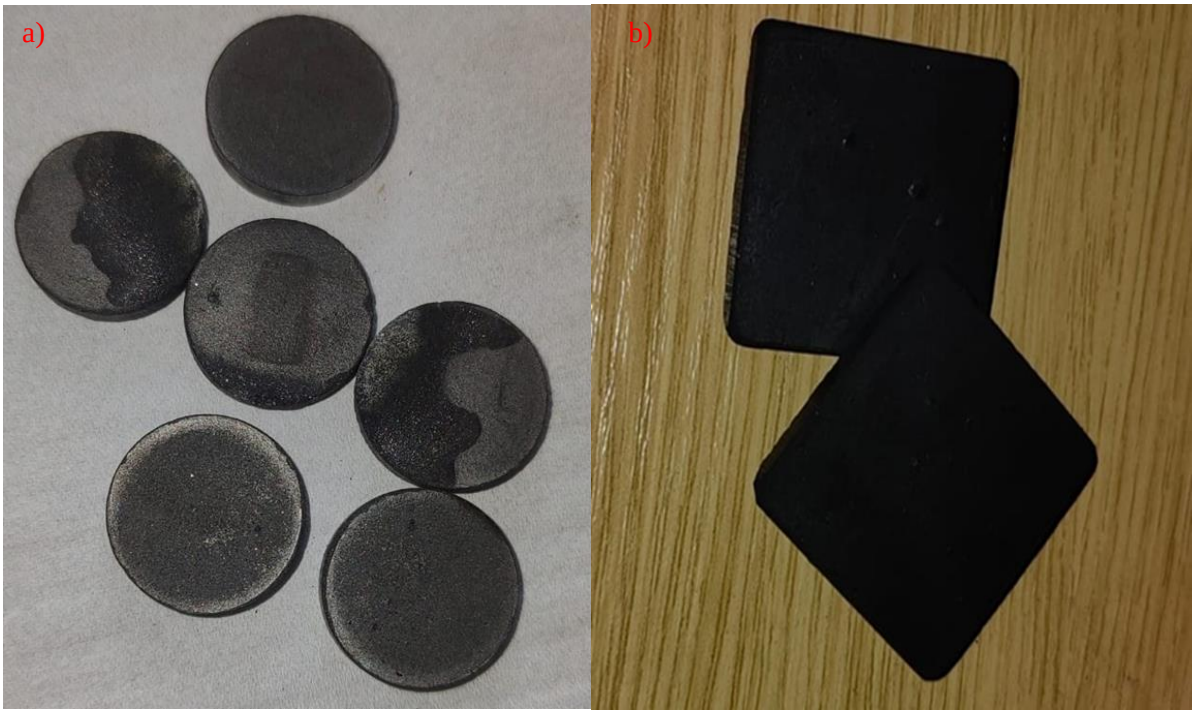

Figure C.8: Composites produced after pyrolysis: (a) circular composites and (b) square composites

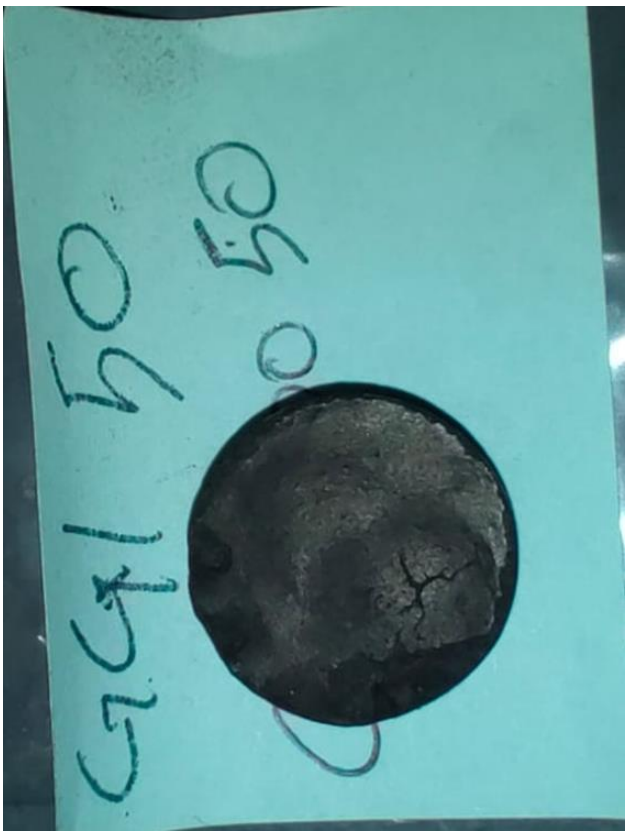

Figure C.9: Cracked GG1 50%/50% CTP composite

Figure C.10: Weighing suspended mass after water immersion test to determine the mass of the composites in water

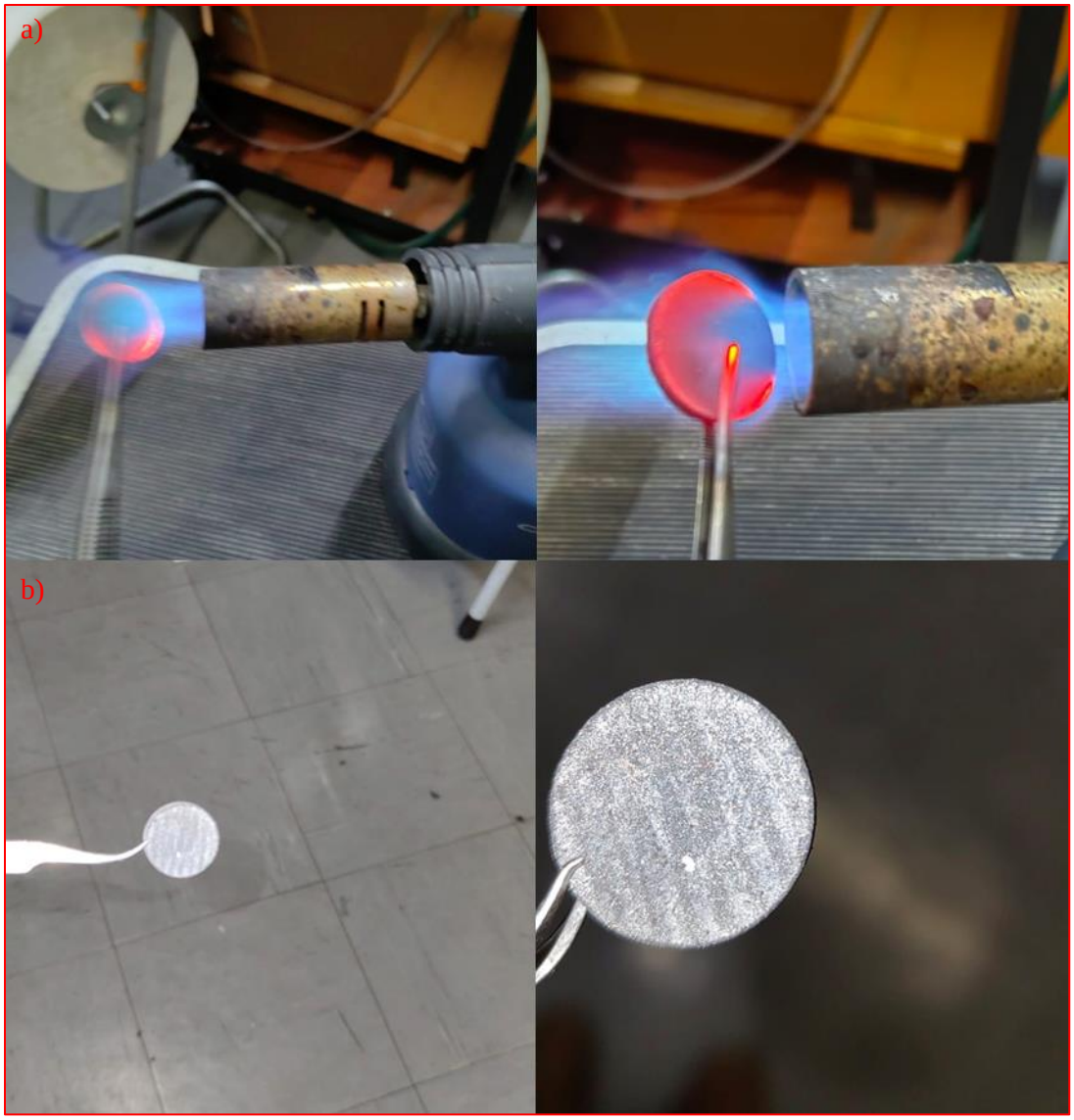

Figure C.11: Flammability of the composites: (a) hot composites and (b) cooled composites